

**LOCAL SCOUR AROUND BRIDGE ABUTMENTS UNDER ICE COVERED
CONDITIONS**

By

Peng Wu

Bsc, Hefei University of Technology, China, 2007

Msc, Hefei University of Technology, China, 2010

DISSERTATION SUBMITTED IN PARTIAL FULFILLMENT OF
THE REQUIREMENTS FOR THE DEGREE OF
DOCTOR OF PHILOSOPHY
IN
NATURAL RESOURCES AND ENVIRONMENTAL STUDIES

UNIVERSITY OF NORTHERN BRITISH COLUMBIA

October 10, 2014

© PENG WU, 2014

ABSTRACT

Local scour refers to the sediment transport around hydraulic structures by flowing water. Excessive scour around the abutment can potentially cause damage to the bridge, which may also result in catastrophic consequences. Abutment scour refers to the local scour generated by the flow passing around bridge abutments. One of the challenging problems for hydraulic engineers is the prediction of maximum scour depth around abutments and pier foundations so that proper provisions can be made in the design and construction to mitigate the consequences.

Despite significant research efforts to improve the understanding of scour related problems, abutment scour is still among the more complex and challenging problems. Over the past few decades, local scour around bridge abutments has received wide attention, and many researchers have contributed various studies on the topic. The current state knowledge on local scour still has insufficiently understood aspects, for example, ice accumulation has never been addressed in the abutment scour research. The impacts of ice cover has never been conducted. To fill this gap, the present research is conducted.

The ice cover can change the channel morphology and flow field. It is well known that river ice affects the vertical and lateral distribution of flow in a channel. Additionally, because river ice affects the flow conditions, it potentially influence sediment transport. Hence, the scour around abutments is affected.

In the present research, a series of large flume experiments are conducted. By adding different simulated ice covers in the flume, ice-covered flow can be generated. By comparing the scour profiles and maximum scour depth around two commonly used abutments in three non-uniform sediments, the ice cover impacts have been investigated. A significant increase can be noticed by adding ice cover. With the increase in ice cover roughness, the maximum scour depth increase correspondingly. Meanwhile, semi-circular abutment can generate a relatively small scour hole. Furthermore, the role of densimetric Froude number, armor layer sediment size, Manning's roughness coefficient are all analyzed in the research. Several empirical equations are developed from present research for the estimation of maximum scour depth around abutments.

TABLE OF CONTENTS

ABSTRACT.....	i
TABLE OF CONTENTS.....	ii
CO-AUTHORSHIP	iv
List of Tables	v
List of Figures.....	vi
ACKNOWLEDGEMENT	ix
1 GENERAL INTRODUCTION.....	1
1.1 Literature review	3
1.1.1 Local Scour characteristics around bridge abutments in open channels.....	3
1.1.2 Ice Covered issues on local scour	8
1.2 Research objectives.....	12
1.2.1 Objective One	12
1.2.2 Objective Two.....	12
1.2.3 Objective Three.....	13
1.3 Research innovations	14
1.4 Outline of dissertation.....	14
2 METHODOLOGY	20
2.1 Theoretical analysis	20
2.2 Experimental study	22
2.2.1 Study site.....	22
2.2.2 Experimental design and construction	22
2.2.3 Measurement apparatus.....	25
2.2.4 Experimental procedures.....	27
3 RESULTS AND DISCUSSION	29
3.1 Impacts of ice cover on local scour around semi-circular bridge abutment.....	30
3.1.1 Methodology	31
3.1.2 Results and discussion	33
3.1.3 Conclusion	46
3.2 Local scour around bridge abutments under ice covered condition: comparing of square abutment and semi-circular abutment.....	49

3.2.1 Experimental setup.....	50
3.2.2 Results and discussion	56
3.2.3 Conclusions.....	63
3.3 Scour morphology around bridge abutments with non-uniform sediment under ice cover	67
3.3.1 Methodology	69
3.3.2 Results and discussion	73
3.3.3 Conclusions.....	79
3.4 Armor layer analysis of local scour around bridge abutments under ice cover	82
3.4.1 Methodology	84
3.4.2 Results and discussion	88
3.4.3 Conclusions.....	100
3.5 ADV measurements of flow field along a round abutment under ice covers	103
3.5.1 Methodology	104
3.5.2 Results and Discussion.....	107
3.5.3 Conclusion	116
3.6 The incipient motion of bed material and shear stress analysis around bridge abutments under ice-cover.....	119
3.6.1 Experimental setup and measurement.....	120
3.6.2 Results and discussion	122
3.6.3 Conclusions.....	129
4 GENERAL CONCLUSION	133
5 APPENDIX.....	135

CO-AUTHORSHIP

For all chapters in this thesis, I was the primary investigator, leading: the design of studies, collection of data and analysis of data. I wrote the manuscripts and was responsible for incorporating comments and feedback on into final versions of the thesis. However, despite the use of first-person singular in writing the thesis, I would like to acknowledge that this work was not conducted in isolation. Faye Hirshfield is my PhD colleague who assisted in all aspects of field work. To acknowledge her contribution, she is included in all publications that stem from my work. Chen Pangpang and Dr. Jun Wang contributed some comments and figures on the manuscripts, so they were included in some publications respectively. Finally, my supervisor, Dr. Jueyi Sui, contributed to experimental design, data analysis of the present research. And he is included in author ship on all resulting publications.

Publications and authorships stemming from this thesis (published or submitted)

Wu P, Hirshfield F, Sui J, Wang J, 2014. Impacts of ice cover on local scour around semi-circular bridge abutment, *Journal of Hydrodynamics*, 2014, 26(1):840-847. (Chapter 3.1)

Wu P, Hirshfield F, Sui J, Chen P, 2014. Local scour around bridge abutments under ice covered condition- an experimental study, IJSR-D-13-00042, *International Journal of Sediment Research*, accepted for publication. (Chapter 3.2)

Wu P, Hirshfield F, Sui J, 2013. Scour morphology around bridge abutment with non-uniform sediments under ice cover, proceedings for the 35th IAHR World Congress, Chengdu, China, September, 2013. (Chapter 3.3)

Wu P, Hirshfield F, Sui J, 2014. Armor layer analysis of local scour around bridge abutments under ice cover, *River Research and Applications*, accepted for publication, published online in Wiley Online Library, DOI: 10.1002/rra.2771. (Chapter 3.4)

Wu P, Hirshfield F, Sui J, 2013. ADV measurements of flow field along a round abutment under ice covers, accepted for publication at the proceedings for 17th Workshop on River Ice, Edmonton, Canada, July 21-24, 2013. (Chapter 3.5)

Wu P, Hirshfield F, Sui J, 2014. The incipient motion of bed material and shear stress analysis around bridge abutments under ice-cover, *Canadian Journal of Civil Engineering*, cjce-2013-0552, published on line 2014-09-09. (Chapter 3.6)

List of Tables

Table 3.1- 1 Experimental running condition summary	34
Table 3.2- 1 Summary of running conditions	54
Table 3.3- 1 Experimental data of small scale flume experiments	70
Table 3.3- 2 Experimental data of small scale flume experiments	72
Table 3.4- 1 Test condition and non-uniform sediment composition of each experiment	87
Table 3.5- 1 The maximum scour depth under different conditions.....	105
Table 5- 1 Experimental data collected at non-uniform sand ($D_{50} = 0.58$ mm)	135
Table 5- 2 Experimental data collected at non-uniform sand ($D_{50} = 0.50$ mm)	136
Table 5- 3 Experimental data collected at non-uniform sand ($D_{50} = 0.47$ mm)	137
Table 5- 4 Scour contours at $D_{50} = 0.58$ mm	138
Table 5- 5 Scour contours at $D_{50} = 0.50$ mm	144
Table 5- 6 Scour contours at $D_{50} = 0.47$ mm	150

List of Figures

Figure 1- 1 A typical local scour around a bridge abutment.....	1
Figure 1- 2 Flow and local scour around a bridge abutment	3
Figure 1- 3 Time evolution of clear-water scour and live-bed scour.....	5
Figure 1- 4 Comparison of velocity and suspended sediment concentration distributions between	9
Figure 1- 5 The velocity distribution of open water, floating smooth and floating rough cover..	11
Figure 1- 6 Bridge abutment (BA) types used in experiments	13
Figure 2- 1 Schematic of force on particle on a sloping bed under ice cover.....	21
Figure 2- 2 The modification plan for the flume at QRRC.....	24
Figure 2- 3 The modification of flume at QRRC.....	25
Figure 2- 4 The dimension of ADV (left) and the sensor head of a ADV (right)	26
Figure 2- 5 Related parameters and Experimental procedure (BA: bridge abutment)	28
Figure 3.1- 1 Dimensions of abutment, ice cover and rough ice cover used in the experiment ...	32
Figure 3.1- 2 Measuring points along the semi-circular abutment	33
Figure 3.1- 3 The local scour around the abutment and the measurement of the scour	34
Figure 3.1- 4 The scour profiles around the abutment under different cover conditions ($D_{50}=0.50\text{mm}$).....	36
Figure 3.1- 5 (a) Cross-section along the semi-circular abutment ($D_{50}=0.50\text{mm}$); (b) Cross- section along the semi-circular abutment under smooth and rough cover ($D_{50}=0.50\text{mm}$).....	39
Figure 3.1- 6 Variation of scour volume around bridge abutment	40
Figure 3.1- 7 (a) Variation of maximum scour depth with the Froude number under different sediment composition (b) The comparison of maximum scour depth in open channel and ice covered condition ($D_{50}=0.50\text{mm}$)	42
Figure 3.1- 8 Dependence of maximum scour depth on related variables.....	43
Figure 3.1- 9 Dependence of maximum scour depth on related variables under ice cover	45
Figure 3.2- 1 (a) The plan and vertical view of the modified flume; (b) The coordinate system and abutments dimensions	52
Figure 3.2- 2 (a) Inside view of the flume; (b) Rough ice cover used in the research.....	53
Figure 3.2- 3 Typical local scour profiles around the square abutment and semicircular abutment	57
Figure 3.2- 4 The variation of maximum scour depth with abutment model	58
Figure 3.2- 5 The variation of D_{50} with scour depth under different conditions	60
Figure 3.2- 6 The variation of maximum scour depth with different sediments and abutments ..	61
Figure 3.2- 7 The variation of maximum scour depth with different covered conditions	63
Figure 3.3- 1 A comparison of flow profiles with (a) and without (b) ice cover.....	68
Figure 3.3- 2 The experimental setup of the small scale flume (left) and large scale flume (right)	69
Figure 3.3- 3 (a) The local scour around the bridge abutment in the small-scale flume and	74
Figure 3.3- 4 The scour contour in the large scale flume	76

Figure 3.3- 5 The sediment samples L1 (left) and L2 (right)	76
Figure 3.3- 6 The cross section of the local scour along the abutment (left) and samples collected (right)	77
Figure 3.3- 7 The sand analysis of samples	77
Figure 3.3- 8 The variation of scour depth with densimetric Froude number in small-scale flume	78
Figure 3.3- 9 The variation of scour depth under smooth ice cover in large scale flume.....	79
Figure 3.4- 1 The layout of the experimental large scale flume	85
Figure 3.4- 2 Dimensions and measuring points of abutments.....	85
Figure 3.4- 3 Experimental flume set up and rough ice cover (up); Armor layer around the square abutment corner (bottom)	86
Figure 3.4- 4 Typical local scour contour around square abutment (left) and semi-circular abutment (right)	89
Figure 3.4- 5 Distribution curves for the non-uniform sediment.....	91
Figure 3.4- 6 Samples of armor layer, fine sediment ridge and related distribution curves.....	92
Figure 3.4- 7 Variation of maximum scour depth with F_o at square abutment (left) and semi-circular abutment (right)	94
Figure 3.4- 8 Variation of maximum scour depth with related variable around square abutment.....	94
Figure 3.4- 9 Variation of maximum scour depth with related variable around semi-circular abutment.....	95
Figure 3.4- 10 Dependence of maximum scour depth on related variables around square abutment.....	95
Figure 3.4- 11 Dependence of maximum scour depth on related variables around the semi-circular abutment	96
Figure 3.4- 12 The impact of ice cover roughness on the maximum scour depth.....	98
Figure 3.4- 13 Regression relationship under ice cover of related variables around square abutment.....	99
Figure 3.4- 14 Regression relationship under ice cover of related variables around semi-circular abutment.....	99
Figure 3.5- 1 Experimental setup.....	104
Figure 3.5- 2 Abutment dimension and coordinate system.	107
Figure 3.5- 3 Contours of scour hole under open channel, smooth cover, and rough cover	109
Figure 3.5- 4 The scour profile along the round abutment under different conditions.....	111
Figure 3.5- 5 The velocity distribution along the abutment under different conditions: open channel (Left), smooth cover (Middle), rough cover (right)	116
Figure 3.6- 1 Sketch of experimental setup and abutment dimension.....	121
Figure 3.6- 2 Incipient motion in the scour hole under ice cover	122
Figure 3.6- 3 Incipient motion of different sediments with the maximum scour depth	125
Figure 3.6- 4 The variation of shear Reynolds number with dimensionless shear stress	127

Figure 3.6- 5 The maximum scour depth variation with dimensionless shear stress around square abutment..... 128

Figure 3.6- 6 The maximum scour depth variation with dimensionless shear stress under ice cover and open channel (square abutment)..... 128

Figure 3.6- 7 The maximum scour depth variation with dimensionless shear stress under smooth ice cover and rough ice cover (semi-circular abutment)..... 129

ACKNOWLEDGEMENT

I would like to express my first thanks to my supervisor, Dr. Jueyi Sui, who has been, and still is helpful and supportive through my entire PhD. His advice on experimental design, writing and data analysis is always helpful. Discussions about my research, but also on the academic research in general, has been really inspiring. I had a great time working with Dr. Sui and lots of ideas for my future research are based on the conversations between us.

During my three years PhD at University of Northern British Columbia, I spent a lot time in the field and received great help from my colleagues and friends. I would like to thank Faye Hirshfield for being my most reliable and helpful colleague and friend, who spend almost two entire field seasons with me from 2011 to 2012, even when it was pouring rain or one meter snow. Anja Forster has been the best field assistant for flume construction in 2011. The work cannot be finished without her help.

I would like to thank my committee members Dr. Jianbing Li, Dr. Liang Chen, Dr. Youmin Tang, Dr. Junjie Gu for their time and support through the last few years. They brought a lot to my thesis, especially by widening my view beyond my research area.

I would also express my thanks to Dr. Ellen Petticrew, Dr. Phil Owens, Dr. Neil Hanlon, Dr. Phil Burton, Dr. Joselito Arocena as my course supervisors in my first year of PhD. Integrating my own research within a wide spectrum of knowledge, and sharing it with people from different fields make me becoming more interested in environmental issues.

I would also like to thank the Institutions that supported my research. The University of Northern British Columbia is really welcoming and supportive of foreign students. The Research Project Awards funding helped a lot during my hard time. The Dr. Max Blouw Quesnel River Research Center, which is the base of my research, has the best manager and staff. Richard Holmes and Samuel Albers provided great help as managers of the research center. Lazlo Enyedy and Howard helped me a lot to finish the flume construction and experiments. I had the best life and work experience in Likely. Friends and people in Likely are greatly acknowledged.

More on the personal side of my life, I would like to say a big thank you to my parents. Also special thanks to Mr. and Mrs. Hirshfield. They always showed support and interest in my work even if it was hard to follow. Being overseas and far from home, I made myself at home in Price George. I want to thank all the cool and wonderful friend I met there and who make my 3-year experience in Prince George so pleasant. My PhD friends, Alex Koiter, Steffi LaZerte, Adrian James, Dominic Reiffarth, Lisha Berzins, Yueting Shao et al. have been the best classmates ever. I would extend my thanks to Heidi, Leah, Ben, Dr. Youqin Wang, Guangji Hu, Lin Bai, Bo Huang for their friendship, encouragement and belief.

1 GENERAL INTRODUCTION

Scour is a natural phenomenon caused by erosion on alluvial or gravel beds by a flowing stream. Local scour refers to the scour caused by an obstruction in the channel (Chang, 2002). Local scour around bridge foundation elements is one of the most common reasons for bridge collapse and has caused huge economic loss around the world (Figure 1-1). For example, in 1987, 17 bridges were destroyed by scour during a flood in New York and New England. During the flooding in Georgia in 1994 over 500 bridges were damaged due to the scour (Richardson and Davis, 2001). According to a nation-wide study conducted by the US Federal Highway Administration, 75% of 383 bridge failures in 1973 involved abutment damage and 25% involved pier damage (Chang, 1973). In 1978, another extensive study indicated that problems caused by local scour at bridge abutments were equal to that at bridge piers (Brice and Blodgett, 1978). Bridge scour has been identified as the most common cause of highway bridge failures and it accounts for about 60% of all bridge collapse in the United States (Deng and Cai, 2009). A study by Kandasamy and Melville (1998) showed that 6 of 10 bridge failures which occurred in New Zealand during Cyclone Bola were related to abutment scour. In China, local scour damaged 49 railway bridges in 1994, resulting in an interruption of railway traffic for 2319 hours (Zhu and Liu, 2012).



Figure 1- 1 A typical local scour around a bridge abutment

It is noted that local scour around bridge foundations has negative impacts on the performance and stability of bridges. In the past few decades, local scour around bridge abutments in open channels has received wide attention, and many scholars have conducted numerous studies on this topic (e.g. Laursen and Toch, 1956; Froehlich, 1989; Melville, 1997; Coleman et al, 2003; Dey 2005a, 2005b). To estimate the maximum scour depth, many relationships and formulae have been developed which can be grouped into four categories: regime approach, dimensional analysis, analytical or semi-analytical approach, and probabilistic approach (Zhang, et al, 2008). In Canada, ice cover can stay up to six months in some northern areas. The formation of ice cover involves complex interactions between hydrodynamic, mechanical, and thermal process (Shen, 2010). Ice cover can result in many problems, such as ice jamming, flooding, restricting the generation of hydro-power, block river navigation and affect the ecosystem balance. (Hicks, 2009). However, to my present knowledge, there is still very little research on the local scour under ice cover.

Field observations indicate that ice cover significantly affects velocity distribution and sediment transport processes in rivers. An imposed ice cover can lead to an increased composite resistance and almost double the wetted perimeter. Understanding river ice process and ice effects on hydraulic structures is important for the design and operation of hydraulic projects. To examine the influence of ice cover on local scour around bridge abutments, the present research is conducted. In the present research, ice cover plays an important variable for the estimation of scour depth around abutments. Compared to an open channel, ice cover changes the hydraulics by adding an extra boundary. Due to the limitations of laboratory study and lack of field data, the flow field in the scour hole is still not clear. The main objectives in this research are to investigate, the local scour development, equilibrium depth estimation, bed evolution, velocity distribution, sediment transport rate and numerical model verification under various ice cover conditions.

1.1 Literature review

1.1.1 Local Scour characteristics around bridge abutments in open channels

The scour occurring around bridge abutments can be grouped into three categories: general scour, constriction scour, and local scour. General scour is the removal of sediment from the bottom of a river channel by the flow of the river. While constriction scour is the removal of sediment from the bottom and sides of the river channel, due to the higher velocity caused by hydraulic structures such as a bridge. Local scour is caused by an acceleration of flow in the vicinity of structures, which may happen around bridge piers, abutments, or other objects that obstruct the flow in different ways (Chang, 2002). Local scour is a dynamic feedback process between turbulent flow and erodible boundaries. The vortex systems and the down flow have high turbulence which is the main cause of local scour. Compared to general scour and constriction scour, local scour can cause serious damage to bridges. So in the following passage, the process of local scour around bridge abutments will be the main interest.

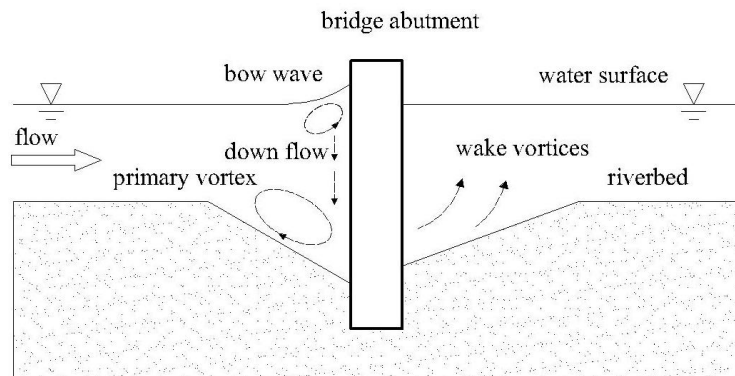


Figure 1- 2 Flow and local scour around a bridge abutment

The flow field around a bridge abutment in natural open rivers is very complex. Moreover, the complexity increases with the development of a scour hole which leads to separation of flow into three vortex flow systems around the abutment. Figure 1-2 shows a schematic diagram of the flow field and scour hole around an abutment. Kwan and Melville (1994) suggested that the scour hole is mainly dominated by a large primary vortex and associated down flow. The primary vortex extends to the downstream of the abutment and loses its identity after some

distance. Near the water surface a vertical pressure gradient is developed due to the stagnation of the approaching flow. At the corner of abutment downstream, the flow accelerates and leads to the development of concentrated vortices, referred to as wake vortices. Wake vortices are created due to the separation of flow upstream and downstream of the abutment corners (Zhang, 2005). Under open channel condition, the flow patterns and maximum down-flow are relatively unaffected by changes in approach flow depth (Kwan and Melville, 1994). Under ice covered conditions, flow fields around the bridge abutments will be significantly changed. This hypothesis will be verified by the experimental study.

Based on whether there is sediment transported by the approaching flow, local scour can be classified into two categories: clear-water scour and live-bed scour (Chabert and Engeldinger, 1956). Clear-water scour takes place in the absence of sediment transport by approaching flow into the scour hole. Live-bed scour occurs when the scour hole is continuously fed with sediment from upstream. The time variation of the clear-water scour and live-bed scour is shown schematically in Figure 1-3. Chabert and Engeldinger (1956) observed that the equilibrium clear-water scour depth is 10% greater than live bed scour depth.

The clear-water scour and live-bed scour are determined by the critical velocity (V_C). The clear-water scour can occur when $V/V_C < 1$, while the live-bed scour will happen if $V/V_C > 1$, in which V is average flow velocity and V_C is the critical flow velocity for sediments. There are many formulae used to decide the value of V_C . In this thesis, the equation from Laursen (1963) will be used for non-uniform sediments,

$$V_C = K_u y_1^{1/6} D_{50}^{1/3} \quad (1-1)$$

in which, y_1 is average flow depth in the main channel or overbank area at the approach section; D_{50} is bed material particle size in a mixture in which 50% percent are smaller; K_u equals to 6.19 (S.I. Units).

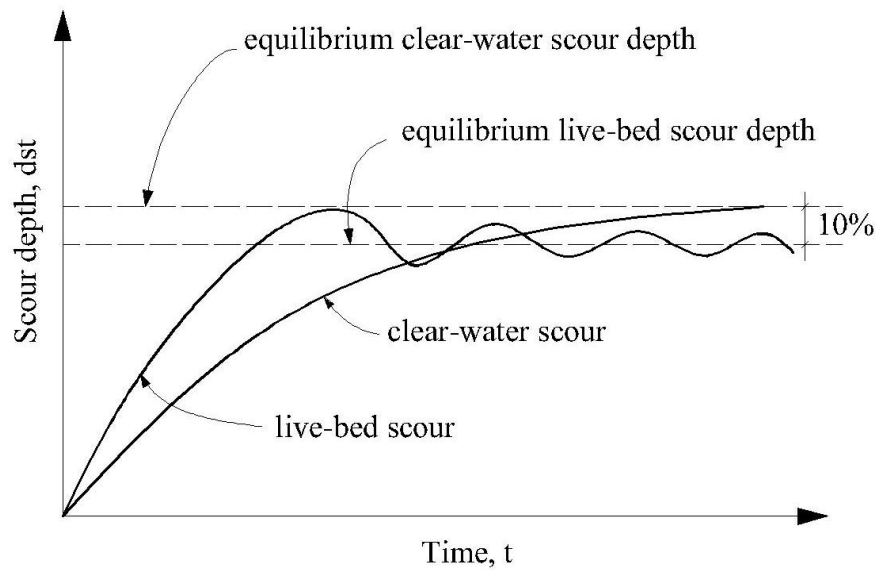


Figure 1- 3 Time evolution of clear-water scour and live-bed scour
(After Chabert and Engeldinger, 1956)

Studies on the local scour around bridge elements in open channels has been widely done in the past few decades and are still of continuous interest for scholars. These studies can be grouped into two categories (Zhang, 2005). One is the prediction of scour depth by using empirical or semi-empirical formulae based on field data or experimental data. The other is numerical simulation. There are basically three types of scour depth estimation formulae from the literature (Lim, 1997): a. the regime approach, which relates the scour depth to the increased discharge or flow at the abutment; b. the dimensional analysis, where relevant dimensionless parameters describing the scour are correlated (most of the past formulas are obtained from this way); c. analytical or semi-empirical approach, which are based sediment transport relationships between approach flow and shear stress around the abutment. A large amount of scour formulae are available in the published literature. However, most of these formulae were derived from limited variables related to the scour development (Barbhuiya and Dey, 2004):

- (a) Variables related to the approaching flow (flow depth, mean velocity, roughness, etc);
- (b) Variables related to bed sediment (grain size distribution, density, cohesiveness, etc);
- (c) Variables related to the flow (water density, dynamic viscosity, gravitational acceleration);
- (d) Variables related to the abutment and channel (abutment size and shape, channel width).

From the 1950s to 1980s, different forms of empirical formulae were presented from earlier studies (e.g. Laursen and Toch, 1956; Laursen, 1963; Shen et al, 1969; Raudkivi and Ettema, 1983). From the 1990s to 2000s was the prosperous development period for scour research, during which many experimental studies were conducted and many formulae were derived. Some of the representative studies include Melville, 1997; Lim and Cheng, 1998; Ettema et al, 1998; Kuhnle et al, 2002; Coleman et al, 2003. A comprehensive review of the investigations on local scour formulae can be found in Melville (1997) and Barbhuiya and Dey (2004). Johnson (1995) compared 7 commonly used and cited formulae with a large set of field data for both clear-water scour and live-bed scour. The results of this study pointed out the necessity for further data collection and experimental research.

For Hydraulic Engineering applications, the concept of equilibrium scour depth in bridge hydraulics is essential for scour prediction. Three of the commonly used formulae for predicting scour depth at abutments for open channels (Laursen, 1963; Melville 1992 and Lim, 1997) are briefly reviewed in the following passage.

1. The Laursen's relationship (Laursen, 1963) was based on scour in a long contraction. For abutments that do not extend over the overbank region into the river channel, Laursen gave the following equation:

$$\frac{L}{y} = 2.75 \left(\frac{d_s}{y} \right) \left[\left(\frac{d_s}{r \cdot y} + 1 \right)^{7/6} - 1 \right] \quad (1-2)$$

In which,

L : the length of abutment

r : the ratio of scour at the abutment to scour in a long contraction.

y : the approach flow depth.

With $r=12$ and using the binomial approximation, the equation can be simplified to:

$$d_s \approx 1.93 (yL)^{0.5} \quad (1-3)$$

2. As defined by Melville and Coleman (2000), the functional relationship between scour depth and other dependent parameters is:

$$d_s = f [\text{flow, bed sediment, bridge geometry, time}]$$

By using dimensional analysis method, Melville (1995, 1997) studied the development of local scour at bridge abutments and developed an equation to estimate the maximum scour depth

under clear water conditions. By plotting many published data of local scour depth d_s at bridge abutment sites and using his own experimental data collected at the University of Auckland, Melville (1997) proposed the following scour prediction equation:

$$\begin{aligned} \frac{d_s}{L} &= 2K_l K_d K_\sigma K_s K_\theta K_G, \quad \frac{L}{y} \leq 1 \\ \frac{d_s}{\sqrt{Ly}} &= 2K_l K_d K_\sigma K_s^* K_\theta^* K_G, \quad 1 < \frac{L}{y} < 25 \\ \frac{d_s}{y} &= 10K_l K_d K_\sigma K_s K_\theta K_G, \quad \frac{L}{y} \geq 25 \end{aligned} \quad (1-4)$$

In which,

d_s : equilibrium local scour depth;

L : abutment length; y : approach flow depth;

K_l : scour depth of flow intensity; K_d : sediment size; K_σ : sediment gradation;

K_s : abutment shape (with values 1 for the vertical wall abutment, 0.75 for 45° wing wall abutment, and 0.5 for 1:1 sloping spill-through abutments);

K_θ : abutment orientation;

K_G : channel geometry;

K_s^* , K_θ^* : adjusted values of K_s and K_θ ;

K_s , K_θ and K_l are all defined through experimental data in Melville's study.

For a vertical wall abutment, under the condition of $1 < L/y < 25$, the formula can be written as $d_s = 2(yL)^{0.5}$, which is close to Laursen's equation.

3. Based on the continuity equation, scour geometry, and a generalized form of the power law formula for flow resistance in an alluvial channel, Lim (1997) proposed an equation for estimation of the maximum equilibrium scour depth. For vertical wall abutments, the scour depth can be simplified to:

$d_s = 1.8(yL)^{0.5}$, which is in close agreement with the formulae derived by Melville (1997) and Laursen (1963).

Currently, even the open channel scour depth estimation is not a standard design because of a lack of reliable data (Hoffmans and Venhij, 1997). According to Melville (1997), “existing design methods...are adequate for prediction of scour depth at abutments sited in channels that can be approximated by a rectangular shape”. For the scour in natural rivers, the formulae mentioned here involve strong empiricism and introduce many uncertainties.

1.1.2 Ice Covered issues on local scour

In northern Canada, many rivers become ice covered in winter. The presence of ice cover causes changes in the properties of the flow such as: velocity profile, bed shear stress distribution, mixing properties, and sediment transport (Lau and Krishnappan, 1985). The riverbed evolution process will be significantly changed compared to that observed in open channels (Sui et al., 2010b). To my knowledge, the literature on the scour under ice cover is still limited (Krishnappan, 1984; Lau and Krishnappan, 1985; Tsai and Ettema, 1994; Beltaos, 1998; Ettema et al, 2000; Wang et al, 2008; Sui et al. 2010b). In the following passage, a brief literature review will be provided on the velocity distribution and sediment transport under ice cover.

Lau and Krishnappan (1981) used the $k-\epsilon$ model to calculate the velocity distribution by using different boundary roughness. Lau and Krishnappan (1985) proposed a method to calculate sediment transport by using $k-\epsilon$ model in covered flows. Under ice covered flows, they found that the reduction in the bed shear stress had very significant effects on the sediment transport. From a series of experiments, it was found that the top ice cover can cause an increase in depth, decrease in average velocity and diffusivity distributions (Figure 1-4). However, the bed shear stress and the eddy viscosity are both smaller than that corresponding free-surface flow values (Krishnappan, 1984).

Ettema et al. (2000) reviewed methods of estimating of sediment transport in ice covered channels and proposed a method to estimate the sediment transport rate by using the parameters acquired from open channels. Wang et al. (2008) conducted an experimental study on the incipient motion of sediment under ice cover and discussed the role of flow velocity and critical shear Reynolds number in this process. Sui et al. (2010b) compared the velocity profile under different flow and boundary conditions. He found that lower critical dimensionless shear stress for incipient motion was needed if the sediment size is smaller. Moreover, the velocity profile

under ice cover is completely different compared to the velocity profile in open channels. The flow in the upper layer is primarily affected by ice cover resistance, whereas the lower portion of the flow is influenced by the channel bed resistance (Sui et al, 2010b).

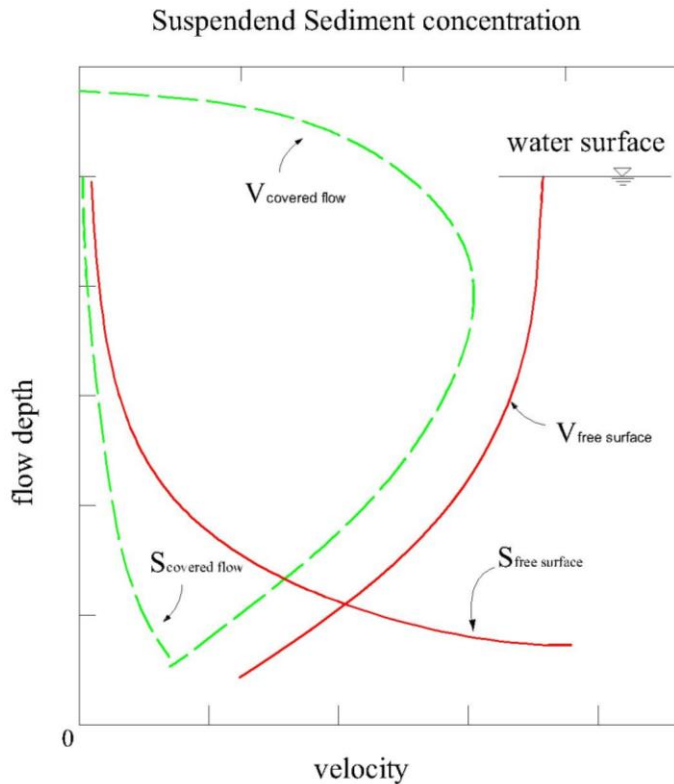


Figure 1- 4 Comparison of velocity and suspended sediment concentration distributions between covered flow and free surface flow (S: sediment transport rate; V: velocity profile. Adapted from Lau et al, 1985)

As mentioned in section 1.1, the local scour can be separated to clear-water scour and live-bed scour. Since it is difficult to measure and track sediments transported from approaching flow, in this research, the clear water scour will be the focus.

In natural rivers, when the flow condition satisfies or exceeds the criteria for incipient motion, sediment particles will start to move. Depending on the size of the bed-material particles and flow conditions, if the motion of the particle is rolling, sliding or sometimes jumping along the bed, it is called bed load transport. If the motion of the particle is supported by the upward components of turbulent currents and remained in suspension for a distance, it is called suspended load transport. Total load is the sum of bed load and suspended load. In most natural

rivers, sediments are mainly transported as suspended load, while the bed load transport rate is about 5-25% of that in suspension (Yang, 2003). In this research, both bed load and suspended load transport rates will be considered.

According to Bagnold (1966), the motion of the bed load particles is assumed to be dominated by gravitational forces, while the effect of turbulence on the overall trajectory of bed load is supposed to be of minor importance. Based on this assumption, van Rijn (1984a) presented a method which enables the computation of the bed load transport rate (q_b) as the product of the saltation height (jumping height, δ_b), the particle velocity (u_b) and bed load concentration (c_b):

$$q_b = u_b \delta_b c_b \quad (1-5)$$

For suspended load, van Rijn (1984b) computed it as the depth integration of the local concentration and flow velocity. The particle fall velocity and sediment diffusion coefficient were studied in detail as the main controlling hydraulic parameters. The proposed relationships for the suspended load transport were also verified by using a large amount of flume data. However, for sediment transport under ice cover, the quality and quantity of data are still limited. Ettema and Daly (2004) reviewed the impacts of river ice on sediment transport. Dimensional analysis of variables associated with flow was used. Sediment transport under ice cover was described in terms of key non-dimensional parameters characterizing the dynamics of flow and sediment interaction. The ice cover can influence water drag on the bed, redistribute flow to generate turbulence, and reduce the rate of flow energy expended along the bed.

Currently, there are two main methods to estimate flow resistance under ice cover in alluvial channels. The first one is to assume that the bed resistance coefficients do not change with ice cover, for example, Manning, Chezy, or Darcy-Weisbach coefficients. The second one is the flow resistance behavior of the bed can be determined by an ice cover flow as a composite of two non-interacting flow layers, with the lower layer of flow affecting the bed topography. Lau and Krishnappan (1985) simulated the sediment transport under ice cover by assuming that the lower layer in a covered flow can be treated as a free surface flow. The top ice cover causes an increase in depth and decrease in average velocity and diffusivity distributions.

The shear stress is also used to characterize the channel scour, which is directly used to quantify resistance to motion. Hains (2004) used the shear stress analysis in experiments with smooth cover and rough ice cover. The results showed that increased shear stresses on the bed will increase bed erosion and scour depth. Hains and Zabilansky (2005) conducted a series of

experiments to establish the sensitivity of various parameters affecting sediment transport processes under ice cover. In their research, approaching flow velocities were selected primarily on clear water scour under both smooth and rough simulated ice covers. Open channel, floating cover and fixed cover experiments were presented. By revising the scour model of Melville and Coleman (2000), two extra parameters were included in the equation: k_{cover} and L_c . The Melville's equation was then modified as:

$$d_s = f [\text{flow, bed sediment, abutment geometry, time, cover } (k_{cover}, L_c)]$$

In which,

L_c = the length of ice cover. k_{cover} = the ice cover factor (roughness, wetted perimeter)

For a floating smooth cover, the velocity profile is gradual, with the maximum velocity approximately at mid-depth. For a floating rough cover, the maximum velocity is also mid-depth but is greater in value than the smooth ice profile (Figure 1-5).

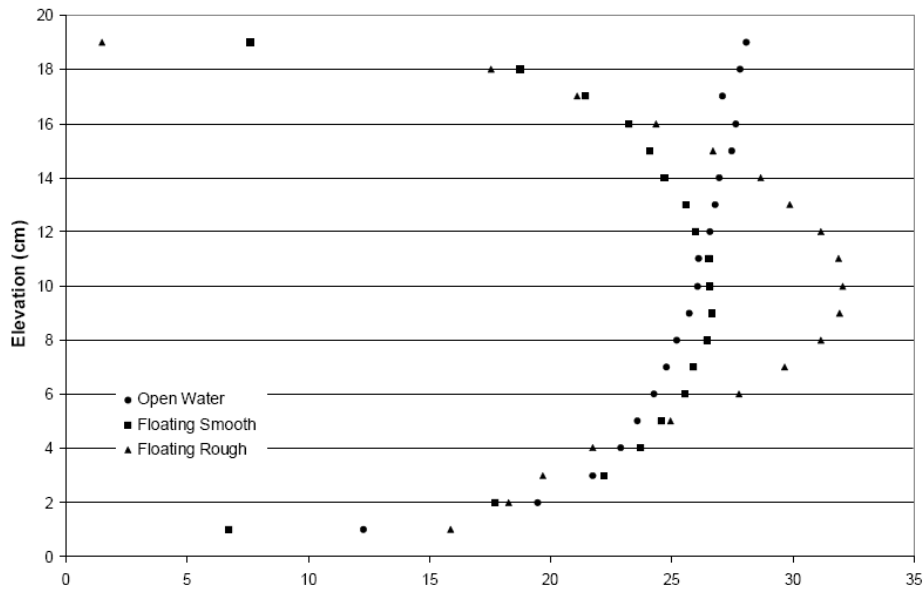


Figure 1- 5 The velocity distribution of open water, floating smooth and floating rough cover
(After Hains and Zabilansky, 2005)

There are also experiments on the local scour under ice cover by using different laboratorial flumes (Ettema, 2000; Wang et al. 2008; Sui et al. 2010b). While most of these studies focus on the velocity distribution, the sediment transport under ice cover is not quantitatively analyzed, which restricts further study of the local scour under ice cover. Only two studies on the

experimental study of local scour around bridge foundations under ice cover can be found (Ackermann et al. 2002; Munteanu and Frenette, 2010). For a better understanding of this phenomenon, more experiments need to be conducted for collecting data and also for the calibration of numerical models in the future.

1.2 Research objectives

Compared to the research of local scour in open channels, the local scour study under covered conditions is very limited. Only a few papers can be found in the literature. For numerical simulation, there is still very limited mathematical model available that can be used in the present research. My study aims at contributing to the understanding of local scour under ice cover and modeling of flow and sediment movement around bridge abutments. The main objectives of this study are listed as follows.

1.2.1 Objective One

The impact of velocity, flow depth and sediment composition

From previous studies, the velocity distribution under ice cover is different to that in open channels. The effect of approaching velocity is incorporated in the scour predicting formulae in the form of flow Froude number or shear velocity (Froehlich, 1989; Kandasamy, 1989). For the bridge abutment scour, Melville (1992) suggested flow depth has different impacts on short abutments ($l/h \geq 1$) and long abutments ($l/h \geq 25$). Characteristics of sediment composition are commonly used in scour depth formulae. Derived from the particle size distribution curves, median sediment diameter d_{50} and geometric standard deviation σ_g ($\sigma_g = (d_{84}/d_{16})^{0.5}$) are the two most widely used sediment parameters in the study of local scour. Dey and Barbhuiya (2004) indicated that for non-uniform sediments, due to the formation of armor-layers in the scour hole, the scour depth is reduced significantly in open channels. Under ice cover, the impacts of different approaching velocity, flow depth and sediment composition on scour hole development are still not clear.

In the experimental study, by changing different approaching velocities, flow depths and sediment compositions, the real-time and maximum scour depth will be measured under ice cover.

1.2.2 Objective Two

Scour development around different types of abutments

Melville (1992, 1997) presented results of laboratory investigations of local scour at bridge abutments and piers in open channels. In the scour depth formulae, Melville used shape factors K_s to account the effect of the shape of abutments on equilibrium scour depth estimation. Semi-circular can produce vortices of feeble strength, while vertical abutment, which is similar to spur-dikes, can produce strong turbulent vortices. A relatively large scour depth is observed around vertical abutments (Barbhuiya and Dey, 2004). In the study, a vertical wall abutment and a semi-circular abutment model will be made to study the shape parameter on local scour. The dimension of the abutment is shown in Figure 1-6.

For the scour under ice cover, different shapes of abutments are still not systematically studied. The value of shape factor in the scour depth formulae has not yet been determined.

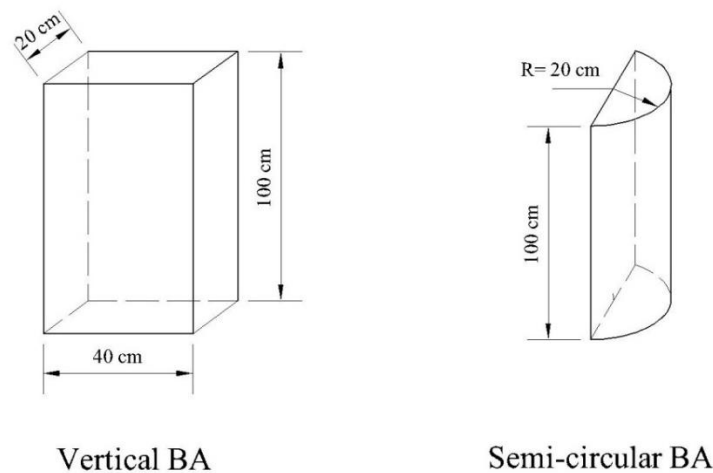


Figure 1- 6 Bridge abutment (BA) types used in experiments

1.2.3 Objective Three

Dimensional analysis of variables for the scour depth including ice cover

Using the Buckingham π theorem, various formulae have been brought up by combining different parameters that affect the scour depth, such as abutment shape, approaching flow, fluid and sediment characteristics, channel geometry, and time. However, none of these formulae has ever incorporated ice cover as a parameter. By using dimensional analysis and data collected from experiments, a relationship between ice cover and other variables will be derived.

1.3 Research innovations

The experimental and numerical research are focused on the local scour around bridge abutment under ice cover conditions. The study has the following innovations:

1. The whole process of local scour around bridge abutment under ice covered conditions will be simulated by a series of large scale flume experiments;
2. The local scour process under different flow conditions, namely, open channel, smooth, rough will be compared;
3. Through Dimensional Analysis, empirical formula to estimate the scour depth under ice covers will be derived.

1.4 Outline of dissertation

The dissertation focuses on the analysis of data from experimental study. Chapter 2 is the methodology and experimental set up. Chapter 3 is the data analysis and discussion, which is separated into several parts. Each section discuss one aspect of ice cover impacts on local scour around bridge abutment. Chapter 3.1 is the analysis of ice cover impacts around the semi-circular abutment. Chapter 3.2 compares both square and semi-circular abutment under ice cover and open channel conditions. In this section, the shape factor of abutment is introduced. By comparing a small scale flume experiments, Chapter 3.3 is introduced to show the impacts of ice cover and non-uniform sediment. The large scale flume experiments shows interestingly different comparing to that from small scale flume experiments. Chapter 3.4 focuses on the analysis of armor layer analysis around abutments. Since the sediments used in the present research are non-uniform, a clear armor layer is noticed around abutments. By including armor layer sediment size, the maximum scour depth is discussed. Empirical equations are also developed. Chapter 3.5 is used to show the analysis of ADV measurements from the experiments. Finally, Chapter 3.6 shows the theory analysis of incipient motion under ice cover. The dimensionless shear stress is calculated and compared.

References

1. Acharya A, (2011). Experimental study and numerical simulation of flow and sediment transport around a series of spur dikes, PhD Dissertation. The University of Arizona, pp: 36.
2. Ackermann N L, Shen H T, Olsson P, (2002). Local scour around circular piers under ice covers. Proceeding of the 16th IAHR International Symposium on Ice, International Association of Hydraulic Engineering Research, Dunedin, New Zealand.
3. Ali K H M, Karim O A, Connor B A, (1997). Flow patterns around bridge piers and offshore structures. ASCE, Water Resources Engineering Conference, 208-213.
4. Bagnold R A, (1966). An approach to the sediment transport problem from general physics. Physiographic and Hydraulic Studies of rivers, Geological survey professional paper, 422-1, Washington.
5. Barbhuiya A K, Dey S, (2004). Local scour at abutments: a review. Proceedings of the Indian Academy of Sciences, Sadhana, October 29, 449-476.
6. Beltaos S, (1998). Logitudianl dispersion in ice covered rivers. Journal of Cold Regions Engineering, ASCE, 12(4): 184-201.
7. Biron P M, Robson C, Lapointe M F, Gaskin S J, (2004). Comparing different methods of bed shear stress estimates in simple and complex flow fields. Earth Surface Processes and Landforms, 29:1403-1415.
8. Brice J C, Blodgett J C, (1978). Countermeasures for hydraulic problems at Bridges. Vol. 1 and 2, FHWA/RD-78-162&163, Federal Highway Administration, US Department of Transportation, Washington D C, US.
9. Chang F F M, (1973). A statistical summary of the cause and cost of bridge failures. Office of Research, Federal Highway Administration, Washington D C, US.
10. Chang H H, Reprint edition (2002). Fluvial process in river engineering. Krieger Publish Company, Malabar, Florida, 80-103.
11. Charbert J, Engeldinger P, (1956). Etude des affouillementsautour des piles de points. Series A, Laboratory National d'Hydraulique. Chatou, France (in French).
12. Chiew Y M, (1995). Mechanics of riprap failure at bridge piers. Journal of Hydraulic Engineering, ASCE, 121 (9): 635-643.
13. Coleman S E, Lauchlan C S, Melville B W, (2003). Clear water scour development at bridge abutments, Journal of Hydraulic Research, 41(5): 521–531.

14. Deng L, Cai C S, (2009). Bridge scour: prediction, modeling, monitoring, and countermeasures-Review. *Practice Periodical on Structural Design and Construction*, 15(2):125-134.
15. Dey S, Barbhuiya A K, (2004). Clear water scour at abutments in thinly armored beds. *Journal of Hydraulic Engineering*, ASCE, 130:622-634.
16. Dey S, Bose S K, Sastry G L N, (1995). Clear water scour at circular piers: a model. *Journal of Hydraulic Engineering*, 121(12):869-876.
17. Dey S, Barbhuiya A K, (2005a). Time variation of scour at abutments, *Journal of Hydraulic Engineering*, ASCE, 131 (1): 11-23.
18. Dey, S, (2005b). Reynolds stress and bed shear in non-uniform-unsteady open channel flow, *Journal of Hydraulic Engineering*, ASCE, 131 (7): 610-614.
19. Dou X, (1980). The stochastic theory and the general law of all flow regions for turbulent open channel flows. *Proc., 1st Int. Symp. on River Sedimentation*, Beijing.
20. Duan J G, He L, Fu X, Wang G, (2009). Mean flow and turbulence around an experimental spur dike. *Advances in Water Resources*. 32: 1717-1725.
21. Ettema R, Braileanu F and Muste M, (2000). Method for estimating sediment transport in ice-covered channels. *Journal of Cold Regions Engineering*, ASCE, 14(3): 130-144.
22. Ettema R, Daly S F, (2004). Sediment transport under ice. *Cold regions research and engineering laboratory*. ERDC/CRREL TR-04-20.
23. Ettema R, Mostafa E A, Melville B W, Yassin A A, (1998). Local scour at skewed piers. *Journal of Hydraulic Engineering*, ASCE, 124 (7): 756-759.
24. Froehlich D C, (1989). Local scour at bridge abutments. *Proc. Natl. Conf. Hydraulic Engineering*, ASCE, pp 13-18.
25. Grimaldi C, Gaudio R, Calomino F, Cardoso A H, (2009). Control of scour at bridge piers by a downstream bed sill, *Journal of Hydraulic Engineering*, ASCE, 135(1): 13-21.
26. Hains D B, (2004). An experimental study of ice effects on scour at bridge piers. PhD Dissertation, Lehigh University, Bethlehem, PA.
27. Hains D B, Zabilansky L, (2005). The effects of river ice on scour and sediment transport, CGU HS committee on river ice process and the environment, 13th workshop on the hydraulic of ice covered rivers, Hanover, NH, September 15-16.

28. Hicks F, (2009). An overview of river ice problems: CRIPE 07 guest editorial Cold regions Science and Technology, 55: 175-185.
29. Hoffmans GJCM, VerheijH J, (1997). Scour Manual, A.A.Balkema, Rotterdam.
30. Johnson P A, (1995). Comparison of pier scour equations using filed data. Journal of Hydraulic Engineering, ASCE, 121 (8): 626-629.
31. Kandasamy J K, (1989). Abutment scour, Report No 458. School of Engineering, University of Auckland, New Zealand.
32. Kandasamy J K, Melville B W, (1998). Maximum local scour depth at bridge piers and abutments. J Hydraul. Res. 36:183-197.
33. Krishnappan B G, (1984). Laboratory verification of turbulent flow model, Journal of Hydraulic Engineering, 110(4): 500-513.
34. Kuhnle R A, Alonso C V, Shields F D, (1999). Geometry of scour hole associated with 90° spur dike. Journal of Hydraulic Engineering, ASCE, 125(9): 972-978.
35. Kuhnle R A, Alonso C V, Shields FD, (2002). Local scour associated with angled spur dikes, Journal of Hydraulic Engineering, 128(12):1087-1093.
36. Kuhnle R A, Jia Y, Alonso C V, (2008). Measured and simulated flow near a submerged spur dike. Journal of Hydraulic Engineering, ASCE, 134(7): 916–924.
37. Kwan R T F, Melville, B W, (1994). Local scour and flow measurements at bridge abutments, Journal of Hydraulic Research, 32(5): 661-673.
38. Lau Y L, (1982). Velocity distributions under floating cover. Can. J. Civ. Eng., 9, 76-83.
39. Lau Y L, Krishnappan B G, (1981). Ice cover effects on stream flows and mixing, Journal of the Hydraulic Division, 107(HY10): 1225-1242.
40. Lau Y L, Krishnappan B G, (1985). Sediment transport under ice cover. Journal of Hydraulic Engineering, ASCE, 111(6): 934-950.
41. Laursen E M, (1963). Analysis of relief bridge scour. J. Hydr. Div., ASCE, 89(3): 93-118.
42. Laursen E M, Toch A, (1956). Scour around bridge piers and abutments. Iowa Highway Research Board Bulletin, No 4.
43. Lim S Y, (1997). Equilibrium clear-water scour around an abutment, Journal of Hydraulic Engineering, 123(3): 237-243.
44. Lim S Y, Cheng N S, (1998). Prediction of live bed scour at bridge abutments. Journal of Hydraulic Engineering, ASCE, 124 (6): 635-638.

45. Lee S O, Sturm T, (2008). Scaling issues for laboratory modeling of bridge pier scour. Proceeding of 4th International Conference on Scour and Erosion, Tokyo, Japan, 111-115.
46. Melville B W, (1975). Local scour at bridge sites. Rep. NO. 117. Department of Civil Engineering, School of Engineering, University of Auckland, Auckland, New Zealand.
47. Melville B W, (1992). Local scour at bridge abutments, Journal of Hydraulic Engineering, 118(4): 615-631.
48. Melville B W, (1995). Bridge abutment scour in compound channels, Journal of Hydraulic Engineering, 121(12): 863-868.
49. Melville B W, (1997). Pier and Abutment scour: integrated approach, Journal of Hydraulic Engineering, 123(2): 125-136.
50. Melville B W, Chiew Y M, (1999). Time scale for local scour at bridge piers, Journal of Hydraulic Engineering, 125(1): 59-65.
51. Melville B W, Coleman S E, (2000). Bridge Scour. Water Resources Publications, LLC. Highlands Ranch, Colorado, US.
52. Molinas A, and Wu B, (2001). Transport of sediment in large sand bed rivers, J. of Hydraulic Res., Vol 39, 135-146.
53. Morales R, Ettema R, Barkdoll B, (2008). Large scale flume tests of riprap-apron performance at a bridge abutment on a floodplain. Journal of Hydraulic Engineering, ASCE, 134(6): 800-809.
54. Munteanu A, Frenette R. (2010). Scouring around a cylindrical bridge pier under ice covered flow condition-experimental analysis. R.V. Anderson Associates Ltd,
55. http://www.rvanderson.com/resource/2010_papers/Scouring%20Around%20Bridge%20Piers%20under%20Ice-cover%20Conditions.pdf
56. Raudkivi A J, Ettema R, (1983). Clear water scour at cylindrical piers. Journal of Hydraulic Engineering, ASCE, 109 (3): 338-350.
57. Richardson E V, Davis S R, (2001). Evaluating scour at bridges. HEC18 FHWA NHI-001, Federal Highway Administration, US Department of Transportation, Washington, DC.
58. Shen H T, (2010). Mathematical modeling of river ice processes. Cold Regions Science and Technology, 62:3-13.
59. Shen H W, Schenider V R, Karaki S S, (1969). Local scour around bridge piers. Journal of Hydraulic Division, ASCE, 95 (6): 1919-1940.

60. Sheppard D M, Odeh M, Glasser T, (2004). Large scale clear-water local pier scour experiments. *Journal of Hydraulic Engineering, ASCE*, 130(10): 957-963.
61. Sui J, Afzalimehr H, Sammani A K, Maherani M, (2010a). Clear-water scour around semi-elliptical abutments with armed beds. *International Journal of Sediment Research*, 25(3): 233-245.
62. Sui J, Faruque M, Balachandar R, (2008). Influence of channel width and tailwater depth on local scour caused by square jets, *Journal of Hydro-environment Research*, Vol. 2, pp. 39-45.
63. Sui J, Wang J, He Y, Krol F, (2010b). Velocity profiles and incipient motion of frazil particles under ice cover. *International Journal of Sediment Research*, 25(1): 39-51.
64. Tsai W F, Ettema R, (1994). Ice cover influence on transverse bed slopes in a curved alluvial channel, *Journal of Hydraulic Research*, 32(4): 561-581.
65. van Rijn L C, (1984a). Sediment transport, part 1: Bed load transport. *Journal of Hydraulic Engineering*, 110(10):1431-1456.
66. van Rijn L C, (1984b). Sediment transport, part 2: suspended load transport. *Journal of Hydraulic Engineering*, 110(11):1613-1641.
67. Wang, J, Sui J, Karney B, (2008). Incipient motion of non-cohesive sediment under ice cover – an experimental study. *Journal of Hydrodynamics*, Vol. 20, No. 1, 117-124.
68. Yang C T, (2003). *Sediment Transport, Theory and Practice*. KRIEGER PUBLISHING COMPANY, Malabar, Florida, pp: 90-140.
69. Zhang H, (2005). Study of flow and bed evolution in channels with spur dykes. PhD Dissertation, Ujigawa Hydraulics Laboratory, Kyoto University, Japan.
70. Zhang H, Nakagawa H, (2008). Scour around spur dikes: recent advances and future researches. *Annals of Disas. Prev. Res. Inst., Kyoto Univ.*, No. 51B: 633-652.
71. Zhao M, Cheng L, Zang Z, (2009). Experimental and numerical investigation of local scour around a submerged vertical circular cylinder in steady currents. *Coastal Engineering*, 57: 709-721.
72. Zedel L, Hay A E, (2002). A three component bistatic coherent Doppler velocity profiler: error sensitivity and system accuracy. *IEEE, Journal of Oceanic Engineering*, 27(3): 717-725.

2 METHODOLOGY

The influence of ice cover on local scour is a complex interaction among the ice cover, fluid flow, sediment, bridge abutment, bed geometry and channel geometry. An ice cover approximately doubles the wetted perimeter of the river, which increases the flow resistance. In the present research, two main approaches will be used: experimental method and analytical study. Experimental study will provide original data of the equilibrium scour depth and profile, which can be used for developing the empirical formulae of scour depth under ice cover. The incipient motion is measured and monitored under ice cover. By conducting physical experiments, dimensional analysis can be employed to determine the effect of ice cover on local scour.

2.1 Theoretical analysis

To predict the location and geometry of local scour in the vicinity of hydraulic structures such as a bridge abutment and spur dike, theoretical analysis of the bed shear stress and turbulence properties is necessary.

In open channels, the measured velocity profiles can be used to calculate the following turbulent flow characteristics: mean velocities in three directions, Reynolds stresses and bed shear stress. Bed shear stresses can be calculated by using four methods (Acharya, 2011). In the present study, the turbulent kinetic energy (TKE) method will be used (Biron et al., 2004), which is as follows:

$$\tau = C_1[0.5\rho(u'^2 + v'^2 + w'^2)] \quad (2-1)$$

Here, ρ is the water density, $C_1=0.19$ is a proportionality constant, u' , v' and w' are flow velocity fluctuations in the longitudinal, transverse and vertical directions, respectively.

For the local scour in open channel, a flow resistance calculation leads directly to the estimation of the shear velocity associated with bed surface drag. To estimate the sediment transport rate under ice cover, it is first necessary to estimate flow resistance (or a relationship between flow depth and mean velocity of the flow), and then the flow drag on the bed. To determine the shear velocity for the incipient motion of sediments, the velocity profile under ice cover has to be measured.

Ice cover alters mean flow distribution and flow turbulence characteristics. The flow velocity profile under ice cover can be categorized into an upper portion and lower portion. Divided by

the locus of the point of the maximum velocity, the upper portion of flow is mainly affected by the ice cover and the lower portion of flow is mainly affected by the river bed (Sui et al, 2010b). The forces acting on a sediment particle under ice cover include hydrodynamic drag, the hydrodynamic lift and the submerged weight, as shown in Figure 2-1. The drag force F_D is in the direction of flow and the lift force F_L is normal to the flow. The drag force F_D is associated with the bed shear stress, while the lift force F_L is also associated with F_D .

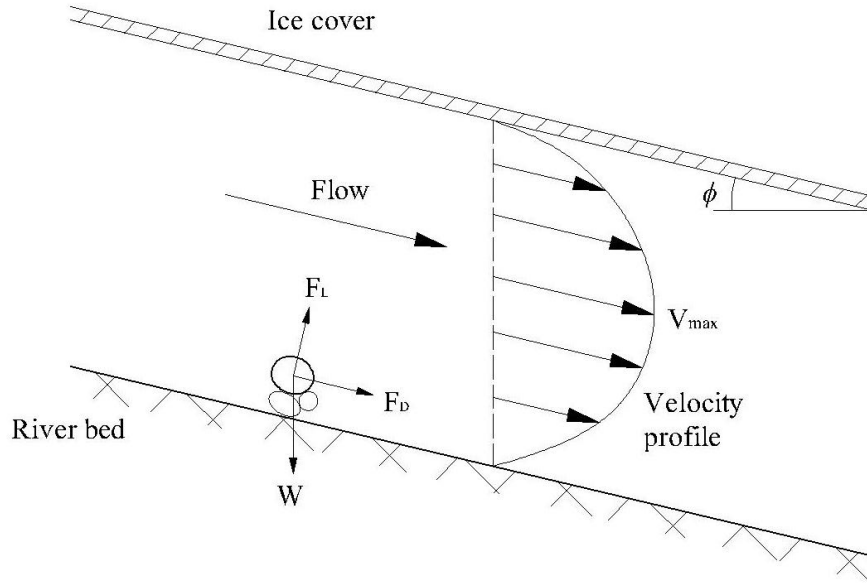


Figure 2- 1 Schematic of force on particle on a sloping bed under ice cover

The shear velocity of approaching flow will be calculated by using the log-law. The critical bed shear velocity can be determined by using the classical Shields Diagram. If the flow velocity profiles are available, the bed shear velocity u_{*c} can be calculated by fitting a least squares regression to flow velocity and distance measurements from near the bed to 20% of the depth using the following equation (Kuhnle et al. 1999; 2002):

$$u_{*c} = \frac{d\bar{u}}{5.75d(\log h)} \quad (2-2)$$

in which \bar{u} is time mean velocity at a distance of h .

The shear Reynolds number will be used here to study the incipient motion of sediment particles.

$$R_e^* = \frac{u_{*c}D_{50}}{\nu} \quad (2-3)$$

in which u_{*c} is the bed shear velocity, D_{50} is the median grain size of sediments and ν is the kinetic viscosity of water.

The dimensionless shear stress will be calculated by using the following equation: $\tau_* = \frac{\rho u_{*c}^2}{g\Delta\rho D_{50}}$,

where $\Delta\rho$ is the difference in mass density between sediment and water, g is the gravity.

In this research, the velocity profile will be measured in the scour hole under simulated ice cover. Once the velocity profile is acquired, the flow resistance and the bed load sediment transport rate can be estimated. Thereby, the suspended sediment transport rate could be calculated based on the bed load transport rate.

2.2 Experimental study

2.2.1 Study site

The experimental research has been conducted at Dr. Max Blouw Quesnel River Research Center (QRRC), Likely, BC. The QRRC is a University of Northern British Columbia (UNBC) based research facility. There are six outdoor flow-through spawning channels in the research center. Each channel has dimensions of 80 meters long, 2 meters wide and 1.3 meters deep. To conduct the experimental research, one channel was modified as an engineering flume during the summer of 2011.

2.2.2 Experimental design and construction

In reviewing the literature on experimental local scour research, only a few studies were conducted in large flumes (Sheppard et al., 2004; Morales et al., 2008). The experimental research, were conducted in a 2m wide flume, and can be treated as a large scale local scour experiment. To my knowledge, this is the first large scale experimental research on the local scour under ice over. A more detailed introduction of the flume will be discussed below.

In 2011, the flume was re-constructed to set up for experimental research. Prior to the modification, the flume had an upstream section and downstream section, which had a length of 39.5m and 38.2m, respectively. The upstream 39.5m has been modified as a holding tank for the purpose of keeping a constant discharge during the experiments. The experimental zone is located in the downstream 38.2m section of the flume. Figure 2-2 shows the modification plan of the flume at the QRRC.

Firstly, to directly observe and record the scour process, two 4m sections of concrete flume wall were replaced with plexiglass. Since the flume has a width of 2 m, it would be too much to cover all the flume bed with sand, so two sand boxes were made by elevating the flume bottom by 30 cm. The sand boxes are 0.3 m deep, 2 m wide and 5.6m and 5.8m long respectively. Other parts of the flume bottom were covered by treated waterproof plywood. Different composition of sands (d_{50}) were put in the sand box to study the effect of sediment composition on local scour. To create different velocities, three input valves were connected together which can adjust the amount of water into the flume. It was measured that this method can produce at least six velocities for the scour simulation. Because of the cold weather and heavy snow in Likely, a roof was also constructed to cover the experimental zone away from leaves, snow and wind. The modification of the flume was finished in November, 2011. Figure 2-3 shows the modification process of the flume at QRRC.

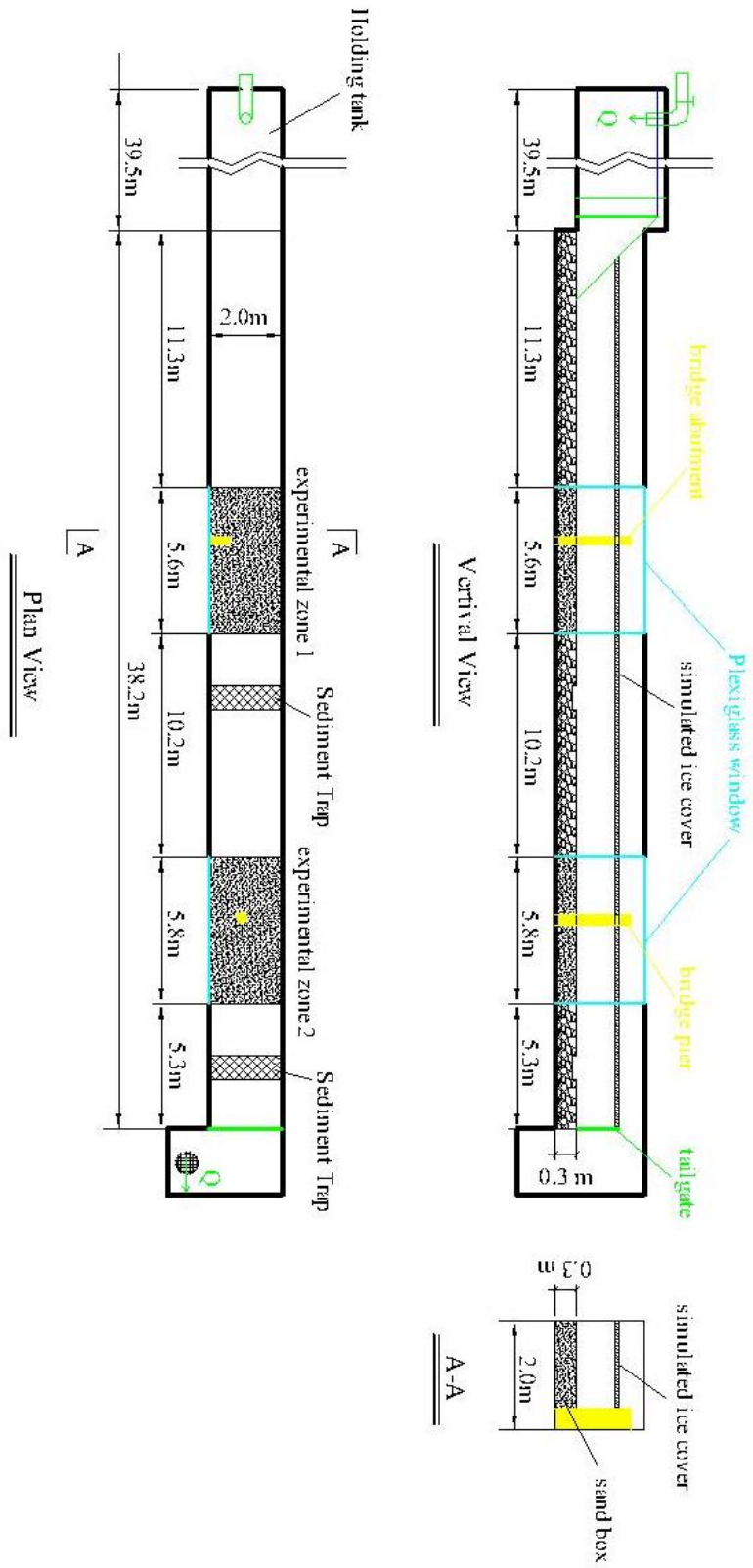


Figure 2- 2 The modification plan for the flume at QRRC



Figure 2- 3 The modification of flume at QRRC

2.2.3 Measurement apparatus

Recently, experimental studies of the local scour have been carried out in laboratory flumes using Laser visualization techniques, Particle Image Velocimetry (PIV), and Acoustic Doppler Velocimeter (ADV) to determine the flow field around bridge abutments, piers and spur dikes. Three dimensional measurements of instantaneous velocity can be used to determine the turbulent properties and the bed shear stress.

In this research, to measure the flow field in the scour hole around the bridge abutment under ice cover, the preferred instrument is a SonTek 10MHz Acoustic Doppler Velocimeter (ADV), which is known for its accuracy, portability, reliability and ease of operation. After the introduction of ADVs in 1990s, they have been widely used to measure the three dimensional flow field in turbulent flows (Zhang et al. 2005; Duan et al. 2009). ADV can measure instantaneous velocities in three dimensions at a given spatial point that can be used to compute the mean velocity, Reynolds stresses, shear stresses, turbulent kinetic energy and other parameters. An ADV consists of a down-looking 3D probe which can be installed to measure instantaneous 3D velocity around the bridge abutment scour hole under ice cover (Figure 2-4). The ADV will be directly connected to a computer to record the transmitted signal.

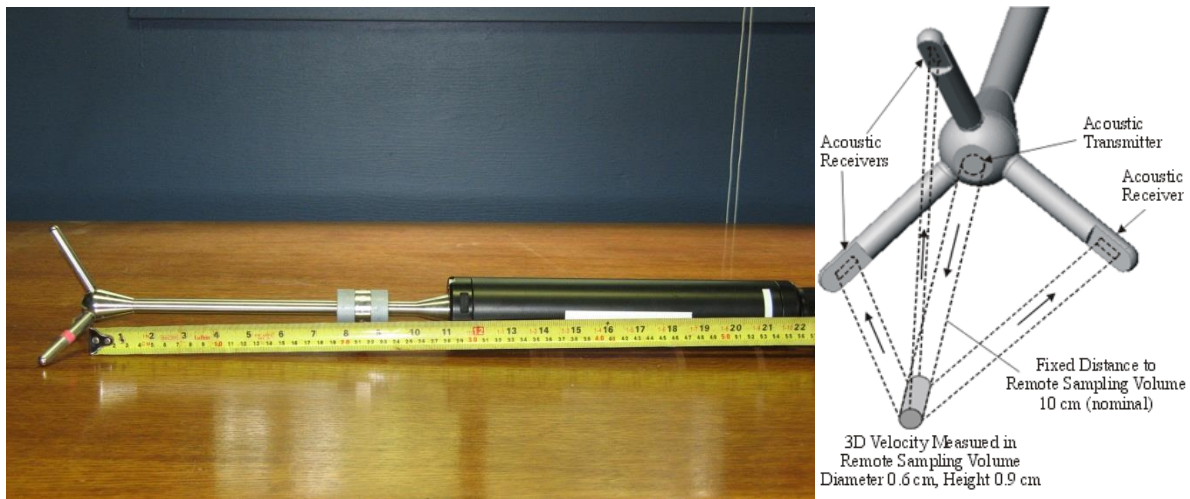


Figure 2- 4 The dimension of ADV (left) and the sensor head of a ADV (right)

By using ADV, Dey and Barbhuiya (2005) studied the turbulent flow field and scour hole around a short abutment. They found that the maximum bed shear stresses were about 3.2 times that of the incoming flow. Kuhnle et al. (2008) suggested the maximum bed shear stresses to be 3 times

that of the incoming flow around a spur dike. These two studies showed similar amplification factor of the bed shear stresses in open channels. ADV was used in this study to decide the amplification factor of bed shear stresses under covered conditions.

Another option for measuring approaching velocity is SonTek IQ, which can be used to measure the 2D velocity in the flume. The SonTek IQ is a monostatic Doppler current meter designed for water level, velocity and flow measurement in the field. With an accuracy of 1% of measured velocity, SonTek IQ can be used in the flume to measure the approaching velocity.

2.2.4 Experimental procedures

An equilibrium scour depth can theoretically be defined as the condition when the dimension of scour hole does not change with time. Various criteria have been proposed in the literature in order to identify the equilibrium state (Grimaldi, et al., 2009). In this study, the criteria from Melville and Chiew (1999) will be used. Namely, the approximate equilibrium state is reached when the variation of scour depth is less than 5% of the width of bridge abutments or piers. To be more practical and relevant to practical engineering, non-uniform sand were used in this study. For non-uniform sediments, an armor-layer should develop on top of the scour hole during experiments. The equilibrium criteria from Melville and Chiew (1999) needs further discussion in this study.

To ensure the repeatability of experiments and isolate other uncertainties, procedures were strictly followed during experiments. However, since the flume is a flow-through type, some of the parameters, such as water temperature, viscosity can not be controlled. The experimental procedures are as follows.

1. The bridge abutment model will be put in the middle of Experimental Zone 1 and fixed to the bottom of the flume. All bridge abutment models here are built by plexiglass to create a clear view from inside of the abutment model. Then non-uniform sediments type 1 will be put in the sand box and be leveled with a scraper blade to the same elevation of the false floor. Since the sediment needs to be re-used, a sediment trap was installed to collect sediment during and after experiments.
2. Before each test, the flume is filled with water slowly and after the required water depth is reached, Styrofoam is put on top of the water as a simulated ice cover. After the depth is

reached, then the experiment is started. In the experimental research, all the abutment models are non-submerged.

3. In the first 2 hours, the scour depth is measured and scour profile is pictured every 10 min. After that, the scour depth and profile is measured every 30 min. A constant discharge can be attained by adjusting the pump in the pump house. The tailgate at the end of flume can be changed to get a certain approaching flow depth. After 24 hours, the scour depth is measured as the final depth.

4. When the equilibrium scour depth is reached, the flow is slowly brought to stop and the water in the flume is drained by gravity. For a better observation of scour hole development, a camera is put inside of the bridge abutment model to record the scour process.

5. The local scour around bridge abutment in open channels is studied. Smooth cover and rough cover are created after open channel test. Around abutment models, velocity is measured by a Acoustice Doppler Velocimeter (ADV) for the real time velocity measurement.

6. After the test for bridge abutment mode, the other abutment model is used to study the shapefactor on local scour under ice cover. Another two different non-uniform sands are used to study the impacts of sediment composition on local scour under ice cover. The procedure of tests is simplified in Figure 2-5.

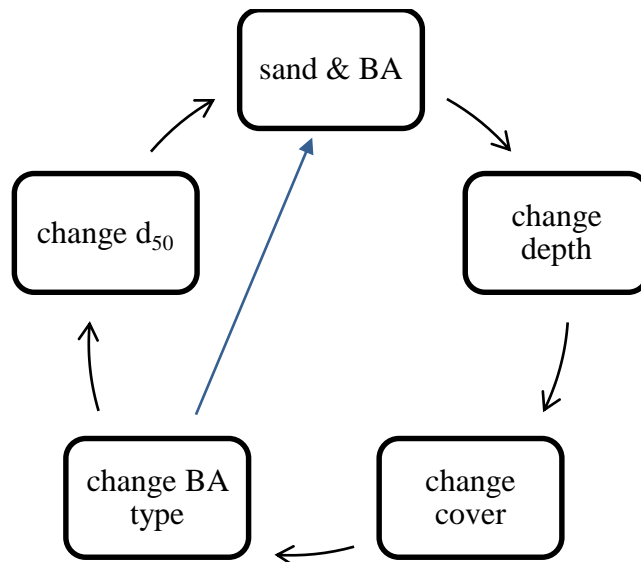


Figure 2- 5 Related parameters and Experimental procedure (BA: bridge abutment)

3 RESULTS AND DISCUSSION

3.1 Impacts of ice cover on local scour around semi-circular bridge abutment

The protrusion of a bridge abutment into the main channel creates disturbance and obstruction to the sediment transport state in the alluvial channel. The flow accelerates and separates at the upstream face of the abutment which creates a down-flow vortex. The direct result is local scour around bridge abutment. The vortex system and down-flow, along with the turbulence, are the main cause of local scour. Essentially, the local scour phenomenon is a dynamic feedback process between the turbulent flow and bed sediment (Zhang et al. 2009).

Bridge scour has been identified as the most common cause of highway bridge failures and it accounts for about 60% of all bridge collapses in the United States (Deng and Cai, 2009). According to Kandasamy and Melville (1998), 6 of 10 bridge failures which occurred in New Zealand during Cyclone Bola were related to abutment scour.

Investigations of bridge failure due to local scour around bridge abutments have been an important topic for hydraulic engineers for many years. In 2011, the National Cooperative Highway Research Program (NCHRP) conducted two reports on the local scour around bridge foundations (NCHRP 175 and 181, 2011). As reviewed in the report, several commonly used equations were compared to estimate scour depth around bridge foundations. However, none of these equations are applicable for the local scour estimation under ice cover.

In the northern region of Canada, rivers can be covered by ice during the winter. Ice cover is a threat to the safety of a bridge and can cause serious problems around local ecosystems. Ice cover presents a different set of geomorphological conditions when compared to that of open flow (Hicks, 2009). The characteristics of flow under ice cover impact the bed-load sediment transport, traverse and vertical mixing and mean flow velocity (Andre and Thang, 2012). However, to date, there is still very limited research on the local scour around bridge infrastructures under ice cover (Ackermann, et al. 2002; Ettema and Daly, 2004; Hains, 2004; Wang et al. 2008; Munteanu and Frenette, 2010; Sui et al. 2009; Sui et al. 2010). Additionally, most of the previous studies were conducted in small scale laboratory flumes (0.5m~1.6m wide). None of these studies were conducted in a large scale flume, which can better simulate the scour phenomenon around abutments. In the present study, one large scale flume (2m wide, 40m long) was used to study the local scour around a semi-circular abutment. To fill this gap, the present chapter was used to investigate the scour pattern and maximum scour depth around a semi-circular abutment under ice cover.

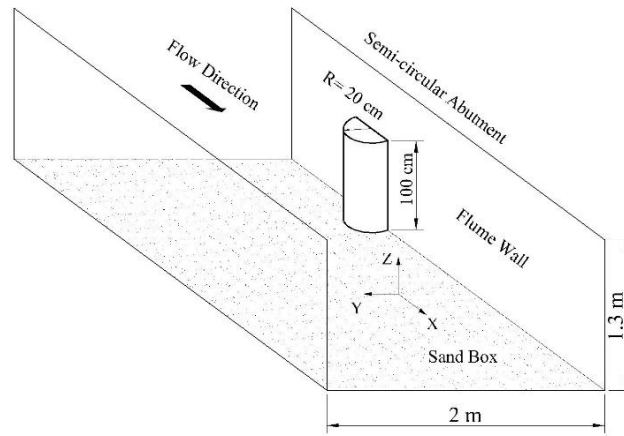
3.1.1 Methodology

Experimental setup

A large flume at the Quesnel River Research Centre, Likely, BC was used. The flume had dimensions of 40m long, 2m wide, 1.3m deep. The slope of the flume bottom was 0.2%. A holding tank with a volume of 90m³ was located in the upstream portion to keep a constant discharge in the experimental zone. At the end of the holding tank, water overflowed from a rectangular weir to the flume. Figure 3.1-1a shows the semi-circular abutment dimension in the flume.

Two sand boxes were created in the flume, with a distance of 10.2m from each other. To make sure the sand box was deep enough for the local scour development, the sand boxes were both dug to a 30cm depth while other parts of the flume were covered by water treated plywood. The velocity range in sand box #1 was 0.16~0.26m/s, while in sand box #2, the range was 0.14~0.21m/s. The semi-circular abutment model was made from plexiglass. Three non-uniform sediments were used with D_{50} s of 0.58mm, 0.50mm, 0.47mm respectively. In the present study, since ice cover was the main focus, two types of ice cover were created, namely smooth cover and rough cover. Both types of ice cover were attached in the experimental zone as a fixed ice cover on top of the water surface (Figure 3.1-1b). The smooth ice cover was the original styrofoam panels while the rough ice cover was made by attaching small Styrofoam cubes to the bottom of the smooth cover (Figure 3.1-1c). The cubic pieces had a dimension of 2.5cm × 2.5cm × 2.5cm. The spacing distance between adjacent cubic pieces is 3.5cm.

(a)



(b)

(c)



Figure 3.1- 1 Dimensions of abutment, ice cover and rough ice cover used in the experiment

Experiment procedure

The following steps were strictly followed in the experimental study.

(1) Before each experiment, the abutment model was leveled and fixed in the sand box to make sure the abutment was vertical to the flume bottom. On the outside surface of the abutment, different measuring lines have been drawn for the purpose of comparing the scour profile at different locations. In all, 13 measuring lines (P ~ Q) were made along the semi-circular abutment (Figure 3.1-2).

(2) At the beginning of each experiment, the flume was slowly filled to avoid initial scouring. After the water depth was reached, the required velocity was applied in the flume.

(3) In front of each sand box, a SonTek IQ was installed to measure the approaching flow velocity and water depth during the experiment. A 10 Hz SonTek ADV was used to measure the velocity in front of the abutment. An adjustable tailgate was installed at the end of flume to

change the water depth. Table 3.1-1 summarizes the experimental conditions for each flume experiment.

(4) After 24 hours, the flume was drained slowly. The scour depth was measured manually along the outside lines of the semi-circular abutment. In all, 27 experiments have been carried out. Some of the data can be found in Table 3.1-1.

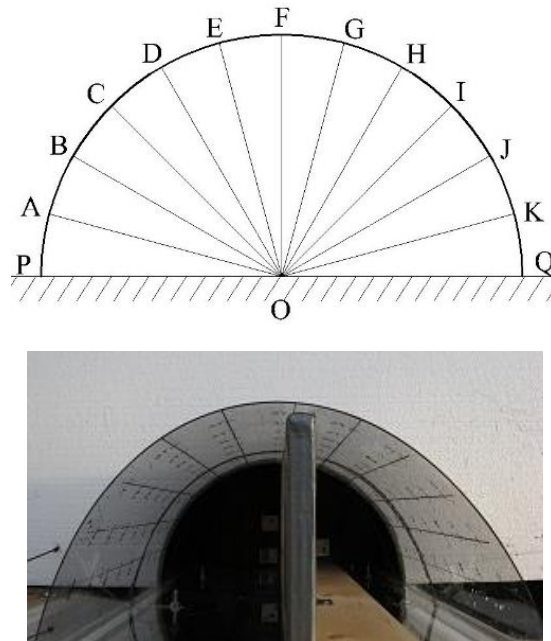


Figure 3.1- 2 Measuring points along the semi-circular abutment

3.1.2 Results and discussion

Local Scour pattern

At the end of each experiment, the local scour was manually measured (Figure 3.1-3). The distance from the abutment outside surface to the boundary of scour hole was measured. The sediment deposition ridges around the abutment can be seen from Figure 3.1-3. The contour of the local scour hole was mapped in the local coordinate system by Surfer 10, Golden Software. Based upon the contour mapping, both the volume of the scour hole and the scour area were calculated (Table 3.1-1).

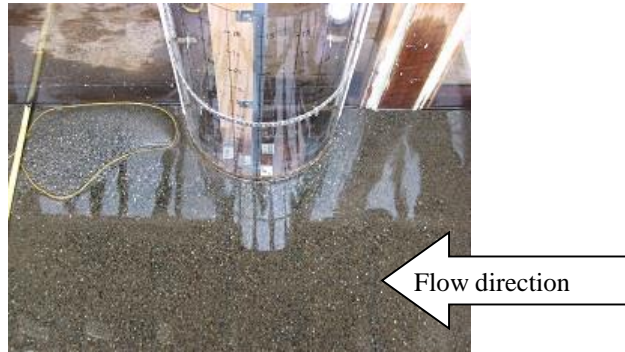


Figure 3.1- 3 The local scour around the abutment and the measurement of the scour

Due to the narrowing effect created by the abutment, we noticed stronger flow turbulence in the experimental zone. When the velocity in the channel was increased, sediment in the toe areas of the abutment was eroded most quickly.

Table 3.1- 1 Experimental running condition summary

D_{50} (mm)	Cover condition	Depth (m)	V (m/s)	Scour volume (cm ³)	Scour area (cm ²)
0.58	open	0.19	0.23	1433.09	1009.79
	open	0.07	0.26	570.46	782.08
	smooth	0.07	0.23	273.33	466.68
	smooth	0.19	0.20	696.74	907.55
	smooth	0.07	0.20	165.88	494.57
	rough	0.07	0.20	238.63	540.96
	rough	0.19	0.20	459.50	376.34
	rough	0.07	0.22	1127.69	715.74
0.47	open	0.19	0.23	19095.9	3335.68
	open	0.07	0.26	16847.2	3401.70
	smooth	0.07	0.23	6520.80	1895.73
	smooth	0.19	0.20	5856.95	1758.72
	smooth	0.07	0.20	187.58	213.61

	rough	0.07	0.20	565.81	469.97
	rough	0.19	0.20	13986.9	3020.83
	rough	0.07	0.22	3224.38	1150.13
0.50	open	0.19	0.23	4140.53	1902.96
	open	0.07	0.26	6295.62	2751.83
	smooth	0.07	0.23	5146.66	2170.39
	smooth	0.19	0.20	5644.58	2600.00
	smooth	0.07	0.20	617.76	765.52
	rough	0.07	0.20	481.45	507.46
	rough	0.19	0.20	2190.03	881.93
	rough	0.07	0.22	10006.2	3367.77

Three different non-uniform sediments were used here. During the scouring process, relatively fine particles moved first and sediment in the scour hole was gradually coarsened. An armor layer formed on the surface of the scour hole which prevented the scour hole from scouring further. After 24h, the armor layer covered the whole area around the bridge abutment. After each experiment, sediment samples were collected at different locations around the abutment. We noticed that at the location from G to I, a secondary scour hole was also developed around the abutment.

The scour hole pattern and geometry around the semi-circular abutment exhibits features similar to those found by Zhang et al. Due to the existence of a primary vortex and wake vortex downstream of the abutment, as well as their interaction, the geometry of the scour area in the upstream is significantly different from that in the downstream. The primary vortex is responsible for the scour hole development, which is analogous to the well-known horseshoe vortex in front of bridge piers (Melville, 1992). At the upstream of the abutment, an obvious scour hole formed while a fine sediment deposition ridge can be seen in the downstream.

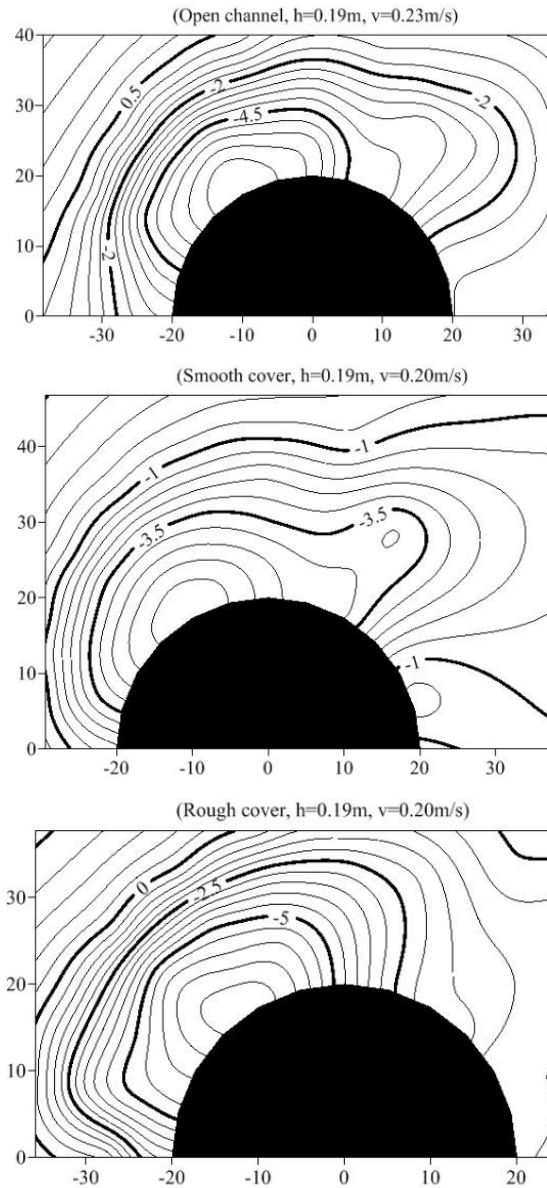


Figure 3.1- 4 The scour profiles around the abutment under different cover conditions ($D_{50}=0.50\text{mm}$)

Figure 3.1-4 shows the contour map plotted under different flow cover conditions with the sediment $D_{50}=0.50\text{mm}$. It can be noted that the maximum scour depth around the semi-circular abutment is located at the upstream surface of the abutment. Additionally, with a decrease in sediment size, maximum scour depth increases correspondingly. Our experiments confirm with the conclusion drawn by Ettema (Ettema et al. 2010) that the reductions in the scour depth for large sediment were due to large particles impeding the erosion process inside of the scour hole

and dissipating some of the flow energy in the erosion area. This is particularly correct for the non-uniform sediment erosion around bridge abutment. Moreover, for the same bed sediment under the same flow condition, ice cover results in a larger maximum scour depth.

Figure 3.1-4 also indicates that the scour pattern in the vicinity of the abutment under ice covers were similar to that in open channels. Under a rough ice cover, due to the effect of the ice cover, the scour depth was increased.

Scour profiles along the abutment

To date, no research has been undertaken for plotting scour profiles along the abutment under ice cover. Hence, scour profiles along the abutment border (From P to Q, refer to Figure 3.1-2) were plotted to show the elevations changing along the semi-circular abutment. Figure 3.1-5a shows the variation in scour depth with different bed sediments under the same flow conditions. Figure 3.1-5b is the cross section of local scour under different conditions. The following points are noted from the figures:

(a) For all the cross sections, it can be found that the maximum scour depth is located close to E, 60° from the flume wall. This is believed to be caused by the primary vortex, which originates at the upstream of the abutment (Dey and Barbhuiya, 2005). The primary vortex is forced by the velocity to drift towards the side of the semi-circular abutment. From Dey's research (2005) on clear water scour, they mentioned that the velocity and scour depth become maximum at 90° to the flume wall. However, from the experimental data, the maximum scour depth happened not at 90° but rather at 60° from the flume wall. This may be due to the non-uniform sediment used in the present research. The locations of maximum scour depth with or without ice cover were all around 60° from the flume wall. A greater number of experiments in ice covered channels will improve the estimation of maximum scour location around the semi-circular abutment.

(b) Moreover, the authors noted that there was a sudden increase in the bed elevation from G to H, which corresponds to the second scour hole noted from the contour diagram. In the literature the second scour hole has been given little attention because of its relatively shallow scour depth compared to the primary scour hole. However, it may explain the migration of the primary vortex flow along the abutment to the downstream, which may explain the downstream wake vortex. Although the reason for the sudden increase in elevation was not clear, one can still note

from Figure 3.1-5 that the upstream surface has a steeper slope (from P to F). The local slope of the scour hole in the downstream (from F to K) is smaller than that in the upstream. Unfortunately, there is no clear trend showing the changes of upstream slope corresponding to the change in bed sediments D_{50} . It is also noted the same results were found by Zhang et al.(2009) on the local scour around the spur dikes in open channels.

(c) The ice cover had a strong impact on the scour depth around the abutment. As shown in Figure 3.1-5b, under rough ice covered conditions, the maximum scour depth increased significantly compared to that in open channel and smooth ice cover. From our understanding, the turbulence caused by rough ice cover moves the maximum velocity closer to the bed compared to that by smooth ice cover, which can be attributed to the deeper scour in the vicinity of the abutment. However, as expected, there were some inaccuracies of the cross section plot due to the limitation of the measurement and profile.

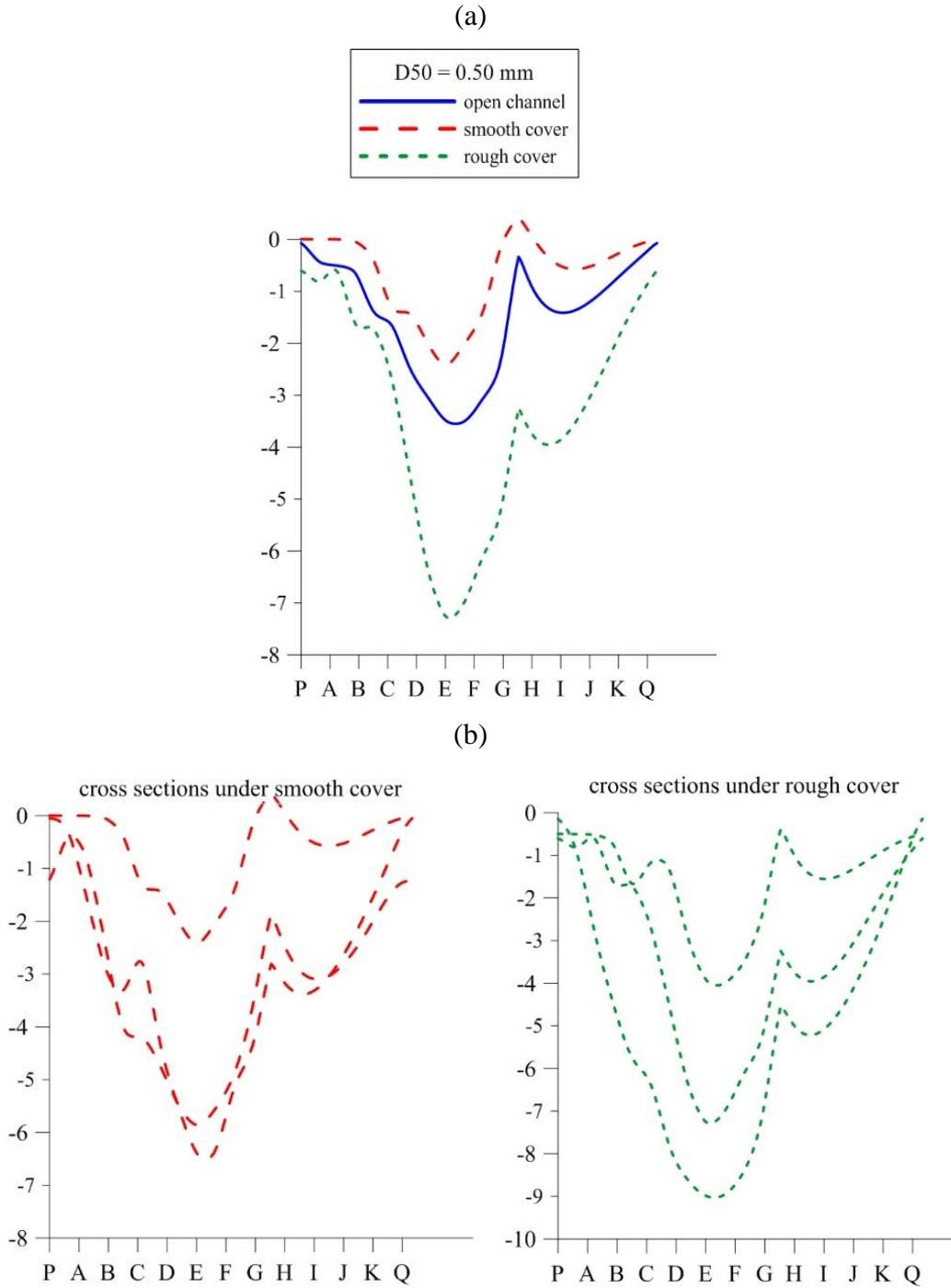


Figure 3.1- 5 (a) Cross-section along the semi-circular abutment ($D_{50}=0.50\text{mm}$); (b) Cross-section along the semi-circular abutment under smooth and rough cover ($D_{50}=0.50\text{mm}$)

Scour volume and scour area

So far, most of the present research conducted on the local scour focuses on the maximum scour depth, while little attention has been paid on the scour volume and scour area. Based on the scour volume and scour area given in Table 3.1-1, the scour volume vs. scour area was plotted in Figure 3.1-6, which shows the scour volume and scour area variation around the semi-circular abutment in open and ice covered channels.

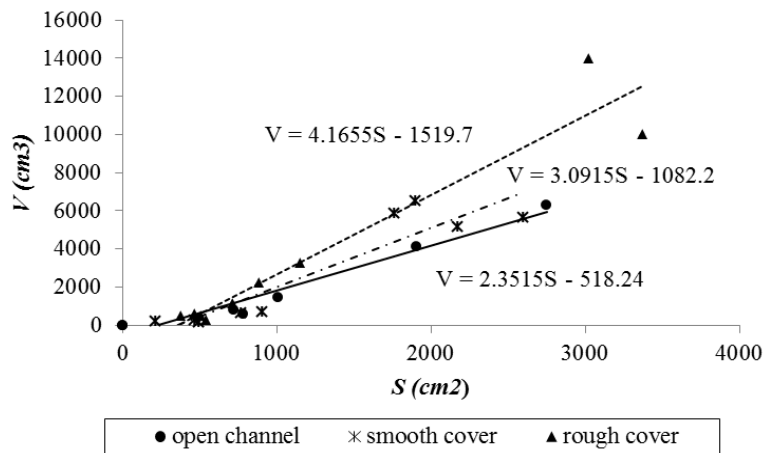


Figure 3.1- 6 Variation of scour volume around bridge abutment

From Figure 3.1-6, the following three relations were developed:

For open channel:

$$V = 2.3515S - 518.24 \quad (3.1-1)$$

Under smooth cover:

$$V = 3.0915S - 1082.2 \quad (3.1-2)$$

Under rough cover:

$$V = 4.1655S - 1519.7 \quad (3.1-3)$$

Since the ratio of scour volume to scour area is the average scour depth. Based on Equation 3.1-1 to 3.1-3, the average scour depths for rough cover, smooth cover and open channel were 4.17 cm, 3.09 cm, 2.35 cm respectively. One should also note that the above equations are practical only under certain conditions, otherwise, the scour volume would be negative. The average scour depth followed a similar trend to the maximum scour depth. With smooth ice cover, the average

scour depth increases by 31.5% compared to that in open channels; for rough ice cover, the increase in average scour depth is 34.7% compared to that under smooth ice cover.

Maximum scour depth

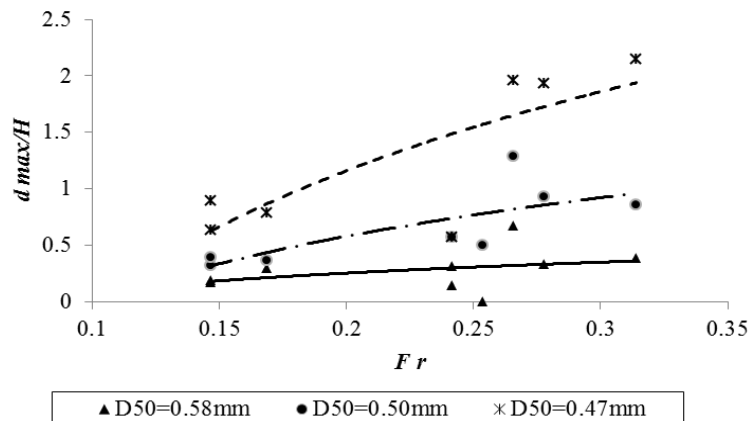
From the author’s understanding, there are still no experimental measurements on the maximum scour under ice cover. For non-uniform sediments, Melville (1997) included sediment non-uniformity in his formula of estimating the maximum scour depth around the bridge abutment under open flow condition. By using sediment size factor K_d as a parameter, the following equations were developed.

$$K_d = 0.57 \log(2.24 \frac{L}{D_{50}}), L/D_{50} \leq 25 \quad (3.1-4)$$

In which L is the projected abutment length and K_d is the particle size factor. When the ratio of $L/D_{50} > 25$, the value of K_d equals to 1 from Melville’s (1992) previous research, which is not practical for the present study. Since the abutment length remains constant, the non-uniform sediments were valued by including the Froude number as defined by the following equation:

$$F_r = U_o / \sqrt{gH} \quad (3.1-5)$$

where g is the gravitational acceleration, U_o is the approaching velocity, H is the approaching flow depth.



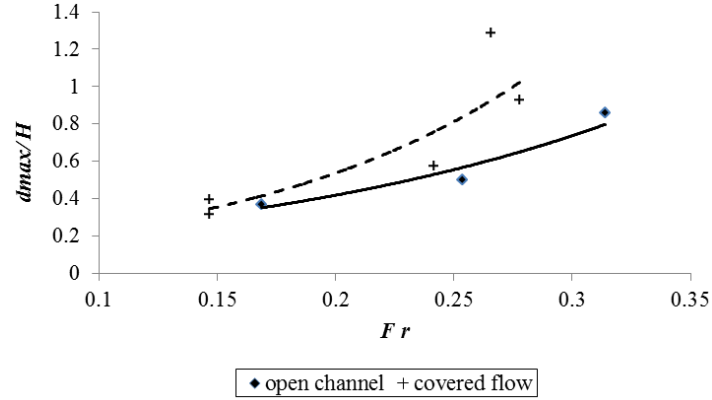


Figure 3.1- 7 (a) Variation of maximum scour depth with the Froude number under different sediment composition (b) The comparison of maximum scour depth in open channel and ice covered condition ($D_{50}=0.50\text{mm}$)

The experimental data from Figure 3.1-7a indicates that under the same flow conditions, fine sediment composition can result in a deeper maximum scour depth. With the same sediment composition, the maximum scour depth increases with the Froude number. An imposed ice cover results in an increased composite resistance, so under ice covered conditions, the maximum scour is more than that in open channels (Figure 3.1-7b). To gain a better understanding of the impact of sediment grain size on the maximum depth, regression analysis was conducted. The maximum scour depth around the semi-circular abutment can be described by the following variables.

$$\frac{d_{\max}}{H} = A \left(\frac{U}{\sqrt{gH}} \right)^a \left(\frac{D_{50}}{H} \right)^b \quad (3.1-6)$$

In all, 27 experiments have been conducted to investigate the relationship between average scour depth and approaching flow depth, in which 9 experiments were in open channels, 9 experiments were under smooth ice cover and 9 experiments were under rough ice cover. By using the regression analysis, the following equations were derived from all the 27 experiments (Figure 3.1-8).

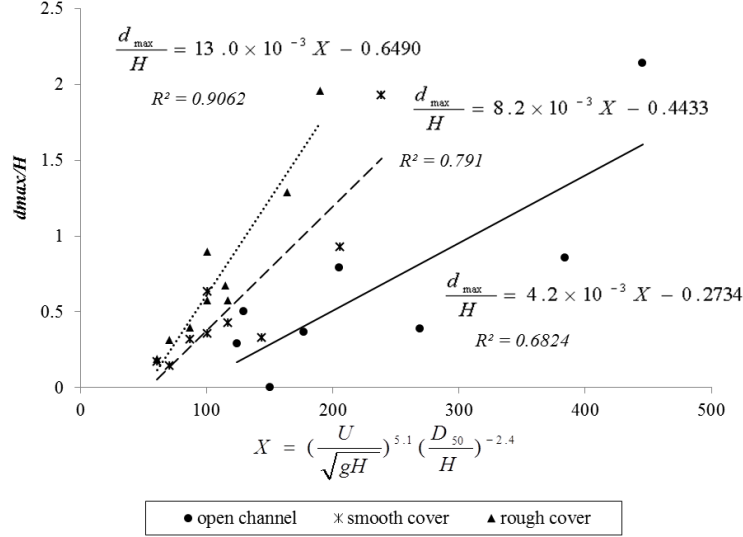


Figure 3.1- 8 Dependence of maximum scour depth on related variables

For open channel:

$$\frac{d_{\max}}{H} = 4.2 \times 10^{-3} \left(\frac{U}{\sqrt{gH}} \right)^{5.1} \left(\frac{D_{50}}{H} \right)^{-2.4} - 0.2734 \quad (3.1-7)$$

For smooth cover:

$$\frac{d_{\max}}{H} = 8.2 \times 10^{-3} \left(\frac{U}{\sqrt{gH}} \right)^{5.1} \left(\frac{D_{50}}{H} \right)^{-2.4} - 0.4433 \quad (3.1-8)$$

For rough cover:

$$\frac{d_{\max}}{H} = 13.0 \times 10^{-3} \left(\frac{U}{\sqrt{gH}} \right)^{5.1} \left(\frac{D_{50}}{H} \right)^{-2.4} - 0.6490 \quad (3.1-9)$$

As reported by Sui et al. (2010), with an increase in velocity and particle size, the maximum scour depth will increase. In the present research, regarding the local scour around the semi-circular abutment, the rough ice cover causes the largest average scour depth compared to those under both smooth ice cover and open channel. Hence, we compared the maximum scour depth under different flow conditions and with different composition of bed sediments. It is interesting to note that the geometric characteristics of the local scour depend mainly on the approaching flow velocity, bed sediment grain size as well as the cover condition.

From Figure 3.1-8 and Equation 3.1-7 to 3.1-9, the impact of sediment distribution is studied. To study the impact of ice cover roughness on the local scour development around the semi-circular abutment, the following dimensional variables under covered flow were considered:

$$\frac{d_{\max}}{H} = A \left(\frac{U}{\sqrt{gH}} \right)^a \left(\frac{D_{50}}{H} \right)^b \left(\frac{n_i}{n_b} \right)^c \quad (3.1-10)$$

where n_i is the ice cover roughness and n_b is the channel bed roughness. According to the Hydraulic Design Handbook (1999), in an un-vegetated alluvial channel, the total roughness n_b consists of two parts. One is grain roughness (n') which is resulting from the size of the particle and the other is skin roughness (n'') because of the existence of the bed forms. The total roughness can be expressed as:

$$n = n' + n'' \quad (3.1-11)$$

However, there is no reliable method of estimating n'' , so in the present research, the grain roughness was used as the channel bed roughness in the analysis. For mixtures of bed material with significant portions of coarse-grain sizes, the following equation from Hager (1999) was used.

$$n' = 0.039 D_{50}^{1/6} \quad (3.1-12)$$

Ice cover presence alters the mean flow distribution and flow turbulence characteristics. For smooth ice cover, because the styrofoam panel has a relatively smooth concrete-like surface, by referring the Mays (1999), the value of 0.013 was adapted. The roughness of the ice cover was changed by attaching small cubes with dimensions of 2.5cm×2.5cm×2.5cm with a distance 3.5cm from each other. By using the results of discharge measurements through the ice and supporting field data related to the observed characteristics of the underside of the ice cover, Carey (1966) calculated Manning roughness coefficient was between 0.01~0.0281. From his calculation, a constant roughness of 0.0251 was used for the winter period. Li (2012) reviewed several methods to calculate the Manning's coefficient for ice cover, the following equation can be used depending on the size of the small cubes.

$$n_i = 0.039 k_s^{1/6} \quad (3.1-13)$$

In which k_s is the average roughness height of the ice underside. So in the present research, the roughness coefficient was calculated as 0.021, which is also in the range of Carey's calculation.

By using the regression analysis, the following empirical equation was developed:

$$\frac{d_{\max}}{H} = 3.0 \times 10^{-5} \left(\frac{U}{\sqrt{gH}} \right)^{9.56} \left(\frac{D_{50}}{H} \right)^{-4.85} \left(\frac{n_i}{n_b} \right)^{1.07} - 0.0511 \quad (3.1-14)$$

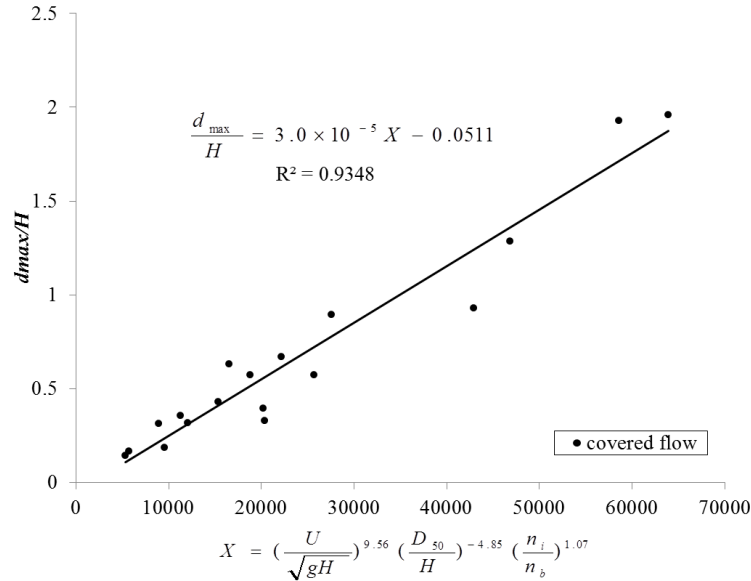


Figure 3.1- 9 Dependence of maximum scour depth on related variables under ice cover

The correlation between maximum scour depth and above three variables is worth mentioning because as indicated in Figure 3.1-9 the regression relationship is strong. Meanwhile, it is also confirmed that the hypothesis for calculation of the ice cover roughness is correct. One can also note that, under the condition of same flow and bed material, the maximum scour depth under rough ice cover is deeper than that under smooth ice cover. However, under the same flow and cover condition, since the index for D_{50} is negative (-4.85), with the decreasing in sediment grain size, the maximum scour depth will increase. With the same bed material and covered condition, the approaching velocity has a positive impact on the maximum scour depth.

To apply this empirical equation in the hydraulic engineering field, the authors assume that during the winter the ice cover can be treated as smooth. While in early spring, with the ice breaking up and ice jamming processes, the ice cover can be treated as rough therefore increasing the flow velocities and increasing the local scour around bridge foundations. In this case, the sediment transport increases and the safety of bridge infrastructures will be threatened. One can note from Equation 3.1-14 that, in the same river, with the increase in ice cover roughness, the maximum scour depth increases. During the ice break up period in spring time, due to the accumulation of small ice chunks under side, local bridge scour should be monitored.

Compared to the research of armor layer development in the paper from Sui et al. (2010), the approaching water depth had a stronger impact on the maximum scour depth compared to

approaching velocity in open channels. However, for ice covered flow, the authors found that approaching velocity has a stronger impact compared to that of the approaching water depth. One drawback regarding the proposed empirical equation is that roughness of only two ice covers were tested.

3.1.3 Conclusion

Experiments have been conducted in a large scale flume to study the impact of ice cover roughness and non-uniform sediment on the local scour around semi-circular abutments. The location of the maximum scour depth along the abutment is 60° from the flume wall. We noticed that the downstream slope in the scour hole is smaller compared to that in the upstream. In this research, the Froude number was also used to investigate the impacts of non-uniform sediment composition on local scour. The scour volume and scour area were calculated and compared to open channel, smooth and rough cover conditions. Under ice cover, the average scour depth was always greater compared to that in open channels. The average scour depth under rough ice cover was 35% greater than that under smooth ice cover. By using dimensional analysis, an empirical equation of the maximum scour depth was developed. The equation indicated that with an increase in sediment grain size, the maximum scour depth decreased correspondingly. In conclusion, ice cover roughness plays an important role for the maximum scour depth development.

References

1. Ackermann N L, Shen H T, Olsson P, Local scour around circular piers under ice covers [C]. Proceeding of the 16th IAHR International Symposium on Ice, International Association of Hydraulic Engineering Research, Dunedin, 2002, New Zealand.
2. Andre R, Thang T, Mean and turbulent flow fields in a simulated ice-cover channel with a gravel bed: some laboratory observations [J]. Earth Surface Processes and Landforms, 2012, Vol. 37, pp: 951-956.

3. Carey K, Observed configuration and computed roughness of the underside of river ice St Croix river Wisconsin [J], Geological Survey Professional Paper, 1966, Vol. 550, Part 2, pp. B192-B198.
4. Deng L, Cai C S, Bridge scour: prediction, modeling, monitoring, and countermeasures-Review [J]. Practice Periodical on Structural Design and Construction, 2009, 15(2):125-134.
5. Dey S, Barbhuiya A K, Turbulent flow field in a scour hole at a semicircular abutment [J], Canadian Journal of Civil Engineering, 2005, Vol. 32, pp. 213-232.
6. Ettema R, Daly S, Sediment transport under ice. ERDC/CRREL TR-04-20. Cold regions research and Engineering Laboratory, 2004, US Army Corps of Engineers.
7. Ettema R, Natako T, Muste M, Estimation of scour depth at bridge abutments, NCHRP 24-20, 2010, The University of Iowa, USA.
8. Hager W H, Wastewater Hydraulics [M]. Berlin: Springer-Verlag, 1999.
9. Hains D B, An experimental study of ice effects on scour at bridge piers [C]. PhD Dissertation, 2004, Lehigh University, Bethlehem, PA.
10. Hicks F, An overview of river ice problems [C] CRIPE 07 guest editorial Cold regions Science and Technology, 2009, 55: pp. 175-185.
11. Kandasamy J K, Melville B W, Maximum local scour depth at bridge piers and abutments [J]. J Hydraul. Res. 1998, 36:183-197.
12. Li S S, Estimates of the Manning's coefficient for ice covered rivers [J], Water Management, Proceedings of the Institution of Civil Engineers, 2012, Vol. 165, Issue WM9, pp. 495-505.
13. Mays L W, Hydraulic Design Handbook [M], McGraw-Hill, 1999, pp. 3.12.
14. Melville B W, Local Scour at bridge abutments [J]. Journal of Hydraulic Engineering, ASCE, 1992, Vol.118 (4), pp. 615-631.
15. Melville B W, Pier and Abutment scour: integrated approach [J], Journal of Hydraulic Engineering, 1997. ASCE, Vol 123(2): 125-136.
16. Munteanu A, Frenette R, Scouring around a cylindrical bridge pier under ice covered flow condition-experimental analysis, R V Anderson Associates Limited and Oxand report, 2010.
17. NCHRP Web-only Document 175, Evaluation of Bridge- Scour Research: Pier scour processes and predictions. 2011, NCHRP Project 24-27(01).

18. NCHRP Web-only Document 181, Evaluation of Bridge-Scour Research: Abutment and Contraction Scour Processes and Prediction. 2011, NCHRP Project 24-27(02).
19. Sui J, Faruque M A A, Balanchandar R, Local scour caused by submerged square jets under model ice cover [J]. *Journal of Hydraulic Engineering, ASCE*, 2009, Vol 135 (4), pp. 316-319.
20. Sui J, Wang J, He Y, Krol F, Velocity profile and incipient motion of frazil particles under ice cover [J]. *International Journal of Sediment Research*, 2010, Vol 25(1), pp. 39-51.
21. Sui J, Afzalimehr H, Samani A K, Maherani M, Clear-water scour around semi-elliptical abutments with armored beds [J]. *International Journal of Sediment Research*, 2010, Vol. 25, No. 3, pp. 233-244.
22. Wang J, Sui J, Karney B, Incipient motion of non-cohesive sediment under ice cover – an experimental study [J]. *Journal of Hydrodynamics*, 2008, Vol 20(1), pp. 177-124.
23. Zhang H, Nakagawa H, Kawaike K, Baba Y, Experimental and simulation of turbulent flow in local scour around a spur dike [J]. *International Journal of Sediment Research*, 2009, Vol. 24, No. 3, pp. 33-45.

3.2 Local scour around bridge abutments under ice covered condition: comparing of square abutment and semi-circular abutment

Local scour is the engineering term used to describe sediment removal around hydraulic structures by running water. It may result in bridge failures as it can undermine piers and abutments that support bridges. The Federal Highway Administration has estimated that over 60% of bridge collapses in the US was from local scour. Luigia et al. (2012) indicated that approximately 50 to 60 bridges fail on average each year in the US. A worldwide survey also indicated that, the main cause of bridge collapse is natural hazards, among which flooding and scour is responsible for around 60% of the failures (Imhof, 2004).

An important consideration in bridge abutment design is to estimate the maximum scour to make sure the bridge foundation can be built deep enough to avoid the possibility of undermining. In the past few decades, local scour around bridge abutments and piers in open channels has received wide attention and many scholars have conducted various studies on this topic (Laursen and Toch, 1956; Froehlich, 1989; Melville, 1997; Coleman et. al., 2003; Dey 2005; etc.). To estimate the maximum scour depth, several formulae have been developed. As reviewed by NCHRP in 2011, five major dimensionless parameter groups are classified for the scour depth estimation formulae.

The first group is Flow and Sediment, which indicates flow interaction with sediment and can be used to classify clear-water or live-bed scour. The second group is Abutment and Sediment scale, which is related to the degree of model scaling. The third group is Abutment and Flow geometry, which will measure abutment dimensions relative to the scale of flow field. The fourth group is Abutment Flow distribution, which is the discharge per unit width in the approach and contracted sections. The fifth group is Scour and Geotechnical Failure, which is the scour that leads to the slope instability which is difficult to model in the laboratory.

The five groups listed above include almost all the variables in the local scour estimation formulae around bridge abutments. However, in the northern areas, ice cover is an issue because it can stay as long as 5 months on some rivers. Ice cover can result in many problems such as ice jamming, flooding, restricting the generation of hydro-power, block river navigation and affect the ecosystem balance (Hicks, 2009). Moreover, ice cover can also significantly change the flow field and change the flow properties around bridge foundations, such as velocity profile, bed shear stress distribution, mixing properties, and sediment transport (Lau and Krishnappan, 1985).

Ettema et al. (2000) developed a method to estimate the sediment transport in ice covered channels. Sui et al. (2000) derived interrelationships of suspended sediment concentrations and riverbed deformation under ice cover in Hequ Reach of Yellow River. Some other researches on the sediment transport and scour under ice including: Ettema and Daly, (2004); Hains and Zabilansky, (2004); Wang et al. (2008). However, to date there is limited research on the local scour around bridge structures under ice cover (Ackermann et al., 2002; Hains, 2004; Sui et al., 2009; Sui et al., 2010a; Sui et al., 2010b). To fill this gap, a series of experiments were conducted to find the parameter that can describe the ice cover impact on the scour depth.

3.2.1 Experimental setup

Based on the previous review of local scour around bridge abutments, flume experiments were designed to evaluate the impacts of ice cover on scour depth. The following three hypotheses were tested in this research.

Hypothesis 1: Shape factor of abutments

Bridge abutments are designed in different sizes and shapes. The shape factor is important in abutment local scour estimation. According to Melville (1992), the effect of shape can be expressed using a shape factor K_s . In open channels, the shape factor for square abutment is 1.0 and for semi-circular one is 0.75. The shape factor was examined under ice covered conditions.

Hypothesis 2: Non-uniform sediment

Most of the existing work on local scour focuses on uniform sediments in small laboratory flumes with very few studies that look at non-uniform sediments. However, a more practical problem for engineers is that natural riverbeds are normally non-uniform. Three non-uniform different sediments were used in this study to see the scour contour and sediment deposition. The maximum scour depths from different non-uniform sediments were also compared.

Hypothesis 3: Ice cover roughness impact

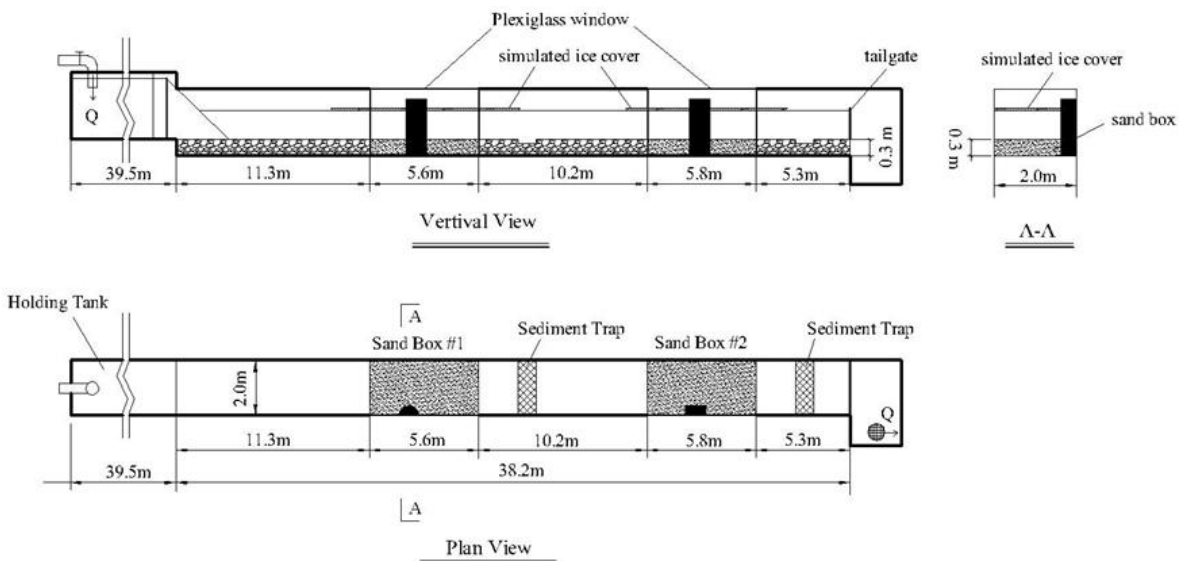
Since the roughness of the ice cover impacts the velocity distribution in the water regime. In this research, two different types of ice cover were created, namely smooth cover and rough cover. The maximum scour depths under different covers were compared.

Experimental design

Experiments were carried out in an outdoor flume in 2012. The flume is 40m long, 2m wide and 1.3m deep. The slope of the concrete bottom is 0.2%. Figure 3.2-1(a) shows the flume geometry and design. Two abutment models were made from Plexiglass to permit observation of the scour process during experiments. The dimensions of the abutment can be found in Figure 3.2-1(b).

A holding tank with a volume of 90m³ was created upstream of the flume. Two valves to adjust flow rate were connected to the holding tank. The flow depth can be adjusted by the tailgate at the end of the holding tank. Two sand boxes were created to simulate riverbed, with a distance 10.2m from each other. Each sand box can have 30cm depth of sediment (Figure 3.2-2). The velocity range in Sand box 1 is from 0.16 to 0.26m/s, while the velocity range in Sand box 2 is between 0.14 and 0.21m/s.

(a)



(b)

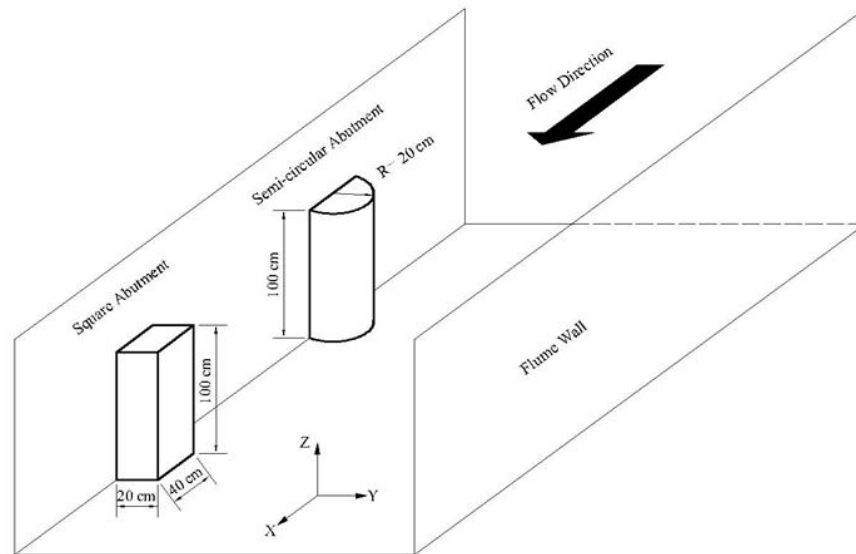


Figure 3.2- 1 (a) The plan and vertical view of the modified flume; (b) The coordinate system and abutments dimensions

Ice cover was simulated by using styrofoam which was fixed around the abutment model to simulate fixed ice cover. To investigate the impacts of ice cover roughness on the maximum scour depth of the scour hole, two types of ice cover were made. Smooth cover was the original Styrofoam. The rough cover was modified by attaching small cubic pieces of Styrofoam to the underside of smooth ice cover. All cubic pieces had the following dimensions: $2.5\text{cm} \times 2.5\text{cm} \times 2.5\text{cm}$. The spacing distance between adjacent cubic pieces is 3.5cm (Figure 3.2-2).

Experiment procedure

Before each experiment, the abutment was installed vertically in the sand box against flume wall. Then the sand box was leveled to maintain the same elevation with false flume floor. At the beginning of each experiment, the flume was slowly filled with water by adjusting the valve in the holding tank. After the required water depth was reached, the valves were fully opened to

start the experiment. The running time for each experiment is at least 24h, which was enough for the maximum scour depth development in large scale flumes from the author's observation.

In front of each sand box, a SonTek IQ was installed to measure the mean approaching velocity and flow depth. A 10 MHz SonTek Acoustic Doppler Velocimeter (ADV) was applied to measure the instantaneous velocity in the scour hole around the abutment at different locations and elevations. After all the velocity measurement was completed, the flume was drained completely and the scour hole was measured. In this section, Surfer 10 was used for contour plotting, which can also provide 3D plotting of the scour profile.



Figure 3.2- 2 (a) Inside view of the flume; (b) Rough ice cover used in the research

One of the main objectives of this research was to compare the maximum scour depth around abutment under different flowing conditions. Herein, the flow depth and approaching velocity are the main available variables. To change the water depth, the adjustable tailgate can be used. Under the same water depth, by adjusting the valve in the holding tank, different approaching velocities can also be acquired. Three different sediments were used to simulate the real local scour in the flume. The D_{50} s are 0.58mm, 0.50mm, 0.47mm respectively. The geometric standard deviations (σ_g) were all larger than 1.4, which can be categorized as non-uniform sediment. In all, 36 experiments were carried out under ice cover and 18 experiments under open flow condition were also conducted. Table 3.2-1 summarizes the experimental conditions for each experiment.

Table 3.2- 1 Summary of running conditions

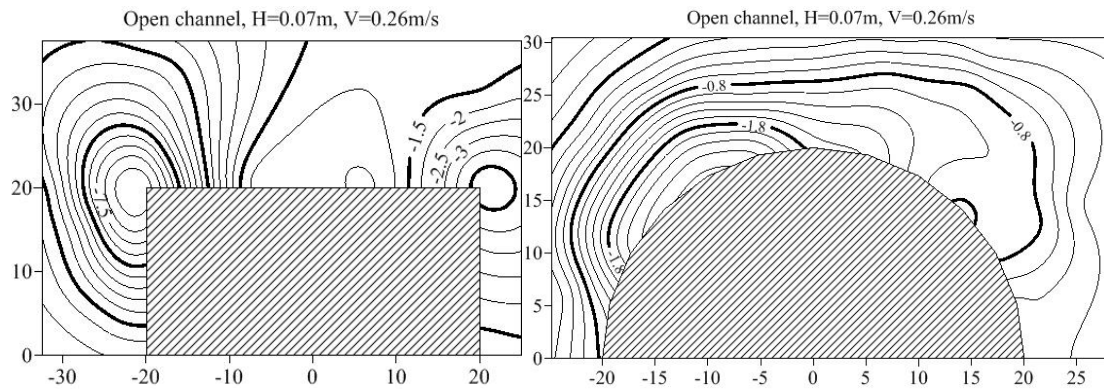
Abutment type	Cover condition	D ₅₀ (mm)	Running time (h)	Flume width (m)	Water depth (m)	Approaching velocity (m/s)
square	open	0.58	24	2	0.07	0.26
square	open	0.58	24	2	0.07	0.21
square	open	0.58	24	2	0.19	0.21
semicircular	open	0.58	24	2	0.07	0.21
semicircular	open	0.58	24	2	0.19	0.23
semicircular	open	0.58	24	2	0.07	0.26
semicircular	smooth	0.58	24	2	0.07	0.23
semicircular	smooth	0.58	24	2	0.19	0.20
semicircular	smooth	0.58	24	2	0.07	0.20
square	smooth	0.58	24	2	0.07	0.20
square	smooth	0.58	24	2	0.19	0.16
square	smooth	0.58	24	2	0.07	0.23
square	rough	0.58	24	2	0.07	0.22
square	rough	0.58	24	2	0.07	0.20
square	rough	0.58	24	2	0.19	0.14
semicircular	rough	0.58	24	2	0.07	0.20
semicircular	rough	0.58	24	2	0.19	0.20
semicircular	rough	0.58	24	2	0.07	0.22
square	open	0.47	24	2	0.07	0.26
square	open	0.47	24	2	0.07	0.21
square	open	0.47	24	2	0.19	0.21
semicircular	open	0.47	24	2	0.07	0.21
semicircular	open	0.47	24	2	0.19	0.23
semicircular	open	0.47	24	2	0.07	0.26
semicircular	smooth	0.47	24	2	0.07	0.23

semicircular	smooth	0.47	24	2	0.19	0.20
semicircular	smooth	0.47	24	2	0.07	0.20
square	smooth	0.47	24	2	0.07	0.20
square	smooth	0.47	24	2	0.19	0.16
square	smooth	0.47	24	2	0.07	0.23
square	rough	0.47	24	2	0.07	0.22
square	rough	0.47	24	2	0.07	0.20
square	rough	0.47	24	2	0.19	0.14
semicircular	rough	0.47	24	2	0.07	0.20
semicircular	rough	0.47	24	2	0.19	0.20
semicircular	rough	0.47	24	2	0.07	0.22
square	open	0.50	24	2	0.07	0.26
square	open	0.50	24	2	0.07	0.21
square	open	0.50	24	2	0.19	0.21
semicircular	open	0.50	24	2	0.07	0.21
semicircular	open	0.50	24	2	0.19	0.23
semicircular	open	0.50	24	2	0.07	0.26
semicircular	smooth	0.50	24	2	0.07	0.23
semicircular	smooth	0.50	24	2	0.19	0.20
semicircular	smooth	0.50	24	2	0.07	0.20
square	smooth	0.50	24	2	0.07	0.20
square	smooth	0.50	24	2	0.19	0.16
square	smooth	0.50	24	2	0.07	0.23
square	rough	0.50	24	2	0.07	0.22
square	rough	0.50	24	2	0.07	0.20
square	rough	0.50	24	2	0.19	0.14
semicircular	rough	0.50	24	2	0.07	0.20
semicircular	rough	0.50	24	2	0.19	0.20
semicircular	rough	0.50	24	2	0.07	0.22

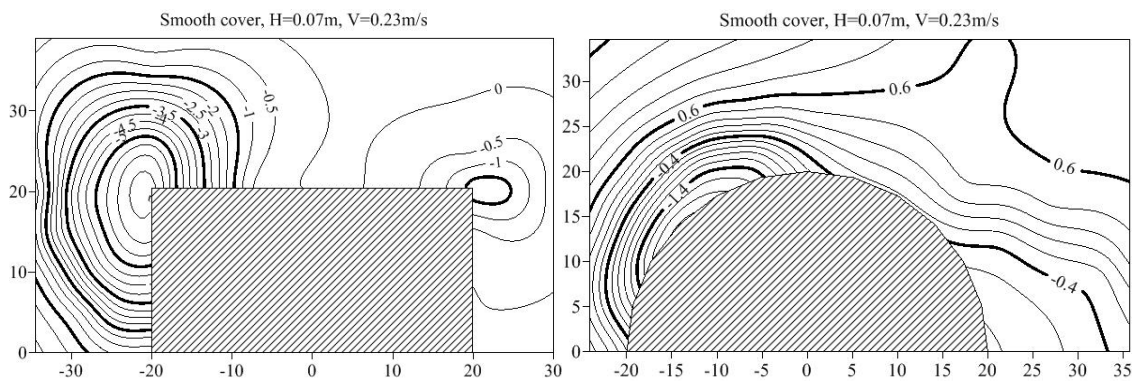
3.2.2 Results and discussion

During the scouring process, a primary vortex was observed in the upstream surface of the square abutment associated with a down flow inside the scour hole in vertical directions. This vortex is formed inside of the scour hole due to the negative stagnation pressure gradient of approaching flow, which explained the location of the maximum scour depth around square abutment. While for the semi-circular abutment, the vertical component of the downward flow is similar to the horseshoe vortex around bridge piers. Values of local flow velocity and bed shear stress increase around the side of the abutment. As reported by Melville (1997), for circular bridge piers, the increases in bed shear velocity that cause the scour occurs at the side of the pier. A similar scouring location was found around the semi-circular abutment in the present research. The maximum scour depth is located around 45 degrees from the flume wall in our cases.

(a)



(b)



(c)

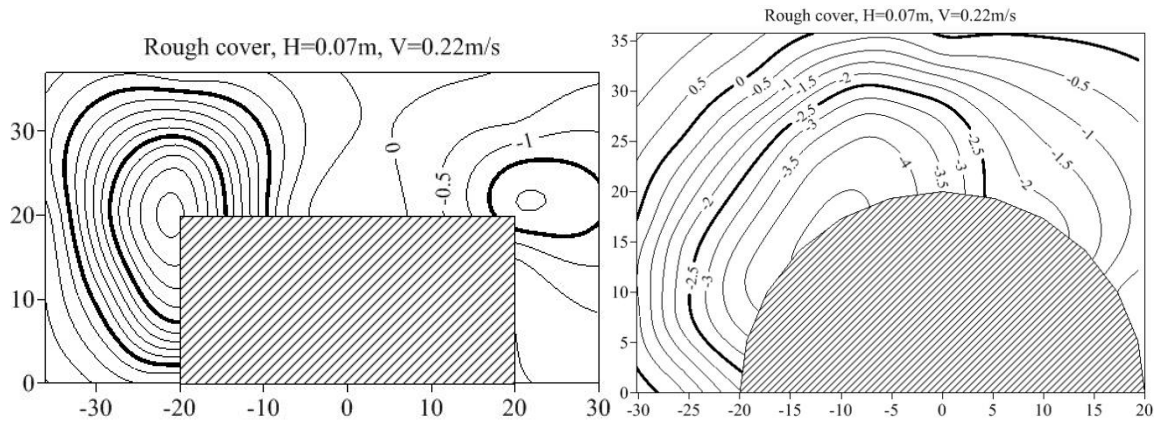


Figure 3.2- 3 Typical local scour profiles around the square abutment and semicircular abutment

The local scour was mapped and contoured by Surfer 10, Golden Software as shown in Figure 3.2-3. Typical scour patterns around square and semi-circular abutments under different covered conditions were mapped. Figure 3.2-3(a) shows the contours in open channels, Figure 3.2-3(b) and Figure 3.2-3(c) shows the contours under smooth and rough ice cover, respectively.

It can be observed that for both types of abutments, the maximum scour depth occurs in the upstream side facing the approaching flow. Around square abutment, there is another relatively smaller scour hole in the corner that faces downstream. For semi-circular abutment, the maximum scour depth is located at the corner which is 45~60 degrees facing upstream. The locations of the maximum scour depth are independent on the covered condition. While for the dimensions of the scour hole, ice cover has an obvious impact. In open channels, around the square abutment, the scour hole has a smaller slope compared to the scour holes under ice covered condition. It is also interesting to note that around semi-circular abutment, the area of scour hole under the cover is larger than that from open channels. With the increase in ice cover roughness, the scouring area increases correspondingly. Around the square abutment, the scour hole keeps a similar pattern with or without ice cover. While for semi-circular abutment, the scour hole under ice cover is larger than that from smooth cover and open channel. Figure 3.2-3(c) also shows a larger deep-scouring area around semi-circular abutment under a rough ice cover.

An analysis on the densimetric Froude number was completed in order to investigate the impact of abutment shape on maximum scour depth. To do this, the densimetric Froude number (F_o) was calculated by using the following,

$$F_o = U_o / \sqrt{g(\Delta\rho / \rho)D_{50}} \quad (3.2-1)$$

In which, g is the gravitational acceleration, U_o is the approaching velocity, ρ is the mass density of water while the $\Delta\rho$ is mass difference between sediment and water. D_{50} is the median grain size of sediments.

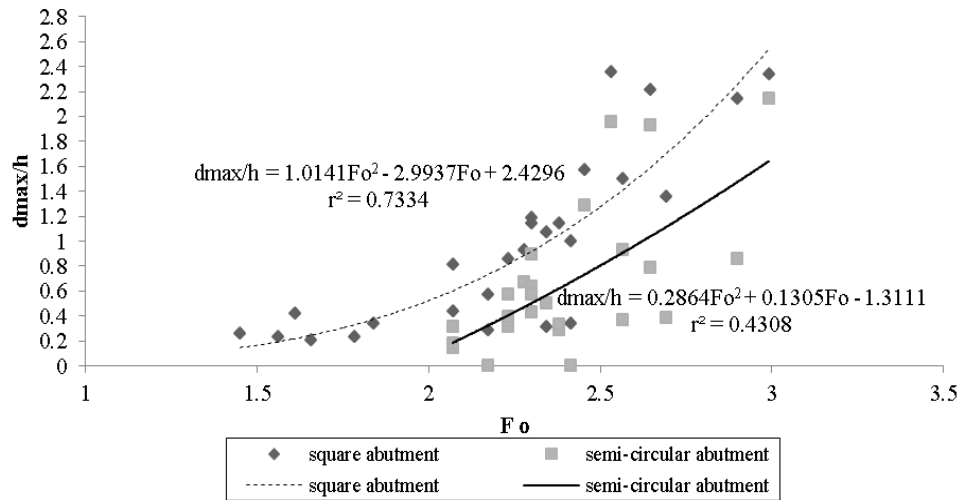


Figure 3.2- 4 The variation of maximum scour depth with abutment model

Overall, 54 maximum scour depth were plotted in Figure 3.2-4, in which 27 were from a square abutment and 27 from a semi-circular abutment. Figure 3.2-4 shows the difference in maximum scour depth between the two types of abutments under different flow conditions. From Melville’s previous research (Melville, 1992), the shape factor for square abutment in open channels is 1.0, while for the abutment with a semi-circular head the value is 0.75. Our data indicate that under covered conditions, the shape factor for semi-circular abutment is smaller than that in open channels. With an increase in ice cover roughness, the value of shape factor decreases.

For square abutment, the following relationship is found between the dimensionless scour depth d_{max}/h and densimetric Froude number F_o :

$$\frac{d_{max}}{h} = 1.0141F_o^2 - 2.9937F_o + 2.4296 \quad (3.2-2)$$

For semi-circular abutment, the relation is:

$$\frac{d_{\max}}{h} = 0.2864F_o^2 + 0.1305F_o - 1.1331 \quad (3.2-3)$$

The two equations can also be written as:

$$\frac{d_{\max}}{h} = f_1(F_o) \quad (3.2-4)$$

$$\frac{d_{\max}}{h} = f_2(F_o) \quad (3.2-5)$$

Here, the range of F_o is 1.3 ~3.0, meanwhile $f_1(1.3) > f_2(1.3)$ and $f_1(3) > f_2(3)$. It is also important to notice that under the same densimetric Froude number condition, the maximum scour depth in the vicinity of square abutment is much larger than that around the semi-circular abutment.

Another important consideration here is to include D_{50} in the relationship between d_{\max} and F_o . By including the median sediment grain size, the connection between flow and sediment can be built under ice covered flow for both abutments. The data and fitting curve from Figure 4 has further strengthened the hypothesis that ice cover has a stronger impact on the maximum scour depth than shape factor of the abutment.

The maximum scour depth with three different bed sediments are compared in Figure 3.2-5. As predicted in the previous hypothesis, the maximum scour depth increases with the decrease of D_{50} . For coarse sand ($D_{50}=0.58$), the maximum scour depth under smooth ice cover is similar to that in open channels, which indicates the smooth cover has less impact on the scour development. However, for fine sediments ($D_{50}=0.50$ and $D_{50}=0.47$), the ice cover has a stronger impact on the maximum scour depth than open channels.

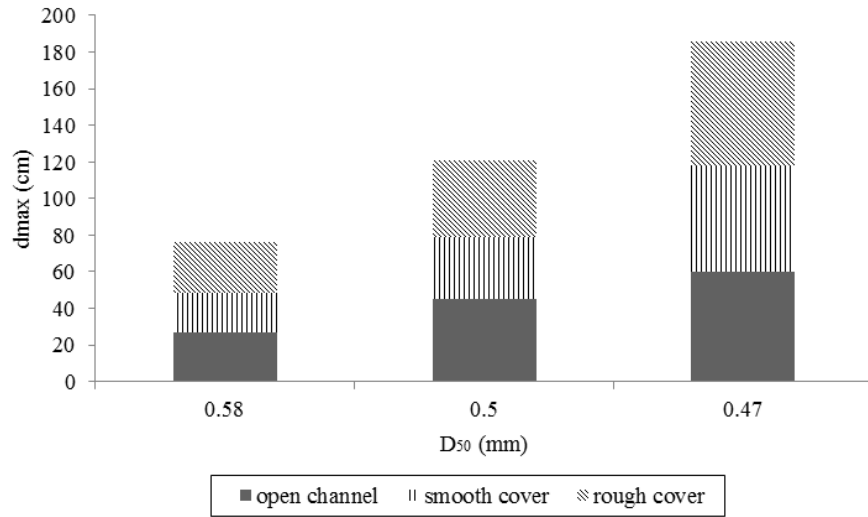


Figure 3.2- 5 The variation of D_{50} with scour depth under different conditions

Under the same flow condition in open channel, results also show that square abutment contributes a higher maximum scour depth compared to that from semi-circular one. With an ice cover as an extra boundary on top, as reported by Sui et al. (2010b), the location of maximum velocity is closer to the channel bed than for the corresponding open channel flow. The increased gradient of the near bed velocity leads to a higher bed shear stress, which contributes the deeper scour hole in covered flow. With the increase of ice cover roughness, the locus of maximum velocity moves closer to the bed compared to the smooth ice cover. This explains the reason of a deeper scour depth under rough ice cover.

Figure 3.2-6 indicates that the variation of the maximum scour depth around the two abutments in open channels, smooth cover and rough cover in different bed sediments.

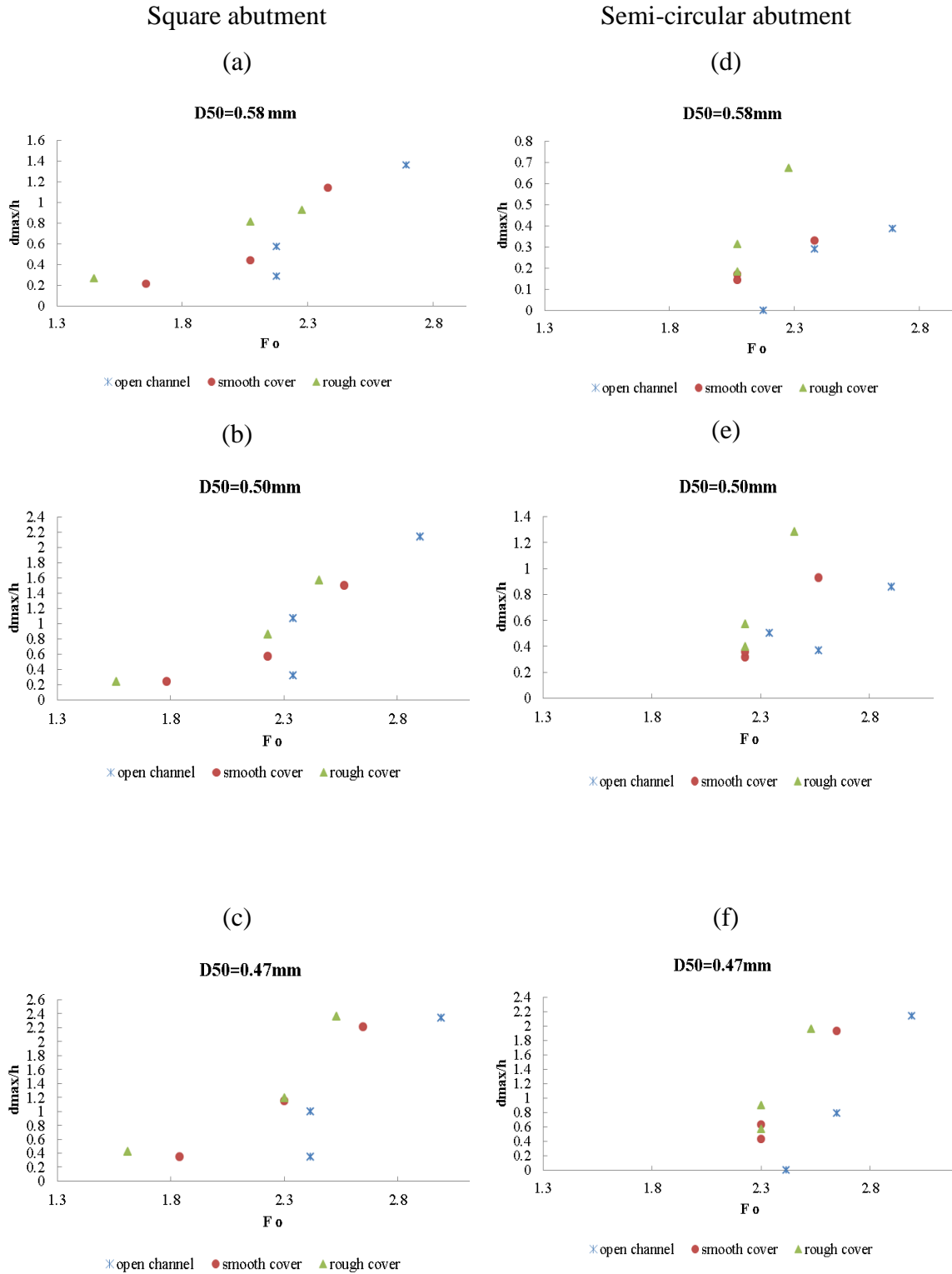


Figure 3.2- 6 The variation of maximum scour depth with different sediments and abutments

Figure 3.2-6 (a) ~ (c) show the variation of maximum scour depth with different bed sediments around the square abutment, while Figure 3.2-6 (d) ~ (f) represent the variation of maximum scour depth with the three sediments around the semi-circular abutment. It is clear that with an increase of F_o , the ratio of maximum scour depth to approach flow depth increases correspondingly under all flow condition with or without ice cover. It can also be seen that under the same densimetric Froude number, with decreasing D_{50} , the scour depth difference between smooth ice cover and rough ice cover also decreases. For both abutments, with the decrease of D_{50} , the impact of ice cover roughness has a more clear impact on the scour depth.

As mentioned above, the impact of the shape factor for semi-circular abutment on scour depth is smaller than that in open channels. To find the impact of shape factors, the derivative of d_{\max}/h to F_o is possible by using Equation (3.2-2) and (3.2-3).

$$\left(\frac{d_{\max}}{h}\right)' = 2.0282F_o - 2.9937 \quad (3.2-6)$$

$$\left(\frac{d_{\max}}{h}\right)' = 0.5728F_o + 0.1305 \quad (3.2-7)$$

By making equation (3.2-6) equals to equation (3.2-7), it is found that when $F_o = 2.11$, the difference between square abutment and semi-circular abutment is the smallest. At this point, the shape factor for semi-circular abutment is 0.66. From the calculation, the shape factor for semi-circular abutment has a range from 0.66 ~0.71.

The following multi-relationship can be used to describe the impact of shape factor on maximum scour depth:

$$\frac{d_{\max}}{h} = f(F_o, K_s) \quad (3.2-8)$$

In which, F_o is the densimetric Froude number and K_s is the shape factor for different abutments. For square abutment, the shape factor has a value of 1, which is same to that in open channels. However, for the semi-circular abutment under ice covered condition, the shape factor will be around 0.66~0.71, which is smaller than that in open channels.

The presence of an ice cover induces a redistribution of the highest velocities compared with the open channel flow around bridge abutments, and thus leads to a higher available energy for the scouring phenomenon. The relationship in Figure 3.2-7 also shows that with an increase in D_{50} , the ratio of maximum scour depth to flow depth decreases. While under the same flow and sediment condition, the ice cover can result in a deeper scour depth. By increasing the

densimetric Froude number, the ratio increases correspondingly under open channel, smooth cover and rough cover. But compared to the ratio in open channels, the rough cover has the largest value and smooth cover has the second largest.

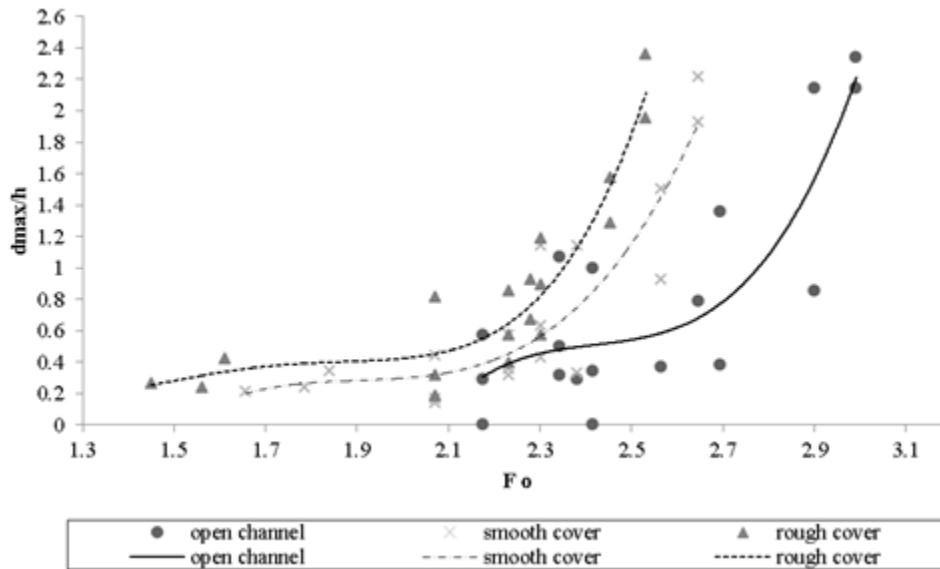


Figure 3.2- 7 The variation of maximum scour depth with different covered conditions

The experimental research conducted by Munteanu and Frenette (2010) showed that, an increase up to 55% of maximum scour depth can be reached around the bridge pier under ice covered conditions. From our study, for bridge abutments under rough ice cover, the increase on maximum scour depth is around 30% ~ 40% for all the sediments. While for the smooth cover, under the same flow condition, the increase of maximum scour depth is less than 30%. From the authors' understanding, the sediment transport under ice cover depends on the flow re-distribution due to ice cover. A rough ice cover can cause more turbulence compared to the smooth ice cover and open channel.

3.2.3 Conclusions

Ice cover plays an important role in the development of local scour hole around bridge abutments. Experiments have been conducted to study the impact of ice cover on bridge abutments with

solid foundations in the soil. Two types commonly used abutments were built, namely semi-circular and square abutments. For three non-uniform sediments, the profiles of local scour around abutments were plotted. By using Buckingham Pi theorem for dimensional analysis, the densimetric Froude number was used as one parameter to investigate the impact of shape factor and ice cover roughness on maximum scour depth around abutments. Results indicate that the impact of shape factor for semi-circular abutments on maximum scour depth is smaller in covered conditions than that in open channels. The range of shape factor is between 0.66 and 0.71. Additionally, ice cover roughness also has a more pronounced impact on the maximum scour depth. However, due to the limitation of experimental data, further experiments can lead to a higher degree of certainty regarding the influence of shape factor on scour for semi-circular abutment under ice covered conditions. Future work will include: flow velocity analysis in the vicinity of bridge abutments under ice cover and analysis of the armor layer.

References

1. Ackermann N L, Shen H T, Olsson P, 2002, Local scour around circular piers under ice covers. Proceeding of the 16th IAHR International Symposium on Ice, International Association of Hydraulic Engineering Research, Dunedin, New Zealand.
2. Coleman S E, Lauchlan C S, Melville B W, 2003, Clear water scour development at bridge abutments, *Journal of Hydraulic Research*, 41(5): 521–531.
3. Dey S, Barbhuiya A K, 2005, Time variation of scour at abutments, *Journal of Hydraulic Engineering*, ASCE, 131 (1): 11-23.
4. Ettema Robert, Daly Steven F, 2004, Sediment transport under ice. ERDC/CRREL TR-04-20. Cold regions research and Engineering Laboratory, US Army Corps of Engineers.
5. Ettema Robert, Braileanu, F, Muste M, 2000, Method for estimating sediment transport in ice covered channels, *Journal of Cold Regions Engineering*, Vol. 14, No. 3, pp. 130-144.
6. Froehlich D C, 1989, Local scour at bridge abutments. Proc. Natl. Conf. Hydraulic Engineering, ASCE, 13-18.
7. Hains D B, 2004, An experimental study of ice effects on scour at bridge piers. PhD Dissertation, Lehigh University, Bethlehem, PA.

8. Hains Decker, Zabilansky Leonard, 2004, Laboratory test of scour under ice: Data and preliminary results. ERDC/CRREL TR-04-09. Cold regions research and Engineering Laboratory, US Army Corps of Engineers.
9. Hicks F, 2009, An overview of river ice problems: CRIPE 07 guest editorial Cold regions Science and Technology, 55: pp. 175-185.
10. Imhof D, 2004. Risk assessment of existing bridge structures. PhD thesis, University of Cambridge, UK.
11. Lau Y L, Krishnappan B G, 1985, Sediment transport under ice cover. Journal of Hydraulic Engineering, ASCE, 111(6), pp. 934-950.
12. Laursen E M, Toch A, 1956, Scour around bridge piers and abutments. Iowa Highway Research Board Bulletin, No 4.
13. Luigia Brandimarte, Paolo Paron, Giuliano Di Baldassarre, 2012, Bridge pier scour: a review of process, measurements and estimates. Environmental Engineering and Management Journal, Vol 11 (5).
14. Munteanu A, Frenette R, 2010, Scouring around a cylindrical bridge pier under ice covered flow condition-experimental analysis, R V Anderson Associates Limited and Oxand report.
15. Melville B W, 1992, Local scour at bridge abutments. Journal of Hydraulic Engineering, ASCE, Vol 118 (4), pp. 615-631.
16. Melville B W, 1997, Pier and Abutment scour: integrated approach, Journal of Hydraulic Engineering, ASCE, Vol 123(2): 125-136.
17. NCHRP Web-only Document 181, 2011, Evaluation of Bridge-Scour Research: Abutment and Contraction Scour Processes and Prediction. NCHRP Project 24-27(02).
18. Sui Jueyi, Wang Desheng, Karney B, 2000, Suspended sediment concentration and deformation of riverbed an a frazil jammed reach, Canadian Journal of Civil Engineering, Vol. 27, 1120-1129.
19. Sui Jueyi, Faruque M A A, Balanchandar Ram, 2009, Local scour caused by submerged square jets under model ice cover. Journal of Hydraulic Engineering, ASCE, Vol 135 (4), pp. 316-319.

20. Sui Jueyi, Afzalimehe Hossein, Samani A K, Meherani M, 2010a, Clear-water scour around semi-elliptical abutments with armored beds. *International Journal of Sediment Research*, Vol 25(3), pp.233-244.

21. Sui Jueyi, Wang Jun, He Yun, Krol Faye, 2010b, Velocity profile and incipient motion of frazil particles under ice cover. *International Journal of Sediment Research*, Vol 25(1), pp. 39-51.

22. Wang J, Sui J, Karney B, 2008, Incipient motion of non-cohesive sediment under ice cover – an experimental study. *Journal of Hydrodynamics*, Vol 20(1), pp. 177-124.

3.3 Scour morphology around bridge abutments with non-uniform sediment under ice cover

Sediment transport, including the erosion of river bed sediment, is a common problem in water resource management. Bridge abutments and piers in rivers are used to support the infrastructure of a bridge and are crucial for the safety of bridges. Bridge abutments extend perpendicularly from the bank into the river flow. The erosion around bridge structures can weaken the structural stability of a bridge and is a public safety concern.

Local scour refers to the erosion of sediment directly around infrastructure by running water. From an engineering perspective, determining the maximum scour depth is important so that provisions can be made in the design and construction (Chang, 2002). The local scour around bridge foundations is an important aspect of river hydraulic engineering as studies have shown that local scour has caused huge economic loss around the world. For example, in 1987, 17 bridges were destroyed in New York and New England and in Georgia in 1994 over 500 bridges were damaged due to the scouring during flood events (Richardson and Davis, 2001). Furthermore, a nation-wide study conducted by the US Federal Highway Administration, found that 75% of 383 bridge failures in 1973 involved abutment damage and 25% involved pier damage (Chang, 1973).

Over the past few decades, local scour around bridge abutments in open channels has received wide attention, and many researchers have conducted numerous studies on this topic (e.g., Laursen and Toch, 1956; Froehlich, 1989; Melville, 1997; Coleman et al, 2003; Dey 2005). These studies can be broadly grouped into two categories (Zhang, 2005). The first is the prediction of scour depth by using empirical or semi-empirical formulae based on field data or experimental data and the second method is based on numerical simulations. There are three main types of scour depth estimation formulae (Lim, 1997): 1) the regime approach, which relates the scour depth to the increased discharge or flow at the abutment; 2) the dimensional analysis, where relevant dimensionless parameters describing the scour are correlated (most of the past formulas are obtained from this way); and 3) analytical or semi-empirical approach, which is based on sediment transport relation between approach flow and increased shear stress at the abutment site.

Natural river beds are composed of non-uniform sediment (i.e., a large range in grain-size), however, very few studies recognize the influence of non-uniform bed sediment on the development and morphology of local scour holes (e.g., Wu et al. 2000; Sui et al. 2010a, Zhang et al. 2012). The direct result of non-uniform sediment transport in alluvial rivers is grain sorting. This can result in the formation of armor layer around the bridge abutment and influence the development and the morphology of scour holes.

In the northern regions of Canada, ice cover on rivers can present numerous engineering challenges as the ice cover can last for several months. River ice formation seasonally affects the water flow and sediment transport in alluvial channels. Field observations indicate that ice cover significantly affects velocity profiles and sediment transport processes in rivers (Figure 3.3-1). A solid ice cover can lead to an increased in the composite resistance and almost double the wetted perimeter. The armor layer and bed morphology of the local scour coupled with non-uniform sediments under ice cover has not been studied extensively.

There is little experimental research on the development and morphology of local scour around bridge abutments under ice cover with non-uniform sediments (Ackermann et al, 2002; Sui et al, 2009, 2010b). A small-scale flume experimental study in open channel with artificial non-uniform sediments was conducted by Sui et al. (2010) and another large-scale flume experiment with simulated ice cover was conducted in 2012 by the authors. The scour morphology of the local scour from these two studies is presented here. In addition, the grain size distribution was also measured around the bridge abutment in the second, large-scale, flume experiment.

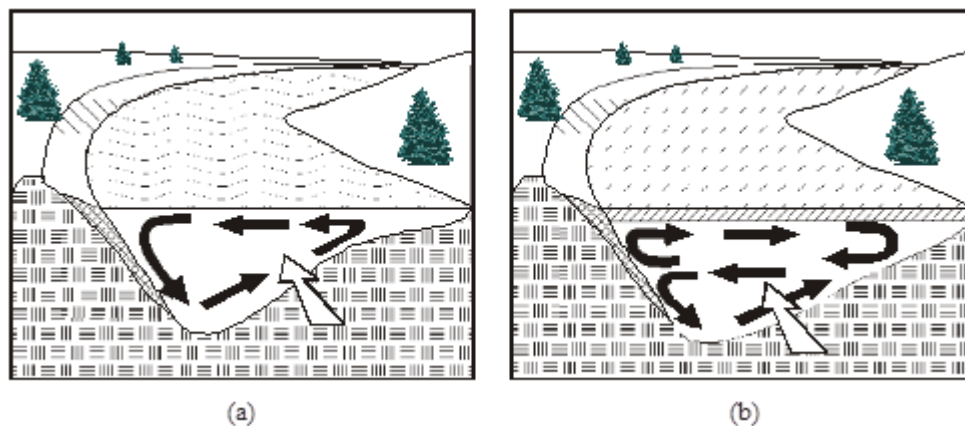


Figure 3.3- 1 A comparison of flow profiles with (a) and without (b) ice cover
(Reproduced from Ettema and Daly, 2004)

3.3.1 Methodology

Small-scale flume experiment

The first experiment was conducted in a 5.6m long, 0.31m wide, 0.4m deep recirculating flume (Sui et al., 2010a). The semi-circular abutment model was used (Figure 3.3-2) and the scour hole morphology was investigated under different flow conditions.

As shown in Figure 3.3-2, the semi-circular abutment was placed in a sediment box which has a dimension of 1m long, 0.3m wide and 0.1m deep. To study the impact of sediment grain size on the local scour development, two layers of uniform sediment with different grain-sizes were put in the sediment box. The flow rate in the flume was controlled by an inlet valve and flow dissipaters were used in front of the flume to reduce the turbulence. The semi-circular abutment model was leveled in the sand box and set against the flume wall. The flume was slowly filled to prevent a scour hole from developing prior to the initiation of the experiment. A weir was installed at the rear of the flume to control the depth of water in the flume and once the appropriate water depth was reached, the valve was adjusted to obtain the desired discharge. In this study, a constant flow depth 0.06m was maintained for each run. A pump was used to circulate the water from the reservoir back to the head.

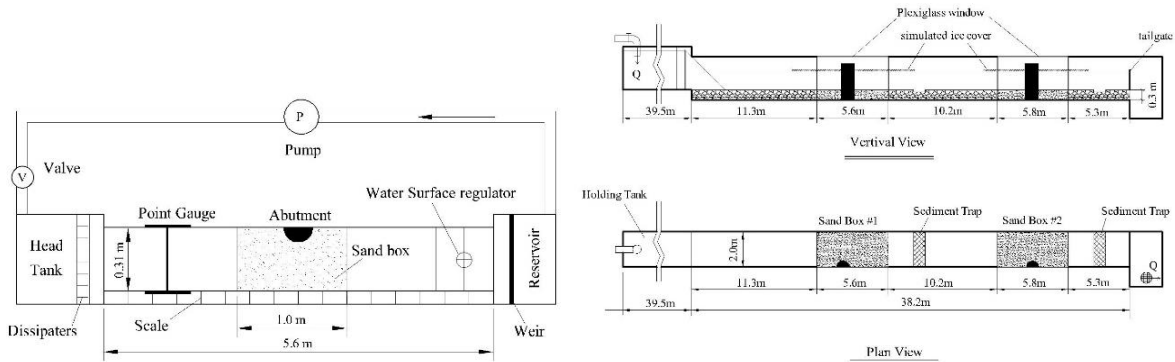


Figure 3.3- 2 The experimental setup of the small scale flume (left) and large scale flume (right)

Observation indicated that the time for achieving maximum scour depth in uniform sediments was approximately 12 hours. Herein, the running time ranges between 12 and 15 hours at which

point the maximum scour depth was carefully measured by using a point gauge with a resolution of $\pm 0.01\text{mm}$.

Table 3.3- 1 Experimental data of small scale flume experiments

H (m)	d (mm)	d_a (mm)	$3d_a$ (mm)	U (m/s)	d_s (m)
0.06	0.26	1.15	3.45	0.24	0.034
0.06	0.26	2.36	7.08	0.34	0.017
0.06	0.26	4.00	12.00	0.41	0.024
0.06	0.52	2.36	7.08	0.34	0.023
0.06	0.52	4.00	12.00	0.41	0.027
0.06	0.84	4.00	12.00	0.41	0.036
0.06	0.26	1.15	3.45	0.28	0.048
0.06	0.26	2.36	7.08	0.39	0.024
0.06	0.26	4.00	12.00	0.47	0.029
0.06	0.52	2.36	7.08	0.39	0.031
0.06	0.52	4.00	12.00	0.47	0.030
0.06	0.84	4.00	12.00	0.47	0.051
0.06	0.26	1.15	3.45	0.31	0.061
0.06	0.26	2.36	7.08	0.44	0.030
0.06	0.26	4.00	12.00	0.53	0.043
0.06	0.52	2.36	7.08	0.44	0.055
0.06	0.52	4.00	12.00	0.53	0.050
0.06	0.84	4.00	12.00	0.53	0.064

Uniform sediments have been used for the purpose of comparison. Three bed materials were used with diameter of 0.26mm, 0.52mm and 0.84mm. Coarse sediment with diameter (d_a) of 1.15mm, 2.34mm and 4.0 mm were overlain on top of the bed material to create an armor layer. From a previous study conducted by Froehlich (1995), the thickness of the armor layer has been designated as $3d_a$. The maximum scour depth of the local scour around bridge abutment are found in Table 3.3-1, in which H is the flow depth, d is the diameter of bed material, d_a is the

median diameter of the armor layer particle, U is the mean flow velocity and d_s is the scour depth near the abutment.

Large-scale flume experiment

The small-scale flume experiment has many advantages including ease of use, greater control of flow and bed conditions and lower power usage. However, compared to the natural rivers, small-scale flumes are not adequate to study the grain-size and ice cover impact on the bed morphology of the local scour. To overcome the limitations of a small-scale flume, a large-scale flume experiment was conducted in 2012. The setup of the large-scale flume can be found in Figure 3.3-2.

As shown in Figure 3.3-2, the flume has a dimension of 40m long, 2.0m wide and 1.3m deep. Two sand boxes with a depth of 0.3m were constructed 10.2m from each other. For the purpose of observing scouring process from outside of the flume, one side of the flume wall in the sand box was replaced by Plexiglass. The semi-circular abutment model was also made from Plexiglass with a radius of 20cm and 1.0m high.

In this large scale experiment, the ice cover was simulated by using styrofoam panel which covered the whole sand box area. To study the bed morphology under different ice covers, a rough ice cover was created by attaching small cubes of the Styrofoam to the underside of the simulated ice cover. The small cubes have a dimension of 2.5cm \times 2.5cm \times 2.5cm, with a spacing distance 3.5cm from each other.

Three different non-uniform sediments were used in this flume. The D_{50} of these three sediments were 0.58mm, 0.50cm, 0.47mm. It is important to note that the non-uniform sediment used here are natural sands which were purchased from a local aggregate mine. The velocity range in sand box 1 was 0.16 - 0.26m/s, while in sand box 2, the range is 0.14 - 0.21m/s. At the beginning of each experiment, the flume was slowly filled by adjusting the valves in the holding tank. To protect the scour from the initial filling of the flume, a template was made to cover the bed material. After the required water depth was reached, the template was removed to start the scouring process. Observations indicated that the running time to reach maximum scour depth around the semi-circular abutment was approximately 24 hours.

To measure the approaching velocity and flow profile around the bridge abutment, a SonTek IQ velocity meter was installed in front of the sand box. The velocity meter also provided flow depth, pressure and temperature. In the sand box, a staff gauge was installed for reading water depth directly. A 10MHz SonTek Acoustic Doppler Velocimeter (ADV) was also used at the end of each experiment to measure the flow field in the scour hole. The ADV measures the phase change caused by the Doppler Shift occurs when the signal reflects off the particles in the flow. The running condition of this large scale flume experiment can be found in Table 3.3-2.

Table 3.3- 2 Experimental data of small scale flume experiments

Running condition	D ₅₀ (mm)	Running time (h)	Flume width (m)	Water depth (m)	Approaching velocity (m/s)
Open channel	0.58	24	2	0.07	0.21
	0.58	24	2	0.19	0.23
	0.58	24	2	0.07	0.26
	0.50	24	2	0.07	0.21
	0.50	24	2	0.19	0.23
	0.50	24	2	0.07	0.26
	0.47	24	2	0.07	0.21
	0.47	24	2	0.19	0.23
	0.47	24	2	0.07	0.26
Smooth cover	0.58	24	2	0.07	0.23
	0.58	24	2	0.19	0.20
	0.58	24	2	0.07	0.20
	0.50	24	2	0.07	0.23
	0.50	24	2	0.19	0.20
	0.50	24	2	0.07	0.20
	0.47	24	2	0.07	0.23
	0.47	24	2	0.19	0.20
	0.47	24	2	0.07	0.20

Rough cover	0.58	24	2	0.07	0.20
	0.58	24	2	0.19	0.20
	0.58	24	2	0.07	0.22
	0.50	24	2	0.07	0.20
	0.50	24	2	0.19	0.20
	0.50	24	2	0.07	0.22
	0.47	24	2	0.07	0.20
	0.47	24	2	0.19	0.20
	0.47	24	2	0.07	0.22

3.3.2 Results and discussion

Local scour pattern and profile

At the end of each experiment, digital photos were taken for the small-scale flume experiment and for the large -scale flume experiment, the local scour was manually measured and then mapped using Surfer 10, Golden Software. The local scour patterns of the small-scale and large-scale flume experiments are compared in Figure 3.3-3.

As reported by Sui et al. (2010), in the small scale flume experiment, the coarse sediment tended to stay in the scour hole because due to the large mass compared to the fine-grained sediment and fine sediments were sheltered behind the coarse sediments. Because coarse particles need more energy to move to the downstream the development of an armor layer depends not only on the approaching velocity, but also the sediment grain size and the thickness of the armor layer. Depending on the conditions of approaching flow and armor layer, the armoring process occurs in the upstream portion of the scour hole. The sediment pile was highly compacted in the upstream portion of the scour area (Sui et al. 2010). However, the downstream portion of the scour was less compaction (Figure 3.3-3(a)).

Figure 3.3-3(a) shows the sediment redistribution around in the small scale flume in open channels. It was also noted that the scour close to the upstream toe area around the abutment was generally deeper. In the downstream side of the abutment, the local scour area is smaller compared to that from the upstream. The scouring process showed that the transport of fine

particles on the bed surface left the large particles that formed a stable armor layer on top of the scour hole.

Figure 3.3-3(b) - (d) showed the grain-size distribution and scour pattern in the large scale flume under ice cover. It was also found that with artificial non-uniform sediments in the small flume there was a thick accumulation of coarse sediment on top of the fine-grained sediment. In contrast, the natural non-uniform sediments, relatively thin ribbons of fine-grained sediment was observed in the scour hole, in-between the coarse sediments. As shown in Figure 3.3-3(c) and (d), the fine sediment ribbon is clearly marked.

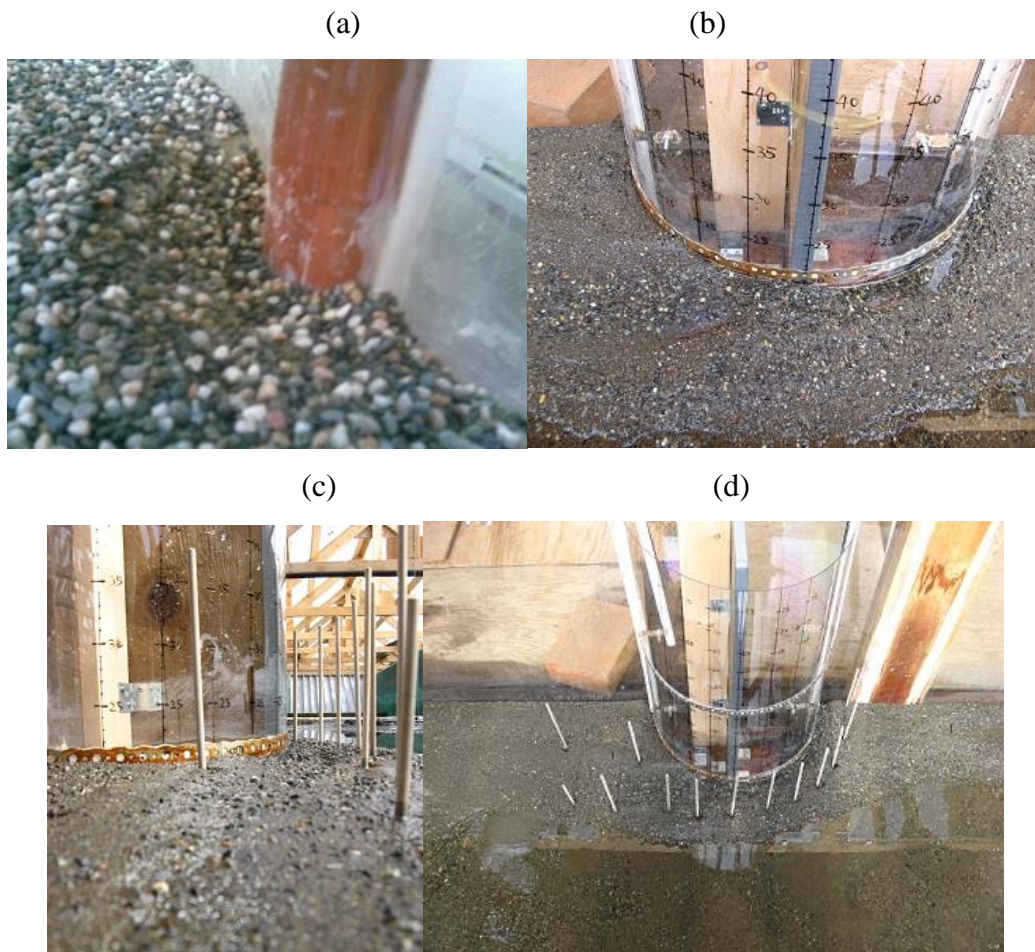


Figure 3.3- 3 (a) The local scour around the bridge abutment in the small-scale flume and
(b) (c) and (d) The local scour around the bridge abutment in the large scale flume

Sediment transport is governed by flow condition, which is often characterized by the bed shear stress and grain-size. From the classical sediment transport theory, fine-grained sediment are more mobile than coarse sediment. However, this conclusion can only be drawn if the material is uniform and the grains are surrounded by identical ones (Hunziker and Jaeggi, 2002). From the small scale flume experiment, with the artificial non-uniform sediment, the medium and coarse particles were also trapped in the scour hole due to their large mass. In the large scale flume under the natural non-uniform sediment, the armor layer was smaller compare to that in the small scale flume. At the same time, two fine sediment ribbons were noticed in the scour hole, which was not detected in the small scale flume experiments. To study the sediment distribution under ice cover, the sediment was sieved and analyzed.

Sediment size distribution around the abutment under ice cover

Properties of sediment include both individual particles and the sediment mixture as a whole. For particles, the size, shape and fall velocity are the main focus, while for sediment mixtures, the size distribution, specific weight, angle of response are part of interest. Due to the large variation in sands used in the large-scale flume experiment, this analysis will focus on samples using the sand with a $D_{50}=0.50$ mm.

For easy interpretation, one local scour contour in the large scale flume under ice cover was used here to illustrate the locations of sample collection. Figure 3.3-4 shows the 2D and 3D contour map of the local scour hole, two sediment samples were collected from L1 and L2. Samples from these two locations are shown in Figure 3.3-5. From Figures 3.3-4 and 3.3-5, the local scour along the abutment under ice cover with natural non-uniform sediments shows a similar trend of the local scour compared to the small-scale flume with artificial non-uniform sediment. The upstream toe area has a deeper scour depth compared to other areas, however, a fine sediment pile was found at location L2. This feature was not present in the small-scale flume experiment, which can illustrate the fine sediment deposition of the non-uniform sediment under ice cover.

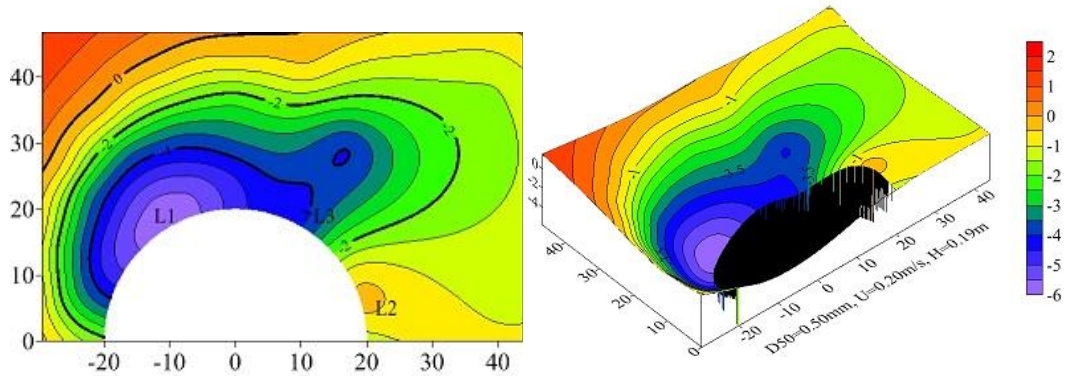


Figure 3.3- 4 The scour contour in the large scale flume



Figure 3.3- 5 The sediment samples L1 (left) and L2 (right)

Figure 3.3-5 shows the sediment sample collected from different locations along the semi-circular abutment. As shown in Figure 3.3-5, the sample in L1 was mainly coarse particles, and in contrast the sample from L2 was comprised mainly by fine sediments. Furthermore, it was observed from the cross section of the scour hole along the abutment is that in the scour hole there is a sudden elevation increase (Figure 3.3-6). To investigate if there is any different of sediment composition, samples were also collected at this location (L3).

The cumulative size distribution from L1, L2, L3 are plotted in Figure 3.3-7. For the purpose of comparison, the sand analysis of the original natural non-uniform sediment was also plotted. It can be found that from the figure that, due to the sediment deposition effect, fine particles were

mainly collected at location L2, while at L2, the large particles of armor layer accounts for most of the sample. However, at L3, the particles were the coarsest and this is likely due to the interaction of the abutment and ice cover. The primary vortex is decreasing before the point L3, while the wake vortex is the strongest at the point L3. Because of the interaction of these two vortices and ice cover, only large particles were trapped at location L3, most of the fine particles were removed by the running water and turbulent vortices. Unfortunately, the relationship between the vortices and sediment movement is difficult to elucidate due to the limited experimental data.

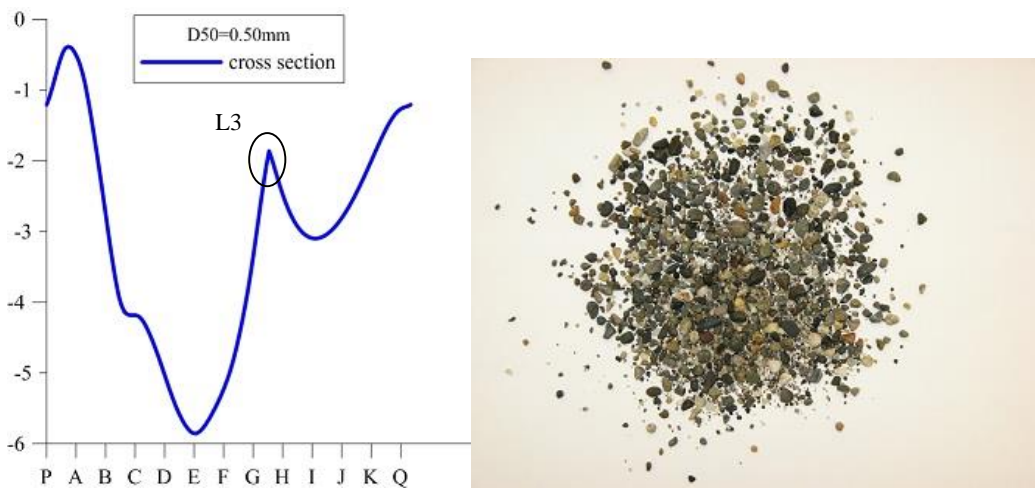


Figure 3.3- 6 The cross section of the local scour along the abutment (left) and samples collected (right)

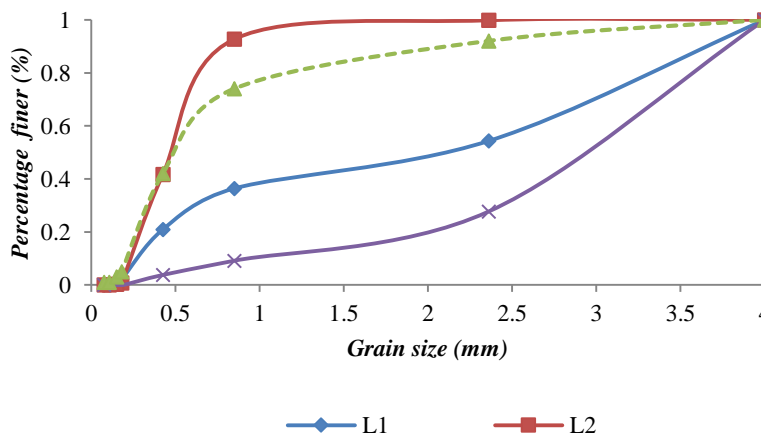


Figure 3.3- 7 The sand analysis of samples

The maximum scour depth analysis

Small scale flume

To study the impact of diameter of bed material on the maximum scour depth (d_s), the densimetric Froude number was used for the small-scale flume analysis, which can be defined in the following equation:

$$F_o = U / \sqrt{g\Delta\rho d} \quad (3.3-1)$$

In which, g is the gravitational acceleration, U_o is the approaching velocity, $\Delta\rho$ is mass difference between sediment and water, d is the diameter of the bed material.

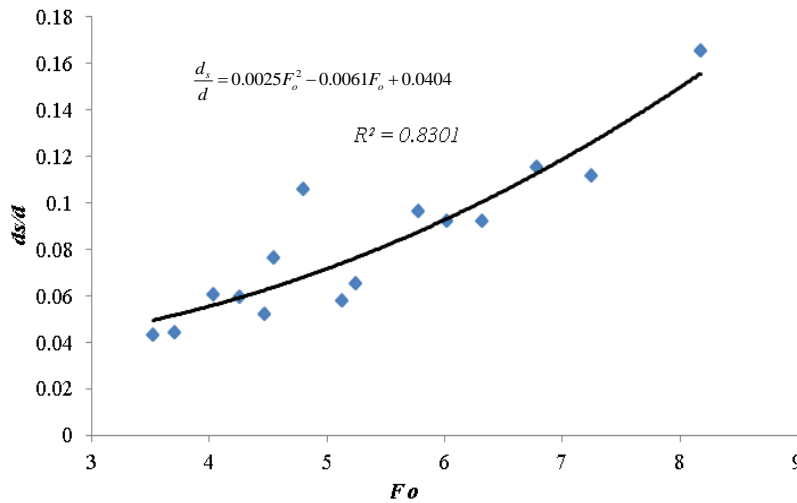


Figure 3.3- 8 The variation of scour depth with densimetric Froude number in small-scale flume

By plotting the maximum scour depth with the densimetric Froude number in the small scale flume, the following relationship can be found under open flow condition:

$$\frac{d_s}{d} = 0.0025F_o^2 - 0.0061F_o + 0.0404 \quad (3.3-2)$$

The maximum scour depth increases with an increase in densimetric Froude number. For natural non-uniform sediments in the large-scale flume, the following analysis was conducted.

Large scale flume

Similarly, under smooth ice cover in the large-scale flume, the maximum scour depth varied with the densimetric Froude number and the data are found in Figure 3.3-9. However, for natural non-uniform sediment the diameter of the bed material was replaced by the D_{50} . It can also be noted from Figure 3.3-8 and Figure 3.3-9 that, for natural non-uniform sediments, a small increase in the densimetric Froude number can change the maximum scour depth significantly compared to that in the artificial non-uniform sediment. In addition, this research demonstrates that the turbulence in the large-scale flume has a strong impact on the scour depth around semi-circular abutments.

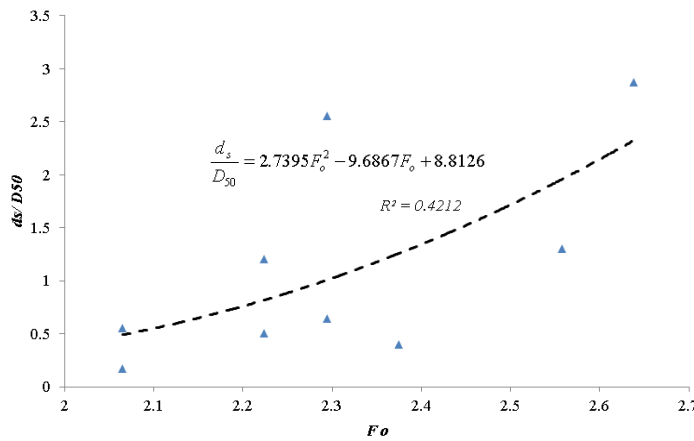


Figure 3.3- 9 The variation of scour depth under smooth ice cover in large scale flume

3.3.3 Conclusions

By using experimental data gained from two flume experiments on the local scour around semi-circular abutments, the bed morphology of the local scour with non-uniform sediment was examined. The small-scale flume experiment with the artificial non-uniform sediment showed the formation of an armor layer and significant erosion around the abutment. The large-scale flume experiment with natural non-uniform sediment showed that under ice cover, at different locations of the abutment, the sediment sorting process was more clear. The armor layer only forms in the scour hole while fine sediment deposition was located at the downstream of the abutment. One relationship of maximum scour depth with densimetric Froude number was also developed for the small scale flume experiment. However, due to the limitation of experimental

data, the relationship between ice cover roughness and sediment movement is not clear and further experimental data are needed to clearly assess this.

References

1. Ackermann N L, Shen H T, Olsson P, 2002, Local scour around circular piers under ice covers. Proceeding of the 16th IAHR International Symposium on Ice, International Association of Hydraulic Engineering Research, Dunedin, New Zealand.
2. Chang F F M, 1973, A statistical summary of the cause and cost of bridge failures. Office of Research, Federal Highway Administration, Washington D C, US.
3. Chang H H, 2002, Fluvial processes in river engineering, Reissue 2002, Krieger Publishing Company, Krieger Drive, Malabar, Florida, pp. 80-104.
4. Coleman S E, Lauchlan C S, Melville B W, 2003, Clear water scour development at bridge abutments, Journal of Hydraulic Research, 41(5), pp. 521–531.
5. Dey S, Barbhuiya A K, 2005, Time variation of scour at abutments, Journal of Hydraulic Engineering, ASCE, 131 (1), pp. 11-23.
6. Ettema R, Daly S F, 2004, Sediment transport under ice, Cold Regions Research and Engineering Laboratory, ERDC/CRREL TR-04-20, pp. 8.
7. Froehlich D C, 1989, Local scour at bridge abutments. Proc. Natl. Conf. Hydraulic Engineering, ASCE, pp. 13-18.
8. Laursen E M, Toch A, 1956, Scour around bridge piers and abutments. Iowa Highway Research Board Bulletin, No 4.
9. Lim S Y, 1997, Equilibrium clear-water scour around an abutment, Journal of Hydraulic Engineering, 123(3), pp. 237-243.
10. Melville B W, 1997, Pier and Abutment scour: integrated approach, Journal of Hydraulic Engineering, 123(2), pp. 125-136.
11. Richardson E V, Davis S R, 2001, Evaluating scour at bridges. HEC18 FHWA NHI-001, Federal Highway Administration, US Department of Transportation, Washington, DC.
12. Sui J, Faruque M A A, Balanchandar R, 2009, Local scour caused by submerged square jets under model ice cover. Journal of Hydraulic Engineering, ASCE, Vol 135 (4), pp. 316-319.

13. Sui J, Afzalimehr H, Samani A K, Maherani M, 2010a, Clear water scour around semi-elliptical abutments with armored bed, *International Journal of Sediment Research*, Vol. 25, No. 3, pp. 233-244.
14. Sui J, Wang J, He Y, Krol F, 2010b, Velocity profile and incipient motion of frazil particles under ice cover. *International Journal of Sediment Research*, Vol 25(1), pp. 39-51.
15. Wu W, Wang S, Jia Y, 2000b, Non-uniform sediment transport in alluvial rivers, *Journal of Hydraulic research*, 38(6), pp. 427-434.
16. Zhang H, 2005, Study of flow and bed evolution in channels with spur dykes, PhD Dissertation, Ujigawa Hydraulics Laboratory, Kyoto University, Japan.
17. Zhang H, Nakagawa H, Mizutani H, 2012, Bed morphology and grain size characteristics around a spur dike, *International Journal of Sediment Research*, Vol. 27, No. 2, pp. 141-157.

3.4 Armor layer analysis of local scour around bridge abutments under ice cover

Local scour is the erosion of sediments in the vicinity of bridge foundations. Depending on if there is a sediment supply from approaching flow, the scour can be categorized as either clear water scour or live-bed scour (Barbhuiya and Dey, 2004). Clear water scour occurs with the absence of sediments transported from upstream while live-bed scour takes place when the scour hole is continuously fed with sediments by the approaching flow.

Local scour is a challenging problem for hydraulic engineers. Most existing studies are conducted in small scale flumes with uniform sediment. Natural river beds are composed of a mixture of different sizes of sand and gravel. Very few studies use natural sand due to its complexity. The finer materials will be transported faster than the coarser materials under the same flow conditions, and the remaining bed material becomes coarser. This coarsening process is stopped once a layer of coarse material completely covers the river bed and protects the finer materials beneath it from being transported. After this process is completed, the river bed is armored and the coarser layer is called armor layer (Yang, 2003).

The incipient velocity for non-uniform sediments varies more in comparison to that of uniform sediment. Advances in the non-uniform sediment movement play a key role in theoretical analysis and engineering practice pertaining to channel and reservoir design, physical sediment model analysis and numerical simulation (Xu et al, 2008).

Meyer-Peter and Mueller (1948) defined the formula describing armor layer sediment size by using one mean grain size of the bed to calculate the sediment size in the armor layer. The following equation was developed.

$$d = \frac{SD}{K_1 \left(n / d_{90}^{1/6} \right)^{3/2}} \quad (3.4-1)$$

where d is the sediment size in the armor layer, S is the channel slope, D is the mean flow depth, K_1 is a constant equal to 0.058 when D is in meters; n is the channel bottom roughness or Manning's roughness, and d_{90} is the bed material size where 90% of the material is finer. Yang (1973) developed his criteria by using the approach velocity to illustrate the incipient motion. For open channels, the logarithmic law for velocity distribution is applied. However, in his equation, the relative roughness effect was treated as constant due to insufficient data. Kuhnle

(1993) conducted flume experiments on the incipient motion of gravel and sand mixtures with different ratios. By calculating critical shear stress for incipient motion, it was found that for gravel-sand mixtures, the gravel showed an increasing critical bed shear stress with increasing grain size. Dey and Barbhuiya (2004) examined clear water scour at abutments in armored beds. It was found that the scour depth with an armor layer in clear water scour is always greater than that without armor layer for the same bed sediment. Around bridge piers, Dey and Raika (2007) noticed that the scour depth with an armor layer is less than that without an armor layer for the same bed sediments when the scour hole is shielded by a compact secondary armor layer. Some recent relevant work on the non-uniform sediment transport can also be found from Khullar et al. (2010) and Jha et al. (2011). Guo (2012) gave a critical review of pier scour in clear water for non-uniform sediments. The flow-structure-sediment factors were analyzed systematically and several empirical equations were reviewed. Zhang et al. (2012) found that the mean grain size and geometric standard deviation of the bed sediments are two important and practical parameters in characterizing the changes in bed morphology and composition around spur dikes. Furthermore, river ice seasonally affects the flow distribution and results in a change in sediment transport in natural rivers around bridge foundations. The impact of ice cover on sediment transport is important for cold regions in the northern hemisphere. The velocity field changes significantly under ice cover due to the presence of an extra boundary layer. As identified by Melville (1992), the primary vortex, together with the down flow are the principal causes of local scour around bridge abutments. With the presence of ice cover, the down flow can be increased, which also increases the sediment transport around bridge abutments.

Regarding the effects of river ice on scour and sediment transport, studies such as Ackermann et al. (2002), Hains (2004), Hains and Zabilansky (2004), Munteanu (2004), Andre and Tran (2012) pointed out that combination of increased ice cover roughness and pressure flow resulted in a larger scour depth. Smith and Ettema's (1997) experiments showed that the two layer assumption was especially inadequate for characterizing flow resistance and sediment transport rates. Ettema et al. (2000) developed a new method for estimating sediment transport and identified the importance of assessing flow resistance attributable to bed surface drag. Li (2012) obtained field estimates of the composite Manning's coefficient associated with ice cover. By using four different methods, winter measurements of ice covered rivers in Canada were analyzed. The results show that the composite Manning's coefficient ranges from 0.013 to 0.040. The results

are useful for modeling ice covered river flow and determining the sediment transport under ice cover.

To date, there is still no research connecting the non-uniform sediment and ice cover. In this research, three non-uniform sediments and two types of ice cover are applied to study the armor layer in the scour hole as well as the impacts of ice cover on the maximum scour depth.

3.4.1 Methodology

One large scale flume was used in this study. The set-up of the flume is indicated in Figure 3.4-1. The flume was 2m wide, 1.3m deep and 38.2m long. Two 0.3m deep sand boxes were created to hold non-uniform sediment. The flume was covered with treated waterproof plywood acting as a false river bed. To compare the shape factor of the abutment as recognized by Melville (1992), two abutments were made from Plexiglass. On the outside surface of the abutment, different measuring lines have been drawn for the purpose of comparing scour profiles at different locations (Figure 3.4-2). For the square abutment, the upstream surface and corner B are the locations of the maximum scour depth from previous studies, so four equal distance lines were made along the upstream surface. While for the semi-circular abutment, 12 lines having an equal central angle of 15° were drawn which are used when describing the scour depth along the abutment.

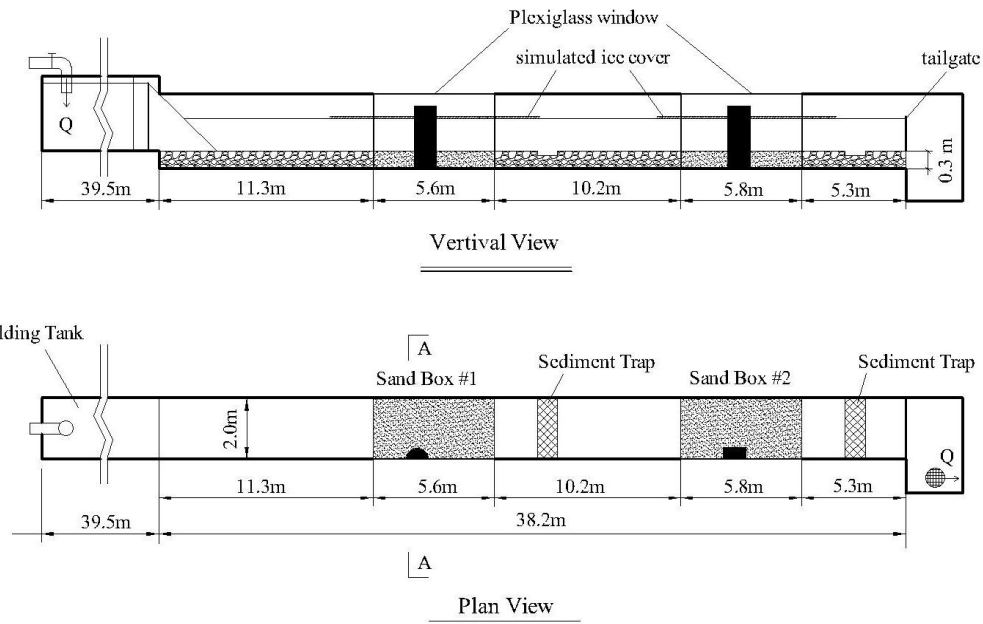


Figure 3.4- 1 The layout of the experimental large scale flume

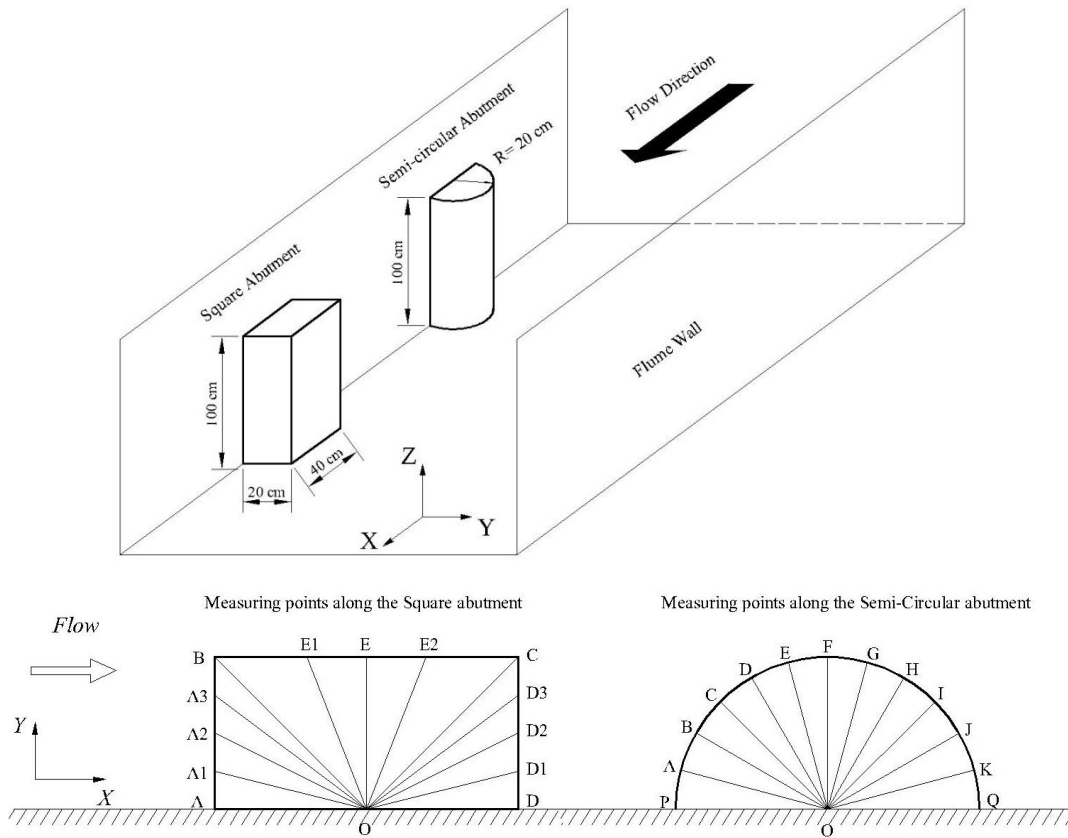


Figure 3.4- 2 Dimensions and measuring points of abutments

Three natural non-uniform sediment mixtures were used in this study. The D_{50s} were 0.58mm, 0.50mm and 0.47mm respectively, with geometric standard deviation (σ_g) of 2.61, 2.53 and 1.89. For all the three sediments, the value of σ_g is larger than 1.4, which can be treated as non-uniform sediments (Dey and Barbhuiya, 2004). Two types of ice covers were used, namely smooth cover and rough cover. Smooth ice cover was constructed from Styrofoam, while the rough ice cover is modified by attaching small cubes to underside of the smooth cover. The small cubes have a dimension of 2.5cm \times 2.5cm \times 2.5cm, with spacing of 3.5cm from each other (Figure 3.4-3).



Figure 3.4- 3 Experimental flume set up and rough ice cover (up); Armor layer around the square abutment corner (bottom)

A 10 MHz SonTek Acoustic Doppler Velocimeter (ADV) was used to measure the flow field at the end of each experiment, which had the equilibrium scour depth. The sampling frequency for ADV was 25Hz. After each experiment, photos of the local scour around the abutment were taken. After measurement was completed, sediment samples from different scour locations were collected. For the square abutment, samples from corner B were collected and for semi-circular abutment samples from location E to F were collected. Additionally, sediment samples from the downstream fine sediment ridge were collected for the purpose of comparison with armor layer. Surface sampling was used in accordance with Ettema (1984). The thickness of the natural armor layer varies from d to $3d$, in which d is the particle size of armor layer (Froehlich, 1995). For this study, surface samples were collected by a small scoop. At the end of each experiment, sediments in the armor layer were sieved and analyzed. The bottom elevations were measured by using the measuring lines on the abutment. The scour contours were plotted using Surfer 10, Golden Software. In all, 54 experiments have been carried out. The experimental conditions are presented in Table 3.4-1.

Table 3.4- 1 Test condition and non-uniform sediment composition of each experiment

Abutment type	Cover condition	D ₅₀ (mm)	D ₁₆ (mm)	D ₈₄ (mm)	D ₉₀ (mm)	depth (m)	Average velocity (m/s)
Square abutment	Open channel	0.58	0.28	1.91	2.57	0.07	0.26
		0.58	0.28	1.91	2.57	0.07	0.21
		0.58	0.28	1.91	2.57	0.19	0.21
		0.50	0.26	1.66	2.09	0.07	0.26
		0.50	0.26	1.66	2.09	0.07	0.21
		0.50	0.26	1.66	2.09	0.19	0.21
		0.47	0.23	0.82	1.19	0.07	0.26
		0.47	0.23	0.82	1.19	0.07	0.21
		0.47	0.23	0.82	1.19	0.19	0.21
	Smooth cover	0.58	0.28	1.91	2.57	0.07	0.20
		0.58	0.28	1.91	2.57	0.19	0.16
		0.58	0.28	1.91	2.57	0.07	0.23
		0.50	0.26	1.66	2.09	0.07	0.20
		0.50	0.26	1.66	2.09	0.19	0.16
		0.50	0.26	1.66	2.09	0.07	0.23
		0.47	0.23	0.82	1.19	0.07	0.20
		0.47	0.23	0.82	1.19	0.19	0.16
		0.47	0.23	0.82	1.19	0.07	0.23
	Rough cover	0.58	0.28	1.91	2.57	0.07	0.22
		0.58	0.28	1.91	2.57	0.07	0.20
		0.58	0.28	1.91	2.57	0.19	0.14
		0.50	0.26	1.66	2.09	0.07	0.22
		0.50	0.26	1.66	2.09	0.07	0.20
		0.50	0.26	1.66	2.09	0.19	0.14
		0.47	0.23	0.82	1.19	0.07	0.22
		0.47	0.23	0.82	1.19	0.07	0.20

		0.47	0.23	0.82	1.19	0.19	0.14
Semi-circular Abutment	Open channel	0.58	0.28	1.91	2.57	0.07	0.21
		0.58	0.28	1.91	2.57	0.19	0.23
		0.58	0.28	1.91	2.57	0.07	0.26
		0.50	0.26	1.66	2.09	0.07	0.21
		0.50	0.26	1.66	2.09	0.19	0.23
		0.50	0.26	1.66	2.09	0.07	0.26
		0.47	0.23	0.82	1.19	0.07	0.21
		0.47	0.23	0.82	1.19	0.19	0.23
		0.47	0.23	0.82	1.19	0.07	0.26
	Smooth cover	0.58	0.28	1.91	2.57	0.07	0.23
		0.58	0.28	1.91	2.57	0.19	0.20
		0.58	0.28	1.91	2.57	0.07	0.20
		0.50	0.26	1.66	2.09	0.07	0.23
		0.50	0.26	1.66	2.09	0.19	0.20
		0.50	0.26	1.66	2.09	0.07	0.20
		0.47	0.23	0.82	1.19	0.07	0.23
		0.47	0.23	0.82	1.19	0.19	0.20
		0.47	0.23	0.82	1.19	0.07	0.20
	Rough cover	0.58	0.28	1.91	2.57	0.07	0.20
		0.58	0.28	1.91	2.57	0.19	0.20
		0.58	0.28	1.91	2.57	0.07	0.22
		0.50	0.26	1.66	2.09	0.07	0.20
		0.50	0.26	1.66	2.09	0.19	0.20
		0.50	0.26	1.66	2.09	0.07	0.22
		0.47	0.23	0.82	1.19	0.07	0.20
		0.47	0.23	0.82	1.19	0.19	0.20
		0.47	0.23	0.82	1.19	0.07	0.22

3.4.2 Results and discussion

Scour morphology and geometry

Figure 3.4-3 shows the experimental setup, local scour morphology and armor layers around the abutments. Figure 3.4-4 shows the contour plotted by Surfer 10 around both square and semi-circular abutment.

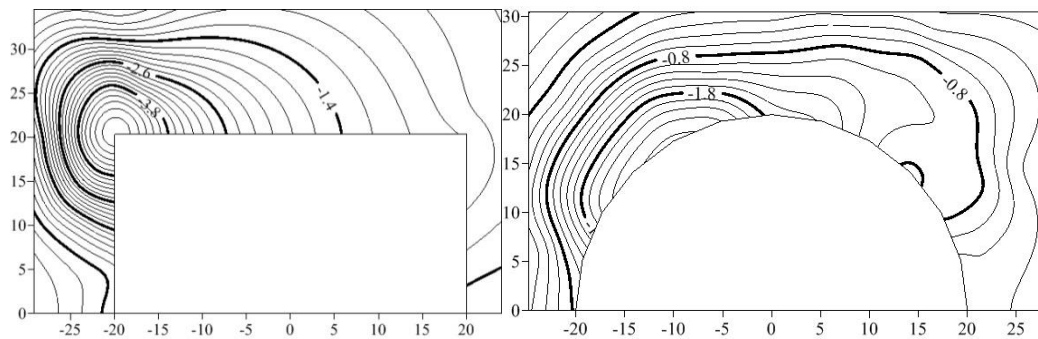


Figure 3.4- 4 Typical local scour contour around square abutment (left) and semi-circular abutment (right)

The geometry of the scour holes under both open channel and ice covered channel share some common features. For the square abutment, two scour holes were developed in the scouring process, one located in corner B, which is also where the maximum scour depth is located. The other smaller scour hole is located at corner C (Figure 3.4-2). For the semi-circular abutment, the maximum scour depth is located between E and F (Figure 3.4-2). For both square and semi-circular abutments, the maximum scour depth is located between 45 to 60 degrees facing the approaching flow. Figure 3.4-3 shows one typical non-uniform scour hole around the square abutment.

As shown in Figure 3.4-3, the scour hole is not completely covered by an armor layer. There are two fine sediment ribbons extending downstream from the main scour hole. For the armor layer development, an earlier formation of the armor layer is detected in the upstream section. Due to the interaction between primary vortex and wake vortex behind the abutment, the geometry of the scour area in the upstream differs substantially from that in the downstream.

Noted by Sui et al. (2010b), the point of the maximum velocity is located at 60% of water depth for smooth ice cover, while 70% under rough ice cover. Due to movement of the maximum

velocity in the transverse direction, stronger turbulence can be generated around the abutment under ice covers. It is also interesting to note that, under the same flow conditions, the area of the armor layer under ice cover is larger than that under open channels. Meanwhile, under rough ice cover, the armor layer area is the largest and extends the longest distance downstream comparing that of smooth ice cover. While in open channels, the armor layer has the smallest area and shortest distance from the abutment.

For non-uniform sediment transport under ice cover, Ettema (2002) mentioned that an imposed ice cover results in an increased composite resistance. The maximum velocity is located between the cover and channel bed, with its vertical location depended on the relative resistance coefficients of the channel bed and cover. With rough ice cover, the location of maximum velocity is lower than that with smooth ice cover and open channel because of the relative large roughness coefficient. Our data of maximum scour depth under rough cover and smooth cover supports the above conclusions.

Grain size analysis of armor layer

In the experimental research, three non-uniform sediments were used. Figure 6-5 shows the sieve analysis of the three sediments. According to United States Standard Test Sieve procedure, the following sieves were selected for the analysis: 4.0mm, 2.0mm, 0.85mm, 0.5mm, 0.25mm, 0.15mm, 0.063mm. The distribution curves were plotted as the “percentage-finer-than” curve; D_{50} , D_{16} , D_{84} , D_{90} are calculated from curves (Figure 3.4-5).

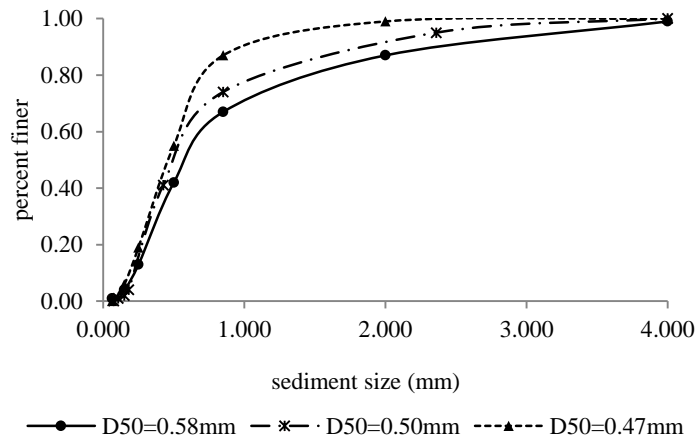
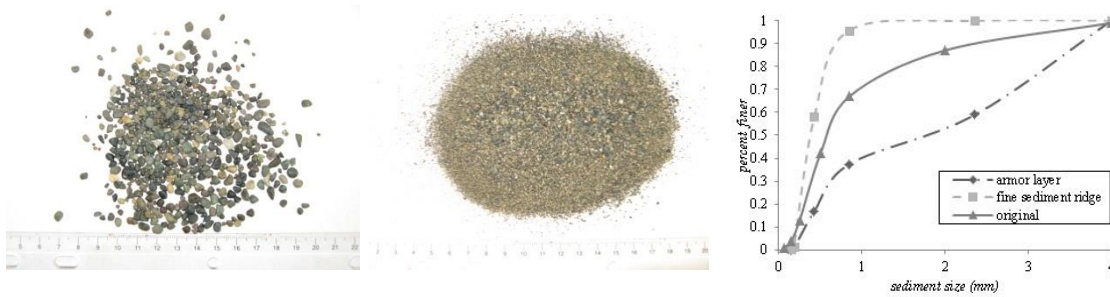


Figure 3.4- 5 Distribution curves for the non-uniform sediment

The armor layer initiated its development from the toe area and then extended to the downside of the abutment. One can see from Figure 3.4-3 that the armor layer covers the outside of the scour hole. However, because the maximum scour depth is located in the upstream of the abutment, only the samples from the larger scour hole were analyzed for this paper. Figure 3.4-6 shows sediment samples of the armor layer and fine sediment deposition of the three uniform sediments. The armor layer generated in $D_{50}=0.58\text{mm}$ sediment is covered by coarser particles. Meanwhile, coarse particles are also found in fine sediment ridge. With the decreasing of D_{50} , more fine sediments can be found in armor layer while less coarse particles are found in the fine sediment ridge. As smaller D_{50} s have less coarse particles, the sediment size in the armor layer decreases. Smaller particles in the armor layer will provide less protection in the river bed around the bridge abutment. A smaller grain size in the armor layer can result in a deeper scour depth.

Samples of armor layer in scour hole samples of deposition of the ridge distribution curve

(a) $D_{50}= 0.58\text{mm}$



(b) $D_{50}= 0.50\text{mm}$



(c) $D_{50}= 0.47\text{mm}$



Figure 3.4- 6 Samples of armor layer, fine sediment ridge and related distribution curves

Effect of armor layer on maximum scour depth

Zhang et al. (2012) pointed out that the extent of the scour hole exhibits a strong relationship with the D_{90} . The maximum scour depth and scour volume decrease with an increase of the D_{90} around a spur dike. Dimensional analysis is used to study the relationship of sediment size of the armor layer and the maximum scour depth.

Dimensional analysis provides a convenient way for building a framework for parameters on which the maximum scour depth depends. Given the complexity of the interaction of various parameters, NCHRP (2011) identified five major groups of dimensionless parameters affecting the maximum scour depth: flow intensity, Froude number, sediment size, abutment and flow geometry, flow distribution and the abutment stability parameter. In this framework, the influence of non-uniform sediment size is unclear, and the roughness of ice cover is not considered. Herein, the maximum scour depth around bridge abutments depends on the following parameters in this study.

$$d_{\max} = f(U, \rho, \rho_s, g, d, n_b, n_i, D_{50}, l, B, H) \quad (3.4-2)$$

where d_{\max} is the maximum scour depth around the abutment; U is the mean approach velocity; ρ and ρ_s is the density of the water and non-uniform sediment respectively; d is the armor layer grain size; n_b is the Manning's coefficient for the channel bed; n_i is the Manning's coefficient of ice cover roughness; D_{50} represents the median grain size; l is the width of the abutment; B is the width of the flume, and H is the approaching flow depth.

For a flow-sediment mixture, the terms g , ρ , and ρ_s should not appear as independent parameters. Additionally, abutment blockage ratio is also kept constant in this study. Equation 3.4-1 is used

to calculate the armor layer sediment size d . Since the armor layer sediment size is the main interest here, d is used in the calculation of the densimetric Froude number.

$$F_o = U / \sqrt{(\rho_s / \rho - 1)gd} \quad (3.4-3)$$

Equation 3.4-2 can be simplified as the following:

$$\frac{d_{\max}}{d} = A(F_o)^a \left(\frac{D_{50}}{d}\right)^b \left(\frac{n_i}{n_b}\right)^c \left(\frac{H}{d}\right)^d \quad (3.4-4)$$

The densimetric Froude number represents the interaction of sediment and flow, D_{50}/d represents the impact of sediment composition on the armor layer particle size, n_i/n_b represents the ice cover roughness and channel bed roughness, and H/d represents the relationship between approaching flow depth to the armor layer particle size.

In all, 54 experiments on the local scour around bridge abutments were conducted, while 18 of which were under open channels for comparison. Under open channels, the ice cover roughness is treated as 0, and Equation 3.4-4 can be written as:

$$\frac{d_{\max}}{d} = A(F_o)^a \left(\frac{D_{50}}{d}\right)^b \left(\frac{H}{d}\right)^d \quad (3.4-5)$$

To study the impact of the independent variables, namely F_o , D_{50}/d , H/d , and n_i/n_b , the following analysis was conducted.

Figures 3.4-6 and 3.4-7 indicate the variation of maximum scour depth to the densimetric Froude number. With the increase in F_o , the value d_{\max}/d increases correspondingly. Around both square and semi-circular abutments, under the same densimetric Froude number, the rough ice cover has the largest relative maximum scour depth. Due to the limitations of experimental data in open channels, the data points around the semi-circular abutment are not as clear as that around square abutment. However, from Figure 3.4-7, under rough ice cover conditions, the scour depth still has the highest value compared to that with smooth ice cover and open channel conditions.

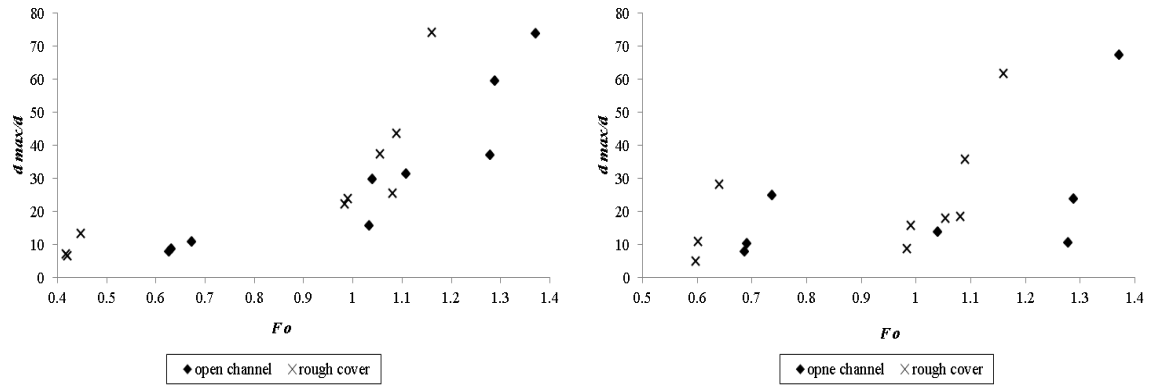


Figure 3.4- 7 Variation of maximum scour depth with F_o at square abutment (left) and semi-circular abutment (right)

Figures 3.4-8 and 3.4-9 compare the variation of the maximum scour depth with different sediment composition and approaching flow depth. Even with the limited experimental data around the semi-circular abutment, an increasing trend is still present for both the square and semi-circular abutment. With the increase in relative flow depth, the maximum scour depth increase correspondingly. Moreover, the square abutment results in a larger scour depth than that of semi-circular abutment under same flow conditions.

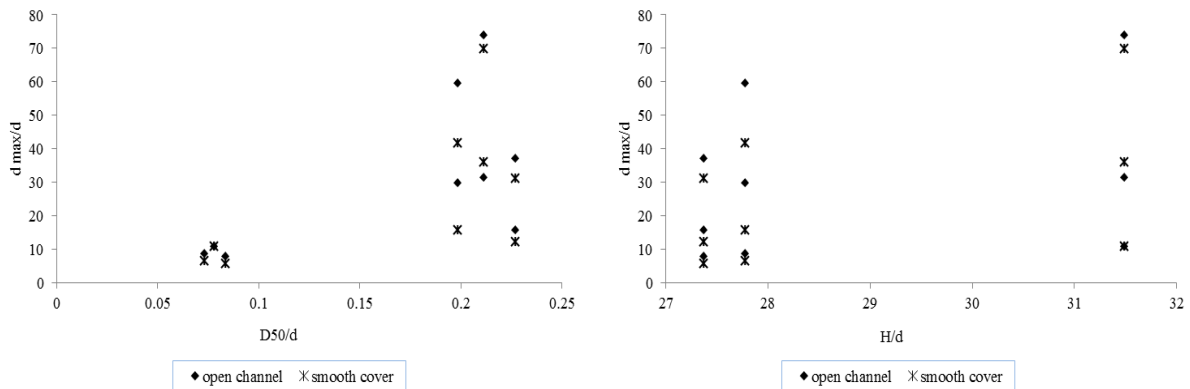


Figure 3.4- 8 Variation of the maximum scour depth with related variable around square abutment

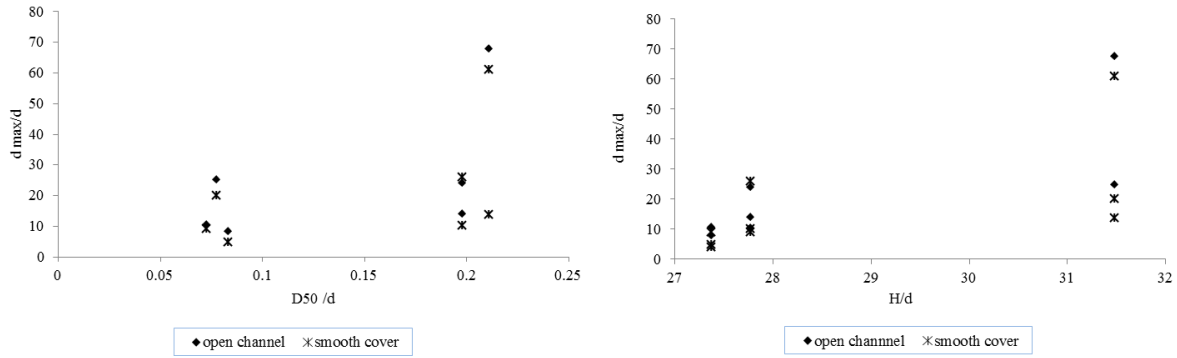


Figure 3.4- 9 Variation of the maximum scour depth with related variable around semi-circular abutment

Figures 3.4-10 and Figure 3.4-11 show the regression relationship of the above variables around the square and semi-circular abutments respectively. For both types of abutments, the rough ice cover leads to a greater dimensionless maximum scour depth compared to that under smooth ice cover and open channel. The slope in the figures 3.4-10 and 3.4-11 indicates that ice covered flow has a large slope compared to that of the open channel.

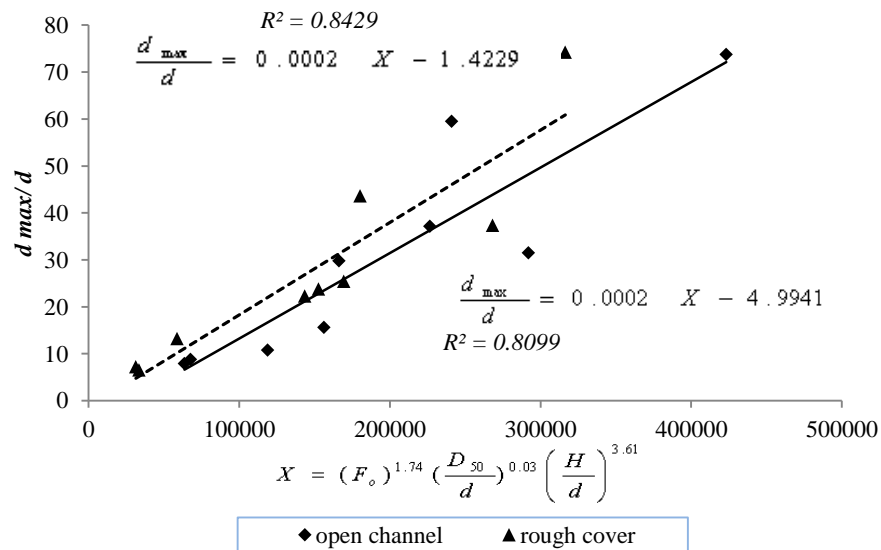


Figure 3.4- 10 Dependence of the maximum scour depth on related variables around square abutment

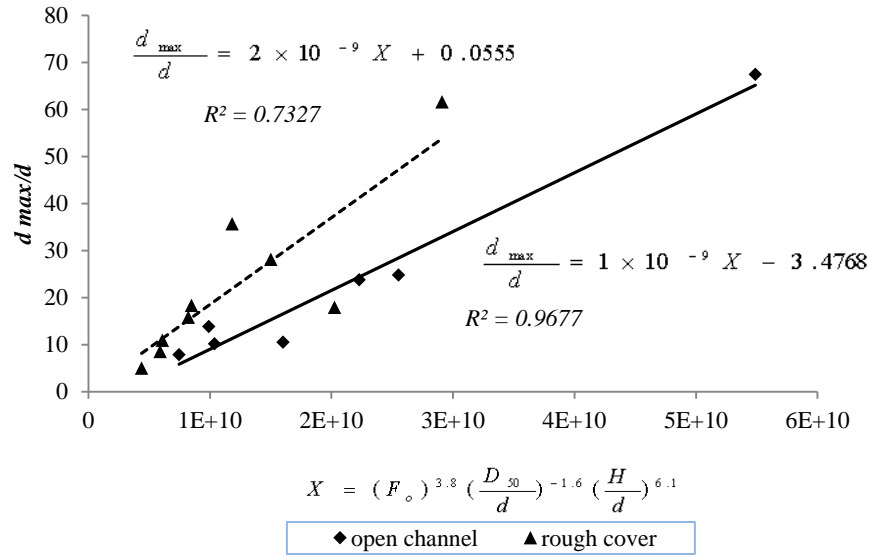


Figure 3.4- 11 Dependence of the maximum scour depth on related variables around the semi-circular abutment

Additionally, under both rough and smooth ice covered conditions, the slope in the scour hole is same for both abutments, while the slope under open channel is smaller. However, under open channel conditions, the semi-circular abutment results in a small slope compared to the square abutment. The following regression relationships are derived.

Around square abutment:

Open channel:

$$\frac{d_{\max}}{d} = 0.0002(F_o)^{1.74} \left(\frac{D_{50}}{d}\right)^{0.03} \left(\frac{H}{d}\right)^{3.61} - 4.9941 \quad (3.4-6)$$

Smooth cover:

$$\frac{d_{\max}}{d} = 0.0002(F_o)^{1.74} \left(\frac{D_{50}}{d}\right)^{0.03} \left(\frac{H}{d}\right)^{3.61} - 5.5206 \quad (3.4-7)$$

Rough cover:

$$\frac{d_{\max}}{d} = 0.0002(F_o)^{1.74} \left(\frac{D_{50}}{d}\right)^{0.03} \left(\frac{H}{d}\right)^{3.61} - 1.4229 \quad (3.4-8)$$

Around semi-circular abutment:

Open channel:

$$\frac{d_{\max}}{d} = 1 \times 10^{-9} (F_o)^{3.8} \left(\frac{D_{50}}{d}\right)^{-1.6} \left(\frac{H}{d}\right)^{6.1} - 3.4768 \quad (3.4-9)$$

Smooth cover:

$$\frac{d_{\max}}{d} = 2 \times 10^{-9} (F_o)^{3.8} \left(\frac{D_{50}}{d}\right)^{-1.6} \left(\frac{H}{d}\right)^{6.1} - 5.2705 \quad (3.4-10)$$

Rough cover:

$$\frac{d_{\max}}{d} = 2 \times 10^{-9} (F_o)^{3.8} \left(\frac{D_{50}}{d}\right)^{-1.6} \left(\frac{H}{d}\right)^{6.1} + 0.0555 \quad (3.4-11)$$

Equations 3.4-6 to 3.4-11 show that H/d has strongest impact on the maximum scour depth compared to other variables. From the derived relationships both the densimetric Froude number (variable index 1.74 and 3.8) and approaching flow depth (variable index 3.8 and 6.1) have stronger impacts on the maximum scour depth than D_{50}/d .

D_{50}/d has the smallest impact for both square and semi-circular abutments. For non-uniform sediments, if the particle size of the armor layer is larger, then the maximum scour depth around bridge abutments is smaller under the same flow conditions. In the practical engineering field, H/d has a relatively large value compared to F_o and D_{50}/d . However, the impact of D_{50}/d is still not neglected for the consideration of maximum scour depth estimation.

Ice roughness and the armor layer

Research on channel roughness has been conducted; however, for calculating ice cover roughness, there are still very few studies that can be referred.

Carey (1966) calculated Manning's roughness coefficient as 0.01~0.0281 by using supporting field data related to the observed characteristics of the underside of ice cover. From his calculation, a constant roughness of 0.0251 was used for the winter period. For this study, for smooth ice cover, the Manning's coefficient of 0.013 was adapted by referring to Mays (1999). For this study, the rough ice cover was created by attaching small cubes with dimensions of 2.5cm×2.5cm×2.5cm. Equation 12 is applied to calculate the Manning's coefficient for rough ice cover by considering the roughness height of the ice cube (Li, 2012).

$$n_i = 0.039k_s^{1/6} \quad (3.4-12)$$

in which k_s is the average roughness height of the ice under side. By using the above equation, the rough ice cover has a Manning's coefficient of 0.021, which falls within the ranges mentioned by Carey (1966). For non-uniform sediment composition with significant portions of coarse-grain sizes, the channel bed roughness is calculated by using the following equation from Hager (1999):

$$n_b = 0.039D_{50}^{1/6} \quad (3.4-13)$$

The values of d_{\max}/d were compared for both smooth and rough cover under almost the same conditions in Figure 6-12. Rough cover causes a greater scour depth compared to open channel around both abutments. However, in some of tests, higher velocity was applied under smooth cover, which caused a larger dimensionless maximum scour depth.

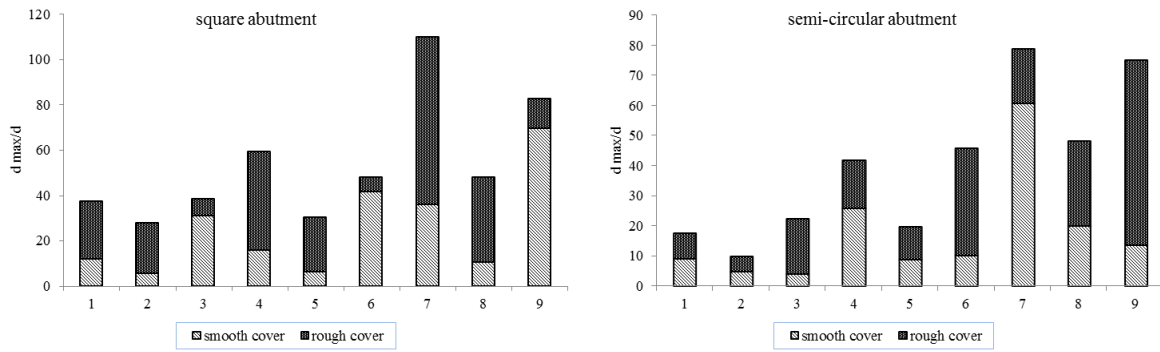


Figure 3.4- 12 The impact of ice cover roughness on the maximum scour depth

Figure 3.4-13 shows the regression analysis around the square abutment under ice cover, as indicated by the following equation:

$$\frac{d_{\max}}{d} = 0.0001(F_o)^{3.73} \left(\frac{D_{50}}{d}\right)^{-1.78} \left(\frac{n_i}{n_b}\right)^{0.77} \left(\frac{H}{d}\right)^{3.01} \quad (3.4-14)$$

Figure 3.4-14 shows the regression analysis for the semi-circular abutment, as indicated by the following equation:

$$\frac{d_{\max}}{d} = 1 \times 10^{-6} (F_o)^{8.60} \left(\frac{D_{50}}{d}\right)^{-4.30} \left(\frac{n_i}{n_b}\right)^{1.00} \left(\frac{H}{d}\right)^{3.00} \quad (3.4-15)$$

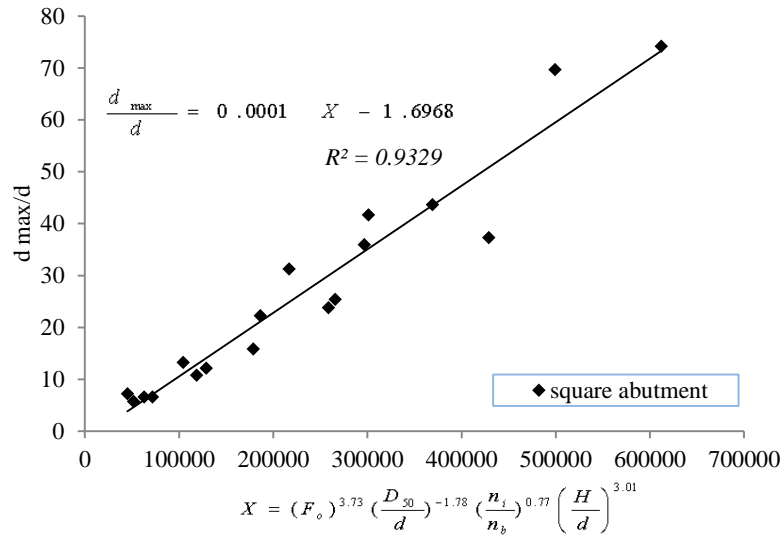


Figure 3.4- 13 Regression relationship under ice cover of related variables around square abutment

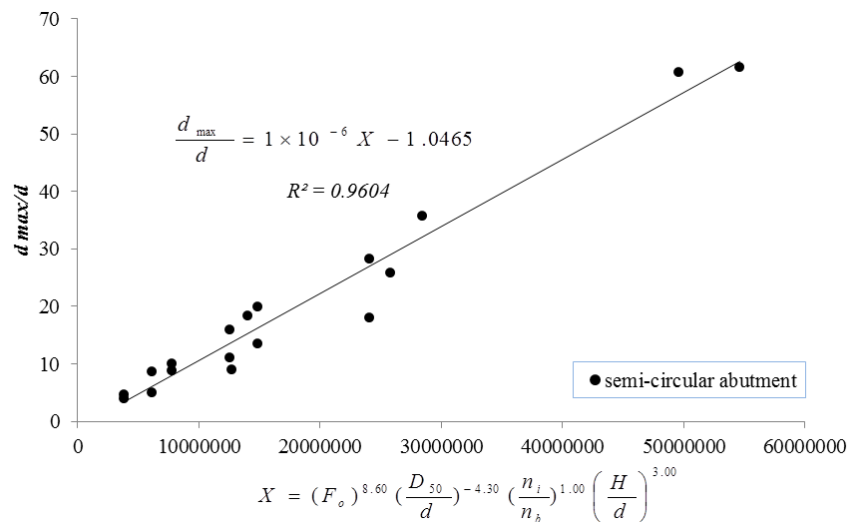


Figure 3.4- 14 Regression relationship under ice cover of related variables around semi-circular abutment

Indexes of independent variables from above equations can be used to indicate the impact of ice cover and armor layer sediment size. Compared to the ice cover roughness, particle size of armor layer sediment has a stronger impact on the maximum scour depth. With the increase in particle diameter of the armor layer, the maximum scour depth decreases correspondingly. Meanwhile, around the semi-circular abutment, the index for n_i/n_b equals to 1. From regression analysis, one can also notice the particle size of the armor layer has a strong impact in reducing the

dimensionless maximum scour depth. This conclusion is in line with a previous study conducted by Sui et al. (2010a). In hydraulic engineering, a mixture of coarse sediments in the vicinity of bridge foundations can reduce maximum scour depth, which has a similar impact as riprap.

3.4.3 Conclusions

By conducting experimental research on the maximum scour depth under ice cover around bridge abutments, the impact of armor layer development and ice cover roughness is discussed. The armor layer grain size has a strong impact on the dimensionless maximum scour depth. With the increase in the particle size of armor layer, the maximum scour depth decreases correspondingly. With the increases in ice cover roughness, the maximum scour depth increases. The relationships between maximum scour depth, water depth, densimetric Froude number, ice cover roughness, and armor layer grain size are derived by using dimensionless analysis. During the period of ice cover formation and during the breakup of ice jams, the roughness of ice cover is beyond our present knowledge. The present study indicates the necessity for further ice scour research as it relates to hydraulic engineering.

References

1. Ackermann N L, Shen H T, Olsson P, 2002, Local scour around circular piers under ice covers. Proceeding of the 16th IAHR International Symposium on Ice, International Association of Hydraulic Engineering Research, Dunedin, New Zealand.
2. Andre R, Thang T, 2012, Mean and turbulent flow fields in a simulated ice-cover channel with a gravel bed: some laboratory observations, *Earth Surface Processes and Landforms*, Vol. 37, pp: 951-956.
3. Barbhuiya A K, Dey S, 2004, Local scour at abutments: a review, *Sadhana*, Vol. 29, part 5, Printed in India, pp. 449-476.
4. Carey K L, 1966, Observed configuration and computed roughness of the underside of river ice, St Croix River, Wisconsin, Professional paper 550-B, US Geological Survey, pp. B192-B198.

5. Dey S, Barbhuiya A K, 2004, Clear water scour at abutments in thinly armored beds, *Journal of Hydraulic Engineering*, ASCE, Vol. 130, No. 7, pp. 622-634.
6. Dey S, Raika R V, 2007, Clear water scour at piers in sand beds with an armor layer of gravels, *Journal of Hydraulic Engineering*, ASCE, Vol. 133, No. 6, pp. 703-711.
7. Ettema R, 1984, Sampling armor-layer sediments, *Journal of Hydraulic Engineering*, ASCE, Vol. 110, No. 7, pp. 992-996.
8. Ettema R, 2002, Review of alluvial-channel responses to river ice, *Journal of Cold Region Engineering*, ASCE, Vol. 16, No. 4, pp.191-217.
9. Ettema R, Braileanu F, Muste M, 2000, Method for estimating sediment transport in ice covered channels, *Journal of Cold Region Engineering*, ASCE, Vol. 14, No. 3, pp. 130-144.
10. Ettema R, Daly S, 2004, Sediment transport under ice. ERDC/CRREL TR-04-20. Cold regions research and Engineering Laboratory, US Army Corps of Engineers.
11. Froehlich D C, 1995, Armor limited clear water construction scour at bridge, *Journal of Hydraulic Engineering*, ASCE, Vol. 121, pp. 490-493.
12. Guo J, 2012, Pier scour in clear water for sediment mixtures, *Journal of Hydraulic Research*, Vol. 50, No. 1, pp. 18-27.
13. Hager W H, 1999, *Wastewater Hydraulics: Theory and Practice*, Springer, Berlin, New York.
14. Hains D B, 2004, An experimental study of ice effects on scour at bridge piers, PhD Dissertation, Lehigh University, Bethlehem, PA.
15. Hains D B, Zabilansky L, 2004, Laboratory test of scour under ice: data and preliminary results, Cold regions research and engineering laboratory, ERDC/CRREL TR-04-09.
16. Jha S K, Bombardelli F A, 2011, Theoretical/Numerical model for the transport of non uniform suspended sediments in open channels, *Advances in Water Resources*, Vol. 34, pp. 577-591.
17. Kuhnle, R A, 1993, Incipient motion of sand-gravel sediment mixtures, *Journal of Hydraulic Engineering*, Vol. 119, No. 12, pp. 1400-1415.
18. Khullar N K, Kothiyari U C, Raju K G R, 2010, Suspended wash load transport of non-uniform sediments, *Journal of Hydraulic Engineering*, Vol. 136, No. 8, pp. 534-543.

19. Li S S, 2012, Estimates of the Manning's coefficient for ice covered rivers, *Water Management, Proceedings of the Institution of Civil Engineers*, Vol. 165, Issue WM9, pp. 495-505.
20. Mays L W, 1999, *Hydraulic Design Handbook*, McGraw-Hill, pp. 3.12.
21. Melville B W, 1992, Local scour at bridge abutments. *Journal of Hydraulic Engineering*, ASCE, Vol 118 (4), pp. 615-631.
22. Meyer-Peter E, Mueller R, 1948, Formula for bed-load transport, *Proceedings of International Association for Hydraulic Research, 2nd Meeting*, Deft, Netherlands, pp. 39-64.
23. Munteanu A, 2004, Scouring around a cylindrical bridge pier under partially ice-covered flow condition, Master thesis, University of Ottawa, Ottawa, Ontario, Canada.
24. NCHRP Web-only Document 181, 2011, Evaluation of Bridge-Scour Research: Abutment and Contraction Scour Processes and Prediction. NCHRP Project 24-27(02).
25. Smith B T, Ettema R, 1997, Flow resistance in ice covered alluvial channels, *Journal of Hydraulic Engineering*, ASCE, Vol. 123, No. 7, pp. 592-599.
26. Sui J, Afzalimehr H, Samani A K, Maherani M, 2010a, Clear-water scour around semi-elliptical abutments with armored beds, *International Journal of Sediment Research*, Vol. 25, No. 3, pp. 233-244.
27. Sui J, Wang J, He Y, Krol F, 2010b, Velocity profile and incipient motion of frazil particles under ice cover. *International Journal of Sediment Research*, Vol 25(1), pp. 39-51.
28. Xu H, Lu J, Liu X, 2008, Non-uniform sediment incipient velocity, *International Journal of Sediment Research*, Vol. 23, No. 1, pp. 69-75.
29. Yang C T, 1973, Incipient motion and sediment transport, *Journal of the Hydraulics Division*, ASCE, Vol. 99, No. HY10, Proceeding paper 10 067, pp. 1679-1704.
30. Yang C T, 2003, *Sediment transport, theory and practice*, Krieger publishing company, Krieger Drive, Malabar, Florida 32950.
31. Zhang H, Nakagawa H, Mizutani H, 2012, Bed morphology and grain size characteristics around a spur dyke, *International Journal of Sediment Research*, Vol. 27, No. 2, pp. 141-157.

3.5 ADV measurements of flow field along a round abutment under ice covers

Local scour is a complex phenomenon resulting from the interaction of the three dimensional turbulent flow around bridge foundations and sediment. Local scour around bridge abutments or piers has been an interesting topic for a long time. As mentioned by Melville (1992), 6 of 10 bridge failures that occurred in New Zealand during Cyclone Bola were related to abutment or approach scour. Luigia et al. (2012) indicated that approximately 50 to 60 bridges fail on average each year in the US. The Federal Highway Administration has estimated that over 60% of bridge collapses in the US is from local scour (NCHRP, 2011).

Bridge foundations should be designed to withstand the effects of scour resulting from designed floods. Estimation of the scour depth at bridge foundations is a problem that has perplexed designers for many years. Improving the understanding of local scour is therefore vital for the engineers responsible for the design of bridge foundations.

In cold regions of northern hemisphere, ice cover is a big issue as it can stay as long as 6 months on some rivers. Ice cover can result in many problems, such as ice jamming, flooding, restricting the generation of hydro-power, block river navigation and affect the ecosystem balance (Hicks, 2009). Numerous researches contributed lots work on the ice related hydrology and hydraulic research (Beltaos, 2000; Prowse, 2001; Ettema and Daly, 2004; Wang, 2008; Sui et al., 2009).

Ice cover can significantly change the flow field and impact of sediment transport in natural rivers. Lau and Krishnappan (1985), Ettema et al. (2000) developed their own methods for estimating the sediment transport under ice cover separately. Sui et al. (2000) derived interrelationships of suspended sediment concentration and riverbed deformation under ice cover at Hequ Reach of the Yellow River. Turcotte et al. (2011) reviewed the sediment transport process in ice affected rivers by documenting a range of unique ice and sediment transport process. Considerable advances have been made concerning ice forces on structures, such as bridges (Brown, 2000) and dams as reported by Morse and Hicks (2005). However, very few researches have ever been conducted regarding the local scour around bridge foundations under different roughness of ice cover. In addition, only a few experiments can be found on the local scour under ice cover (Ackermann et al. 2002, Hains and Zabilansky, 2004; Sui et al. 2010). To date, there is still no research measure the flow field in the scour hole around bridge abutment

under ice cover. To fill this gap, a series of flume experiments were conducted in 2012. The objectives of this research are as following.

- a. Compare the flow field measured by ADV in open channel and under ice cover around the semi-circular abutment.
- b. Compare the scour depth around the bridge abutment at different locations.
- c. Study the impact of sediment composition on the maximum scour depth by introducing a dimensionless particle parameter.

3.5.1 Methodology

A series of experiments were conducted in a large scale flume with the dimension of 40m long, 2m wide and 1.3m deep. The flume is located at Quesnel River Research Center, Likely, BC, Canada. The slope of the flume bottom is 0.2%. A holding tank was made in the upstream of the flume with a volume of 90m³ to keep a constant discharge rate in the experimental zone. Two valves were connected to adjust water into the holding tank for the purpose of changing the flow velocity. From the holding tank, water overflowed from a rectangular weir to flow dissipaters in the experimental zone. One sand box was created in the flume with depth of 30cm. Figure 3.5-1 shows the setup of abutment and ice cover in the large scale flume.



Figure 3.5- 1 Experimental setup

Since ice cover is the main interest here, we made two types of ice cover for the research, namely smooth cover and rough cover. A smooth ice cover was created from the original Styrofoam. A

rough ice cover was created by attaching small cubes of the Styrofoam to the underside of the smooth ice cover. The small cubes have a dimension of 2.5cm × 2.5cm × 2.5cm, with a spacing distance of 3.5cm from each other. Meanwhile, three different natural non-uniform sediments were used in the study. The D_{50} of the three sediments were 0.58cm, 0.50cm and 0.47cm. One round abutment with the diameter of 20cm was made from plexiglass. The dimensions of the abutment and coordinate system can be found in Figure 3.5-2. In front of the sand box, a SonTek IQ was installed in the bottom of the false floor to measure the approaching flow velocity, water depth, water temperature, etc. Meanwhile, a staff gauge was also installed in the sand box for depth measurement. A 10 MHz SonTek ADV was used to measure the flow field in the vicinity of the abutment. Table 3.5-1 summarizes the experimental conditions and some preliminary results for each flume run.

Table 3.5- 1 The maximum scour depth under different conditions.

Cover condition	D_{50} (mm)	D_{16} (mm)	D_{84} (mm)	Water depth (m)	Average velocity (m/s)	Maximum scour depth (cm)
Open channel	0.58	0.28	1.91	0.07	0.21	0.0
	0.58	0.28	1.91	0.19	0.23	5.5
	0.58	0.28	1.91	0.07	0.26	2.7
	0.50	0.26	1.66	0.07	0.21	3.5
	0.50	0.26	1.66	0.19	0.23	7.0
	0.50	0.26	1.66	0.07	0.26	6.0
	0.47	0.23	0.82	0.07	0.21	0.0
	0.47	0.23	0.82	0.19	0.23	15.0
	0.47	0.23	0.82	0.07	0.26	15.0
Smooth cover	0.58	0.28	1.91	0.07	0.23	2.3
	0.58	0.28	1.91	0.19	0.20	3.2
	0.58	0.28	1.91	0.07	0.20	1.0
	0.50	0.26	1.66	0.07	0.23	6.5
	0.50	0.26	1.66	0.19	0.20	6.0
	0.50	0.26	1.66	0.07	0.20	2.5

	0.47	0.23	0.82	0.07	0.23	13.5
	0.47	0.23	0.82	0.19	0.20	12.0
	0.47	0.23	0.82	0.07	0.20	3.0
Rough cover	0.58	0.28	1.91	0.07	0.20	2.2
	0.58	0.28	1.91	0.19	0.20	3.5
	0.58	0.28	1.91	0.07	0.22	4.7
	0.50	0.26	1.66	0.07	0.20	4.0
	0.50	0.26	1.66	0.19	0.20	7.5
	0.50	0.26	1.66	0.07	0.22	9.0
	0.47	0.23	0.82	0.07	0.20	4.0
	0.47	0.23	0.82	0.19	0.20	17.0
	0.47	0.23	0.82	0.07	0.22	13.7

To make sure each experiment had the same conditions, the following steps were strictly followed in the experimental study.

(1) Before each experiment, the abutment model was leveled and fixed in the sand box to make sure the abutment is upright to the flume bottom. On the outside surface of the abutment, different measuring lines have been drawn for the purpose of measuring scour depth. In all, 13 measuring lines (P ~ Q) were made for the round abutment (Figure 3.5-2).

(2) At the beginning of each experiment, the flume was slowly filled up by adjusting the valves in the holding tank. One template was made to cover the scour zone from initial scouring. After the required water depth was reached, the valves were adjusted to get a certain flow rate in the flume and the template was then removed to start the experiment. The duration of scour experiments was 24 hours; enough for the maximum scour depth development in a large flume from the authors' observation.

Because the main interest of the research here is the flow field in the scour hole. The down-looking ADV was used. The sampling interval is 0.04s. At each measuring point, the measurement last at least 20s.

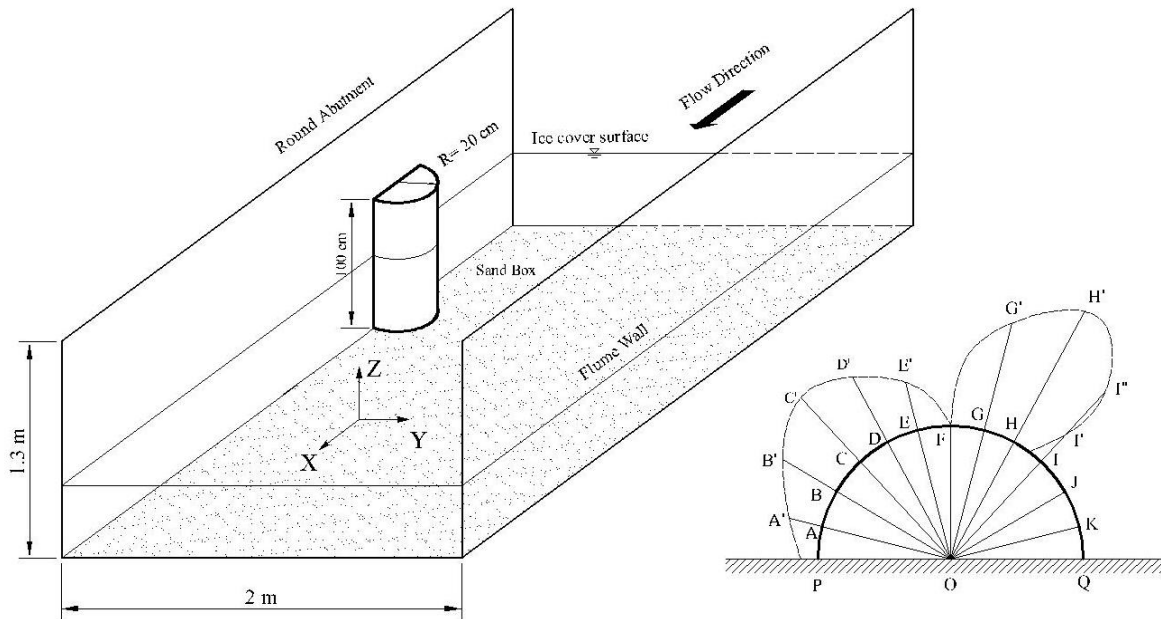
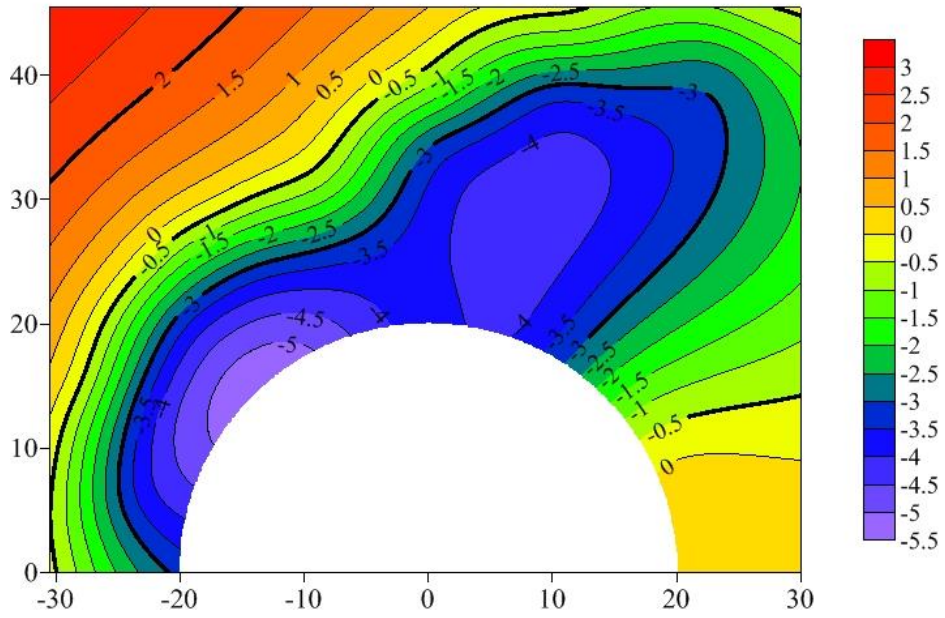


Figure 3.5- 2 Abutment dimension and coordinate system.

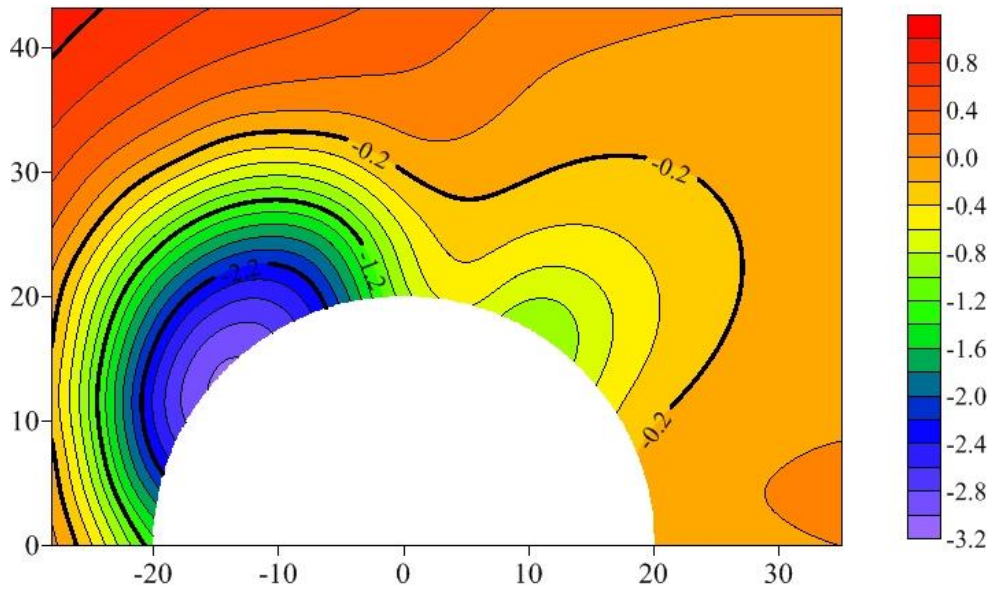
3.5.2 Results and Discussion

At the end of each experiment, photos were taken for the scour profile around the bridge abutment. Meanwhile, by measuring the scour depth along the outside line of the abutment, the profiles of the scour hole were plotted by using Surfer 10, Golden Software. Figure 3.5-3 shows the typical scour profile under open channel, smooth cover and rough cover.

open channel, $h=0.19\text{m}$, $v=0.23\text{m/s}$



smooth cover, $h=0.19\text{m}$, $v=0.20\text{m/s}$



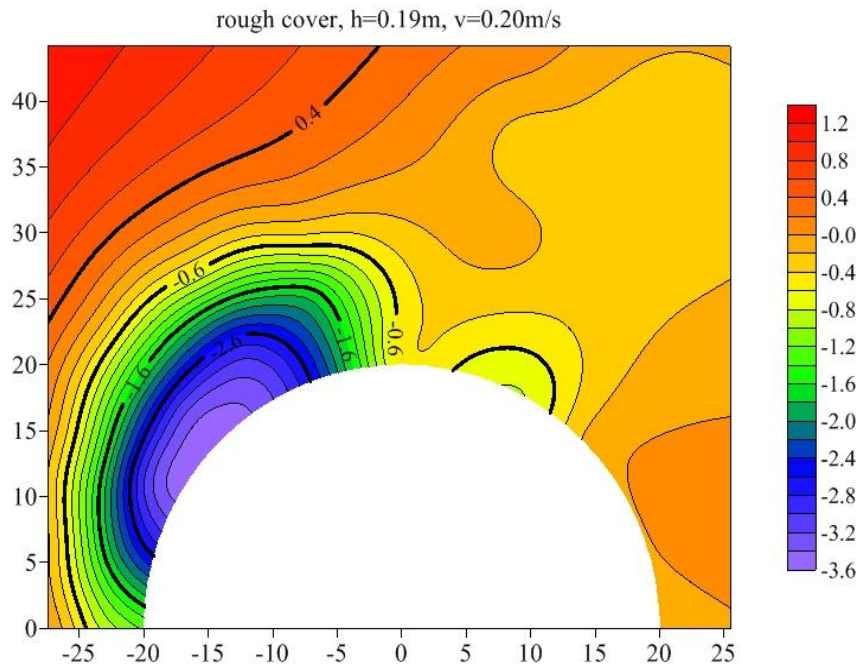


Figure 3.5- 3 Contours of scour hole under open channel, smooth cover, and rough cover

Scouring process and contours

From our observation, the scour started from the toe area of the abutment. In the first two hours, one large scour hole has already been formed. The maximum scour depth is located at the corner which is around 50° facing upstream. With the developing of scour hole, more sediment moves out to the downstream, which can also be seen from the pile of fine sediment ridge from Figure 3.5-3. The location of the scour hole is independent on the covered condition. While for the dimensions of the scour hole, from Figure 3.5-4, it can be seen that ice cover roughness has a more obvious impact on the profile of the scour. Under rough ice cover, the scouring area is larger compared to that under smooth cover.

During the scouring process, a primary vortex was observed in the upstream of the abutment. As mentioned by Dey and Barbhuiya (2005), around the bridge pier, the horseshoe vortex is the primary reason for scouring. While under ice cover, several small horseshoe vortexes can be detected in the scour hole. The horseshoe vortex had the direction of clock wise. Meanwhile, some horizontal vortexes were also noticeable.

In the downstream of abutment, a fine sediment ridge can be seen from the outside of Point J and K to downstream. From our observation, under rough ice cover, the ridge has a longer length compare to that under smooth ice cover.

As shown in Figure 3.5-4, one can clearly notice the location of the maximum scour depth around the bridge abutment. The profiles along the measuring points (A ~ K) are different under ice covers compare to that in open channels. Please also note that the approaching velocity in open channels is larger that those in covered channels. Following three observations are noted.

(1) In open channel, the maximum scour occurs around C and D, while under ice covers, the maximum depth locates between B and C. Additionally, under rough ice cover, the maximum scour depth closes to B. From our understanding, with an increase in ice roughness, we can make the assumption that in the upstream of the abutment, extra shear stress caused by the ice cover impacts location of maximum scour depth.

(2) In open channel, one fine sediment ridge can be noticed along from J to Q. However, there was no clearly fine sediment ridge under ice covers along the abutment. From our observation, fine sediment ridge locates at a distance downstream away from the abutment under ice covers. And with the increase in roughness of ice cover, the start point of fine sediment ridge further from the abutment.

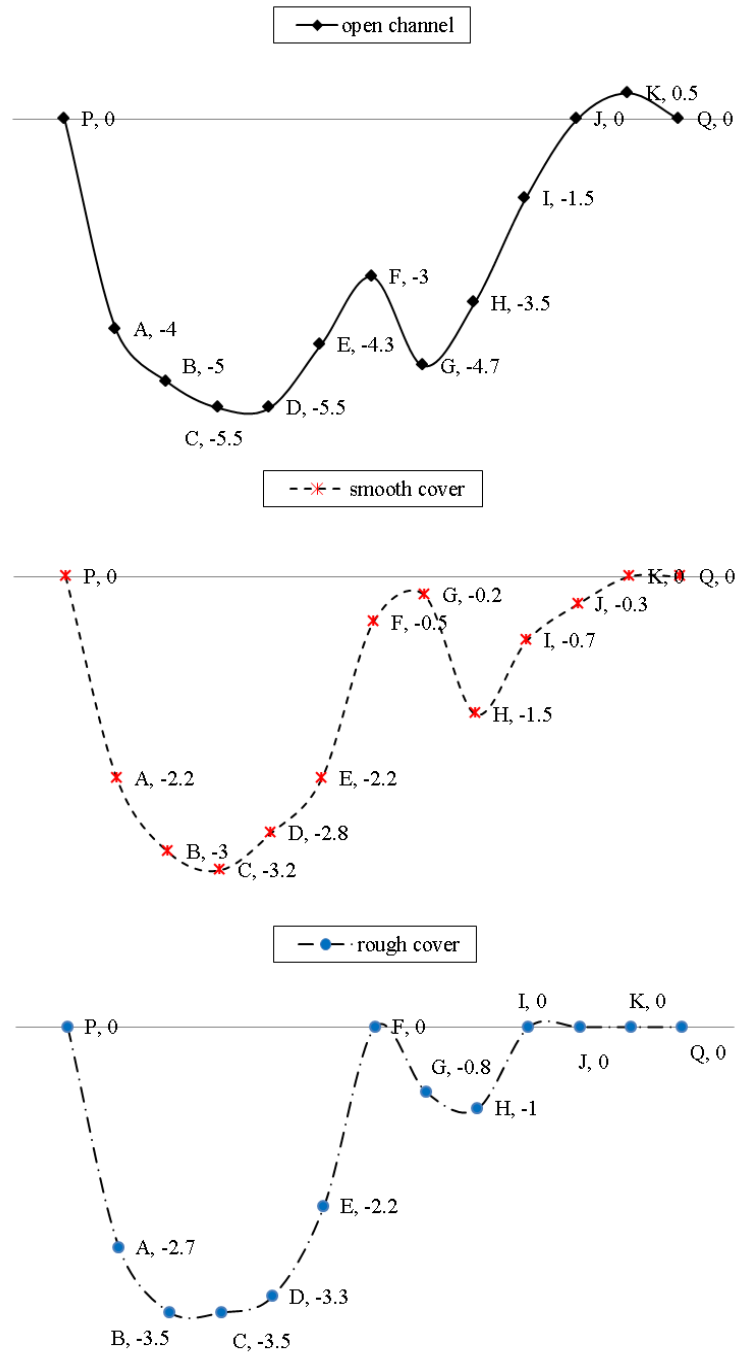


Figure 3.5- 4 The scour profile along the round abutment under different conditions

(3) Two scour holes can be noted along the abutment. One locates in the upstream surface of the abutment, the other locates between measuring points F to I. Meanwhile, along the abutment, F

is the dividing point of two scour holes. Under ice covers, the elevation at F is close to the original channel bed.

(4) From our observation, under ice covers, the scouring process takes more time to reach the maximum scour depth. In open channels, in the large scale flume, the scour hole develops fast in the first 3 hours. While under ice cover, due to the increased opposing resistance, the scouring time is longer than that in open channels. Additionally, with the increase in roughness, the scouring process under rough cover is longer than that under smooth ice cover.

Velocity distribution under ice cover

As reported by Sui et al. (2010), due to the increased wetted perimeter of flow caused by ice cover, the composite resistance increased correspondingly. The upper portion of the flow is mainly affected by the ice cover, while the lower portion is mainly influenced by the channel bed. The maximum velocity locates between the cover and channel bed. However, in the vicinity of the abutment, inside the scour hole, the flow field has never been studied.

By using one down-looking ADV, 3D instantaneous velocity can be measured along the abutment. One should evaluate two parameters provided in the ADV file, which is signal-to-noise ratio (SNR) and the correlation (COR), to ensure the ADV measurements can provide an accurate representation of the flow velocity (Wahl, 2000). According to the manufacturer, the SNR is a function of turbidity, the amount of particulate matter in the flow. COR is an indicator the relative consistency of the behavior of the scatters in the sampling volume during the sampling period. Here we used the following standard: $SNR > 15$ db, and $COR > 70\%$. The WinADV software program developed by the Bureau of Reclamation's Water Resources Research Laboratory was used to filter the ADV data from poor quality or erroneous data based on the two parameters mentioned above. The velocity field from the upstream surface of the abutment to the downstream was measured. Figure 3.5-5 shows the Reynolds-averaged velocity measured along the abutment from A to K under open channels, smooth cover and rough cover. The following findings have been noticed.

(1) From Point A to I, one can notice that in open channels, the velocity component in the Z direction is small compared to the X and Y components at the same elevation. Meanwhile, compare with the value in Z direction under smooth cover and rough cover, the velocities in the

Z direction in open channels are so small being close to zero. From our understanding, ice cover imposed extra force to the flow downwards which creates a higher velocity component in the Z direction.

(2) From Point J to K, the velocity component is larger than that from A to I in open channels. J and K are the only two locations that have large Z direction velocity component under open channel condition. Additionally, the fine sediment ridge was located close to this zone. Due to the boundary layer of the flume wall, small downward vortexes can be generated in the downstream of the abutment. Our ADV measurement also proved this assumption.

(3) Under ice covered condition from Point A to F, all the measured velocity components in Z direction have negative value. However, in the downstream, from G to H, the velocity component in Z direction has positive value. Based on this, we make the following assumption: in the upstream, the primary vortex moves downwards, while in the downstream, the vortex moves upwards from the bottom.

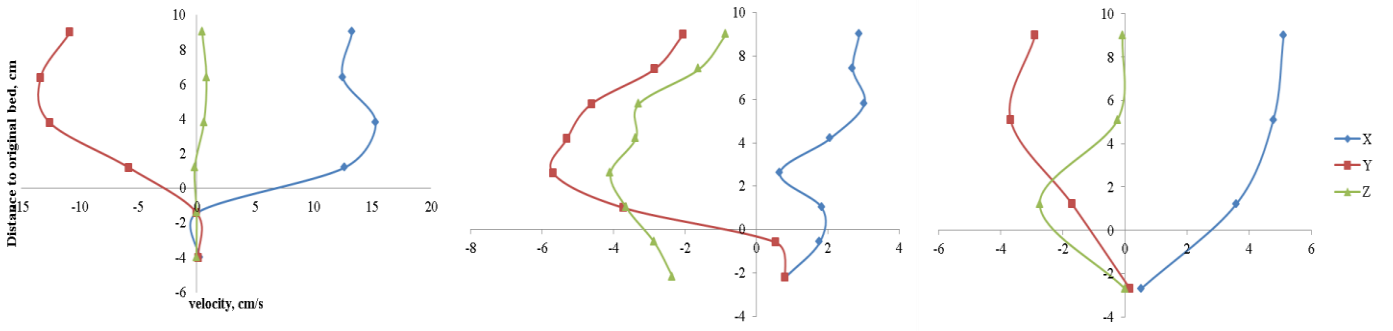
(4) In the upstream of the abutment, velocity component in the X direction is always positive, while the Y component has the trend from positive to negative. At Point C to E, the Y direction velocity is the least compared to that in other points. In other words, the Y direction velocity component decreases along the abutment in the upstream surface till the maximum scour depth. After that, the Y velocity component increases again to the downstream. Meanwhile, we make the conclusion that the Y direction velocity contributes less to the maximum scour depth compared to the velocity component in the X and Z direction.

(5) As mentioned above, in open channels, the maximum scour depth locates between C and D. While under ice cover, the maximum scour depth locates between B and C. From our ADV measurement, we also notice that, in open channels, the X direction velocity contributes most to the scour hole development. While under ice covered condition, the Z direction velocity has the largest impact.

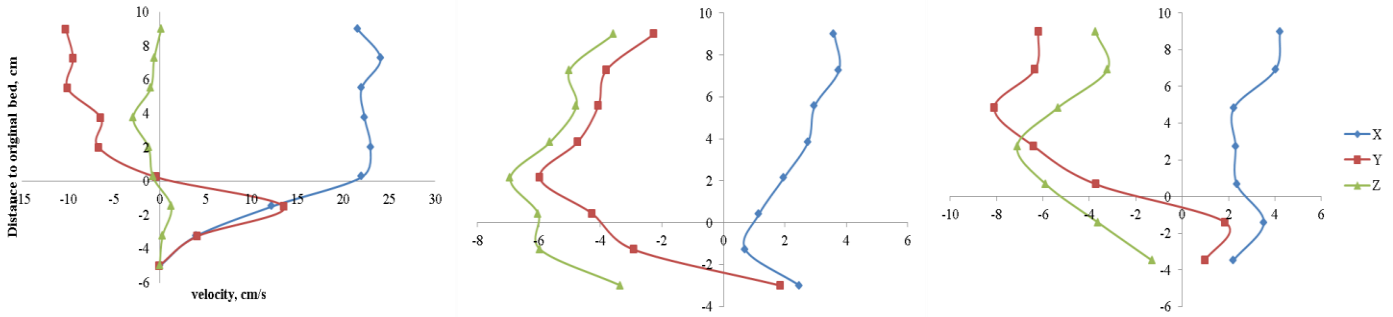
(6) With the increase in ice cover roughness, the gradient of velocity in all the three directions decreases, which can be found from the ADV measurements at all points.

(7) No scour hole was observed in the downstream of the abutment under ice cover. However, from I to K, velocity components are highly turbulent compared to that without ice covers.

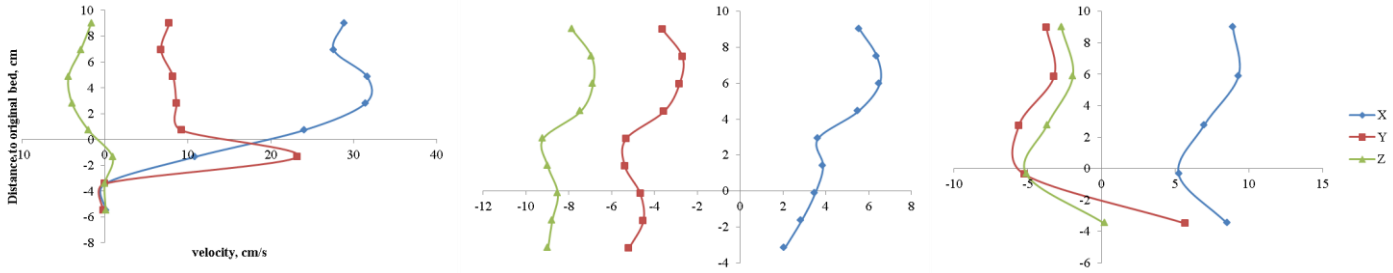
Point A



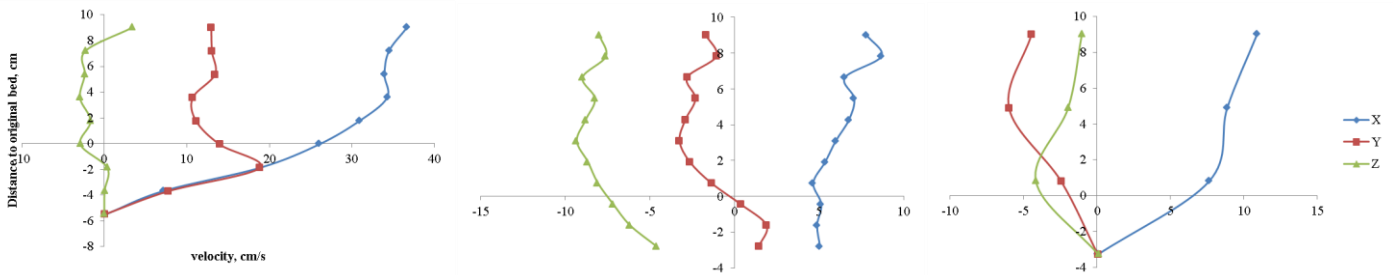
Point B



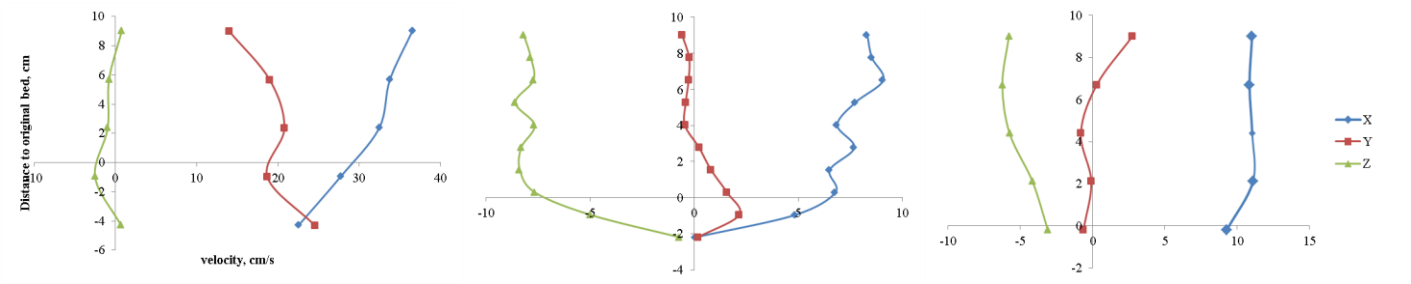
Point C



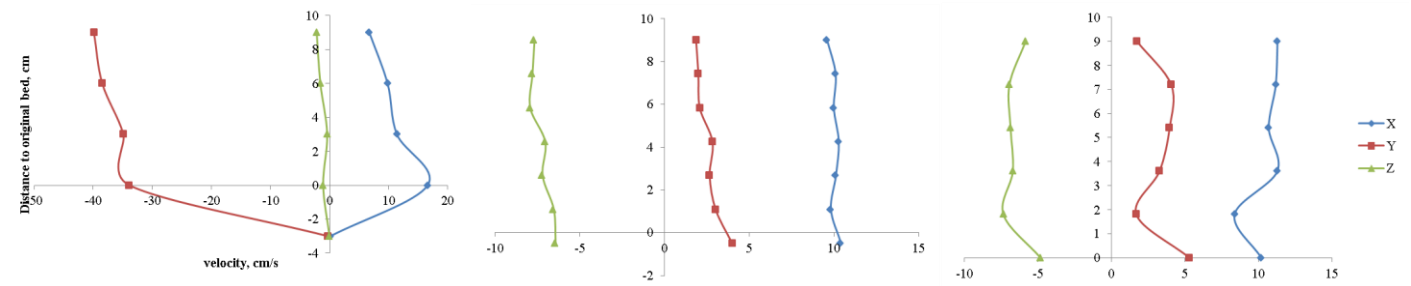
Point D



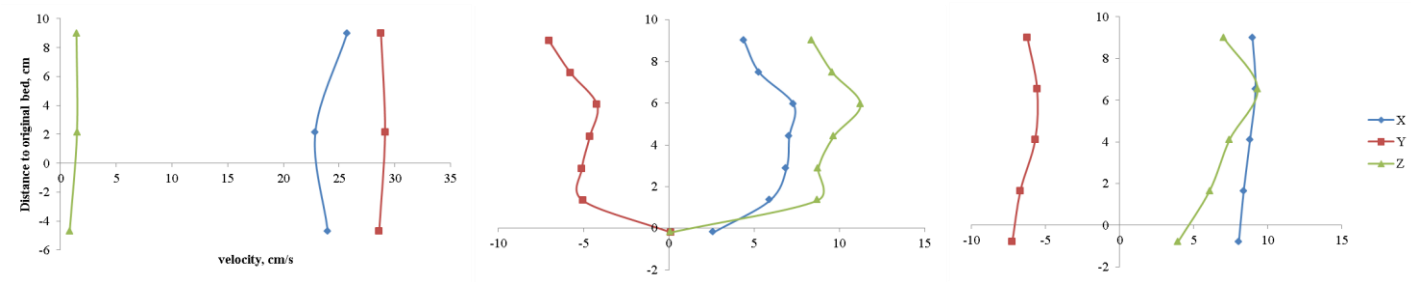
Point E



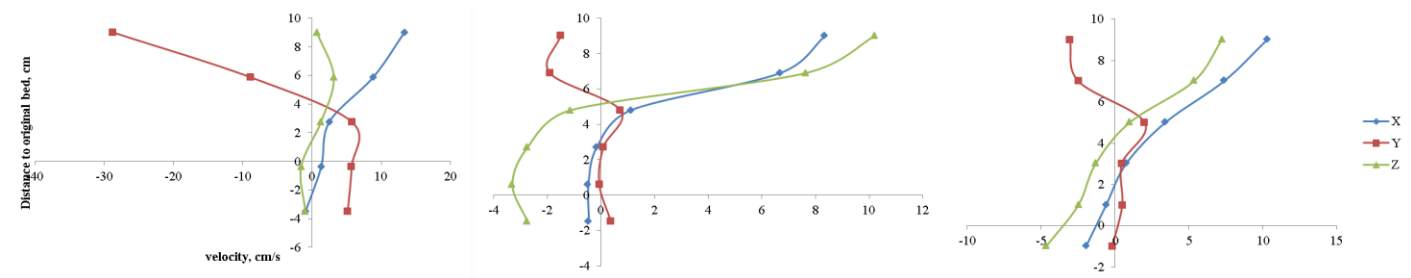
Point F



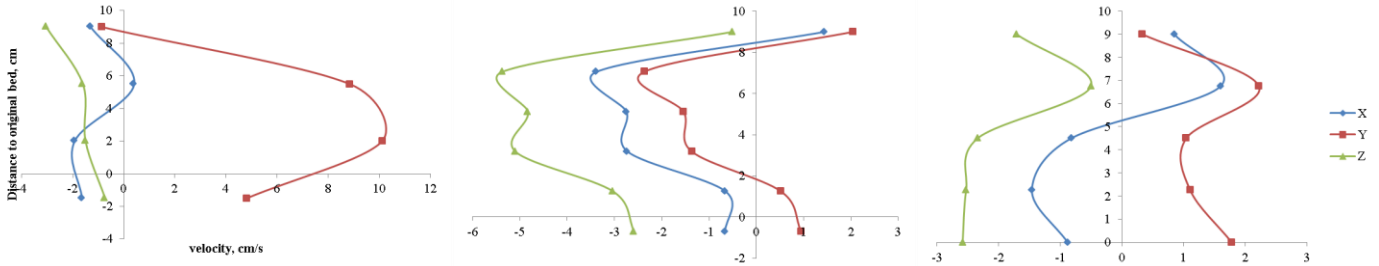
Point G



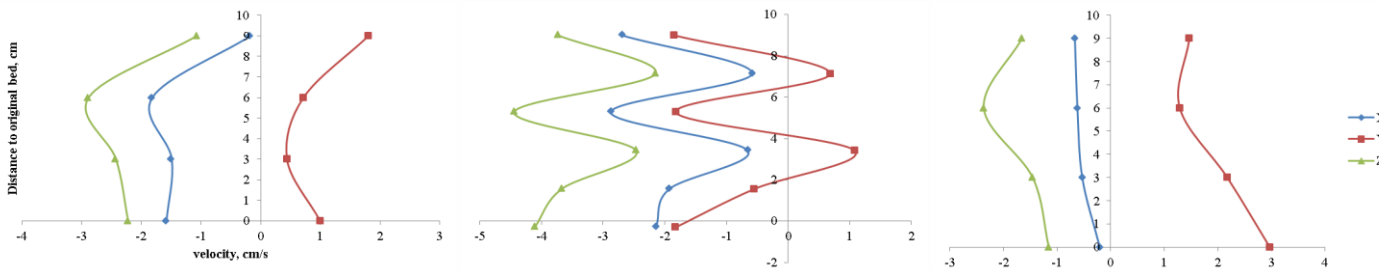
Point H



Point I



Point J



Point K

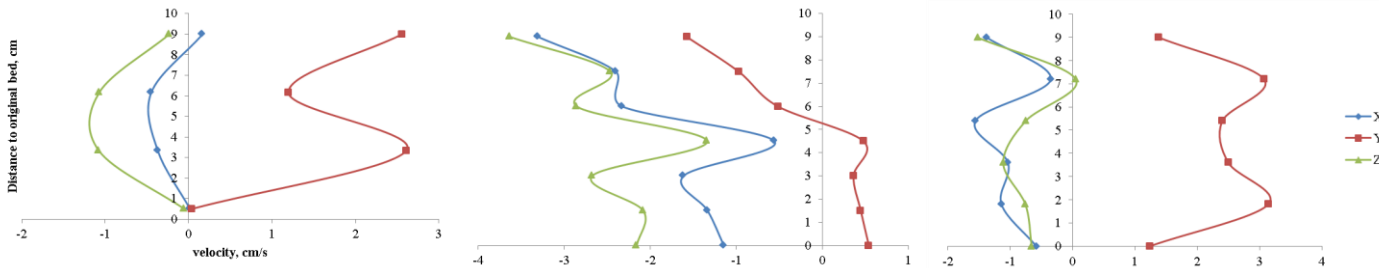


Figure 3.5- 5 The velocity distribution along the abutment under different conditions: open channel (Left), smooth cover (Middle), rough cover (right)

3.5.3 Conclusion

The local scour under ice covers were conducted in a large flume in 2012. Equal distance measuring lines were made along the round abutment to measure the 3D flow velocity in the scour hole. We found that in open channels, the maximum scour depth locates at the upstream surface of the abutment with an angle about 50°, while under ice cover, the angle is around 60°.

By using a down-looking 3D ADV, the flow field at different locations and elevations were measured. Compared to the flow in open channel, the velocity component in Z direction contribute much to the development of scour hole under ice covers. Based on the comparison of flow distribution, the velocity field around the abutment was analyzed under open channel and ice covered conditions.

References

1. Ackermann N L, Shen H T, Olsson P, 2002. Local scour around circular piers under ice covers. Proceeding of the 16th IAHR International Symposium on Ice, International Association of Hydraulic Engineering Research, Dunedin, New Zealand.
2. Beltaos S, 2000. Advances in river ice hydrology. Hydrological Processes. Vol. 14, pp. 1613-1625.
3. Brown T G, 2000. Ice loads on the piers of Confederation Bridge, Canada. Structural Engineer, Vol. 78, pp. 18-23.
4. Dey S, Barbhuiya A K, 2005. Turbulent flow field in a scour hole at a semicircular abutment. Canadian Journal of Civil Engineering, Vol. 32, pp. 213-232.
5. Ettema R, Braileanu, F, Muste M, 2000. Method for estimating sediment transport in ice covered channels. Journal of Cold Regions Engineering, Vol. 14, No. 3, pp. 130-144.
6. Ettema R, Daly S F, 2004. Sediment transport under ice. ERDC/CRREL TR-04-20. Cold regions research and Engineering Laboratory, US Army Corps of Engineers.
7. Hains D, Zabilansky L, 2004. Laboratory test of scour under ice: Data and preliminary results. ERDC/CRREL TR-04-09. Cold regions research and Engineering Laboratory, US Army Corps of Engineers.
8. Hicks F, 2009. An overview of river ice problems: CRIPE 07 guest editorial Cold regions Science and Technology, 55: pp. 175-185.
9. Lau Y L, Krishnappan B G, 1985. Sediment transport under ice cover. Journal of Hydraulic Engineering, ASCE, 111(6), pp. 934-950.
10. Luigia B, Paolo P, Giuliano D B, 2012. Bridge pier scour: a review of process, measurements and estimates. Environmental Engineering and Management Journal, Vol. 11 (5).

11. Melville B W, 1992. Local scour at bridge abutments, *Journal of Hydraulic Engineering*. ASCE, Vol. 118, No. 4, pp. 615-631.
12. Morse B, Hicks F, 2005. Advances in river ice hydrology 1999-2003. *Hydrological Processes*, Vol. 19, pp. 247-263.
13. NCHRP Web-only Document 181, 2011. Evaluation of Bridge-Scour Research: Abutment and Contraction Scour Processes and Prediction. NCHRP Project 24-27(02).
14. Prowse T D, 2001. River-Ice ecology: Part A. Hydrologic, geomorphic and water-quality aspects. *Journal of Cold Regions Engineering*, Vol. 15, pp. 1-16.
15. Sui J, Wang D, Karney B, 2000. Suspended sediment concentration and deformation of riverbed and a frazil jammed reach. *Canadian Journal of Civil Engineering*, Vol. 27, 1120-1129.
16. Sui J, Faruque M A A, Balanchandar R, 2009. Local scour caused by submerged square jets under model ice cover. *Journal of Hydraulic Engineering*, Vol. 135, No. 4, pp. 316-319.
17. Sui J, Wang J, He Y, Krol F, 2010. Velocity profile and incipient motion of frazil particles under ice cover. *International Journal of Sediment Research*, Vol. 25, No. 1, pp. 39-51.
18. SonTek, 2001, Acoustic Doppler Velocimeter (ADV) principles of operation, SonTek ADV technical manual, SonTek, San Diego.
19. Turcotte B, Morse B, Bergeron N E, Roy A G, 2011. Sediment transport in ice affected rivers. *Journal of Hydrology*, Vol. 409, pp. 561-577.
20. Wahl T L, 2000, Analyzing data using WinADV. Joint Conference on water resources engineering and water resources planning and management, Minneapolis, Minnesota, pp. 1-10.
21. Wang J, Sui J, Karney B, 2008. Incipient motion of non-cohesive sediment under ice cover – an experimental study. *Journal of Hydrodynamics*, Vol. 20, No. 1, pp. 177-124.

3.6 The incipient motion of bed material and shear stress analysis around bridge abutments under ice-cover

Local scour refers to the scour caused by river obstructions such as bridge abutments, piers, and other objects that obstruct the flow (Chang, 2002). It has been identified as an important issue by civil engineers for a long time. Excessive scour can cause structural failure and even result in the loss of life. According to Melville (1992), 29 of 108 bridge failures in New Zealand between 1960 and 1984 were attributed to abutment scour. Over the past few decades, local scour around bridge abutments has received worldwide attention: Laursen and Toch, 1956; Froehlich, 1995; Melville, 1997; Coleman et al, 2003; Dey and Barbhuiya, 2005. However, almost all of these studies were conducted in open channels.

In the Northern Hemisphere, winter lasts up to six months, which is a big challenge for hydraulic engineers to estimate scour condition around bridges. To fill this gap, some researchers started to look at this problem from an experimental approach (Ackermann et al., 2002; Hains, 2004; Munteanu, 2004; Ettema and Daly, 2004; Sui et al., 2009, 2010; Munteanu and Frenette, 2010) and numerical approach (Beltaos, 2000; Wang et al., 2008).

Ackermann et al. (2002) investigated the effects of ice cover on local scour around bridge piers. By using uniform sediments, the author's found that for equivalent averaged flow velocities, the existence of an ice cover could increase the local scour depth by 25%~35%. For live bed scour, a rough cover gave a slightly larger scour depth than smooth cover. Munteanu (2004) conducted experiments on local scour around cylinders and found that under clear water conditions local scour increased up to 55 percent. Sui et al. (2010) mentioned that the flow velocity profiles under ice cover appear to be identical regardless of the average flow velocity and flow depth. As reported by Wang et al. (2008), under ice covered conditions, flow velocity profiles can be divided into the upper portion which is from the ice cover bottom to the point of the maximum velocity, and the lower portion, which is from the channel bed to the maximum velocity. When the channel bed and ice cover have different resistance coefficients, the maximum velocity will be closer to the surface with the smallest resistance coefficient.

In practice, dimensionless shear stress is used to study the incipient motion. Dey and Barbhuiya (2005) investigated the three dimensional turbulent flow properties around a short vertical wall abutment both upstream and downstream of the scour hole in open channels. By using the

Reynolds stresses, the bed shear stresses were also calculated. From their experiments, the maximum bed shear stresses were about 3.2 times that of the incoming flow. Duan et al. (2009) examined the Reynolds stresses around a spur dike. It was found the Reynolds stress was 2-3 times that of the incoming flow. Since the abutment and spur dike have similar contraction impact on the flow, all three studies showed the similar amplification factor of bed shear stress in open channel flow.

For non-uniform sediments, finer materials can be transported faster than coarser materials under constant flow conditions. The remaining coarser layer is called armor layer (Yang, 2003). With the development of an armor layer, further sediment transport is inhibited. Non-uniform sediment makes up typical bed composition in natural rivers.

To date, there are no known experimental studies on clear water scour around bridge abutments under ice covered conditions with non-uniform sediments. The effects of ice cover and armor layer have to be considered in the analysis of local scour. In this study, we started with a particle force analysis under ice cover by introducing armor layer particle size. Then the dimensionless shear stress was calculated.

3.6.1 Experimental setup and measurement

Experiments were conducted in a 40m long, 2m wide and 1.3m deep flume located at Quesnel River Research Center, BC, Canada (Figure 3.6-1a). The flume had a bottom slope of 0.2% and a 90m³ volume holding tank was located in the upstream section of the flume to keep a constant flow rate in the experimental zone. At the end of the holding tank, water overflowed from a rectangular weir to flow dissipaters in the experimental zone. Two types of ice cover were used in the research, namely smooth cover and rough cover. The ice cover was 6m long, which covered the experimental sand box area completely. Two abutment models were made from plexi-glass, semi-circular and square abutments (Figure 3.6-1b). The abutment model was located in the sand box to simulate a bridge abutment with a solid foundation in the floodplain. A smooth ice cover was created from Styrofoam panels, while a rough ice cover was created by attaching small cubes of the Styrofoam to the underside of the smooth ice cover. The small cubes had dimensions of 2.5cm × 2.5cm × 2.5cm, with a spacing distance of 3.5cm from each other. In this study, three different natural non-uniform sediments were used in the flume. The D₅₀ of the

three sediments was 0.58cm, 0.50cm and 0.47cm with geometric standard deviations (σ_g) larger than 1.4.

To maintain clear water scour conditions, the approaching velocity was carefully chosen in this series of experiments. A SonTek IQ was installed for flow velocity and water depth measurement. We also used a 10 MHz SonTek down looking ADV for scour hole velocity measurements. The sampling rate of the ADV was 10Hz. ADV measurements were mainly located at four points around square abutment, A, B, C, D. Around the semi-circular abutment, the measurement points (from A to K) were along measuring lines marked on the abutment (Figure 3.6-1b).

For the ADV measurement, two values were used to ensure the measurements can provide an accurate representation of the flow velocity: signal-to-noise ratio (SNR) larger than 15db and the correlation (COR) between 70% and 100%. Then the data was analyzed by WinADV (Wahl, 2000).

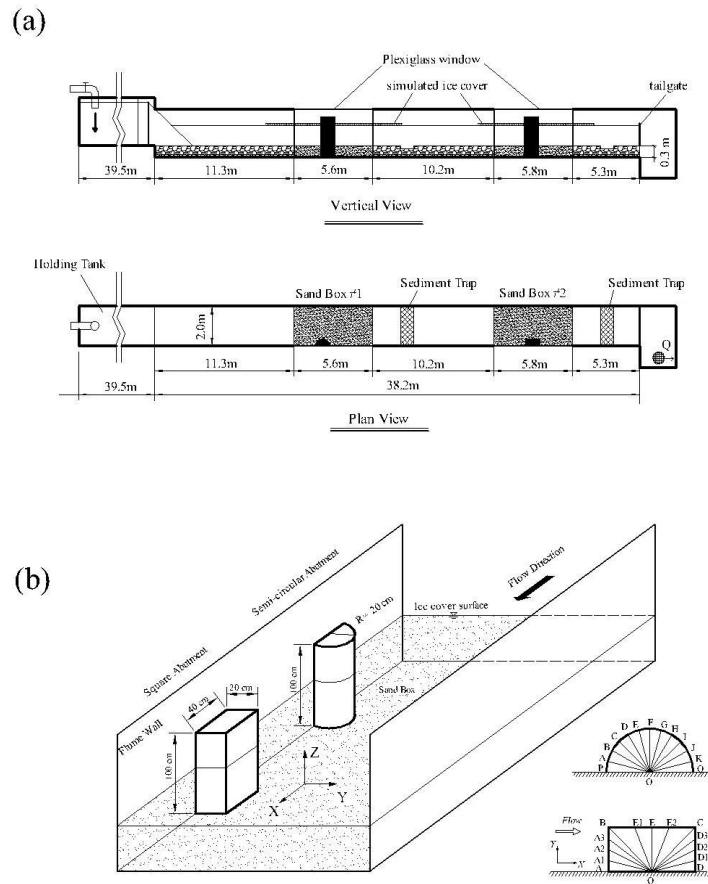


Figure 3.6- 1 Sketch of experimental setup and abutment dimension

3.6.2 Results and discussion

Incipient motion under ice cover

The presence of ice cover in the channel altered the flow characteristics to a great extent. From our observation, the incipient motion started from the toe area of the abutment. Around the square abutment, the scour started at point B and extends to A and E. While around the semi-circular abutment, the scour was firstly observed between Point D and E.

The forces acting on a sediment particle at the bottom of the scour hole under ice cover are shown in Figure 3.6-2. For most natural rivers, the river slopes are small enough that the component of gravitational force acting on the particle in the direction of flow can be neglected. As shown in Figure 3.6-2, the forces to be considered related to the incipient motion are the drag force F_D , lift force F_L , submerged weight W , and the resistance force F_R . The angle of the scour hole with vertical abutment is α .

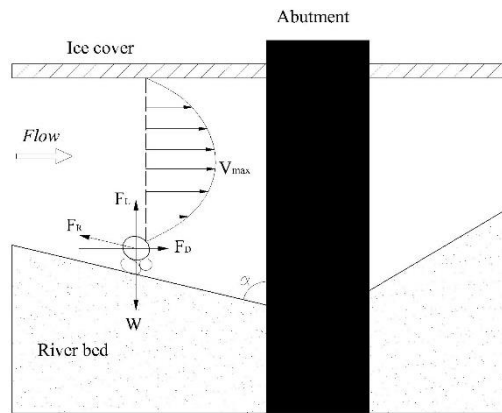


Figure 3.6- 2 Incipient motion in the scour hole under ice cover

The scour angle was calculated by measuring the upstream facing scour distance and maximum scour depth. For the square abutment, the distance from Point B to upstream was measured, while for the semi-circular abutment, since the maximum scour depth was located between Point D and E, the larger distance outwards from D and E was used. We found that around the square abutment, the average scour angle was 65° , while the average scour angle around the semi-circular abutment was 74° . From the perspective of preventing local scour, the larger the scour

angle, the better. Our study indicates the idea that streamline-like abutments cause less local scour depth under ice-covered condition.

A sediment particle is at a state of incipient motion when the following conditions have been satisfied:

$$\begin{cases} F_D = F_R \sin \alpha \\ W = F_L + F_R \cos \alpha \end{cases} \quad (3.6-1)$$

By using Yang's criteria (2003) for incipient motion, the drag force can be expressed as:

$$F_D = C_D \frac{\pi d^2}{4} \frac{\rho}{2} V_d^2 \quad (3.6-2)$$

where C_D is the drag coefficient at velocity V_d , ρ is the density of water, and V_d is the local velocity at a distance d above the bed. In open channels, the shear velocity, shear stress or flow velocity profile can be calculated by using the logarithmic distribution law. The lift force acting on the particle can be obtained as:

$$F_L = C_L \frac{\pi d^2}{4} \frac{\rho}{2} V_d^2 \quad (3.6-3)$$

where C_L is the lift coefficient at velocity V_d .

The submerged weight of the particle can be given by:

$$W = \frac{\pi d^3}{6} (\rho_s - \rho) g \quad (3.6-4)$$

By applying Equation 3.6-2 to 3.6-4 to Equation 3.6-1, the following relationship can be found:

$$V_d = \sqrt{\frac{4}{3} \frac{\Delta \rho}{\rho} g d \frac{1}{C_D \text{ctg} \alpha + C_L}} \quad (3.6-5)$$

The lift coefficient and drag coefficient can be determined by experiments. Since the sediments used here are non-uniform sediment, in Equation 3.6-5, the diameter of the sediment particle will be replaced by D_{50} , and the following can be derived.

$$V_d = \sqrt{\frac{4}{3} \frac{\Delta \rho g}{\rho} \frac{1}{C_D \text{ctg} \alpha + C_L} D_{50}} \quad (3.6-6)$$

From Equation 3.6-6, one can note that, with the increase in scour angle, the velocity needed to move the particle in the scour hole will increase correspondingly. When the scour angle is equal to 90° , the velocity reaches maximum. However, when the scour angle is less than 90° the critical

velocity for incipient motion in the scour hole will be smaller compared to that with flat beds under the same flow conditions.

Regarding the drag coefficient C_D , since the Reynolds number in this research was larger than 10^5 , the Stokes Law cannot be applied. By referring the relationship between drag coefficient and Reynolds number for a sphere, developed by Graf and Acaroglu (1966), the value of C_D can be determined. For the lift coefficient C_L , the lift coefficient was a function of shape and density of the sediment particle. If $C_L = \beta C_D$, the trail and error method was used to get the value of β in this research.

Around the square abutment, the maximum scour depth was located around Point B, herein, the measurements at B were used to calculate the near bed velocity. While for the semi-circular abutment, the maximum scour depth was located between Point D and E, so the measurements at these two points were used.

Under ice cover, if the flow velocity profile was available, as suggested by Kuhnle et al. (2008), the bed shear velocity can be calculated by fitting a least square regression to flow velocity and distance measurements from near the bed to 20% of the depth using the following:

$$U_{*c} = \frac{d\bar{u}}{5.75d \lg h} \quad (3.6-7)$$

in which, U_{*c} is the critical bed shear velocity, \bar{u} is the mean flow velocity at a distance of h .

However, if the velocity profile was not available, the logarithmic velocity distribution assumption was one of the generally accepted methods for calculating the shear velocity based on Prandtl and Einstein correction factor (Einstein, 1950).

$$U_{*c} = \frac{\bar{u}}{5.75 \log_{10} \left(\frac{12.27 \chi R_h}{D_{50}} \right)} \quad (3.6-8)$$

Where R_h is the channel hydraulic radius, \bar{u} is the average cross sectional velocity, D_{50} is used to represent the particle size since the sediment used in this research is non-uniform sediment, χ is the Einstein multiplication factor, here we used $\chi=1$, and the ice cover can be included in the channel hydraulic radius. The critical shear velocities were calculated based on Equation 3.6-8.

At the end of each experiment, an armor layer developed around the bridge abutment. To assess the impacts of armor layers, Meyer-Peter and Mueller (1948) developed the following equation by using one mean grain size of the bed to calculate the sediment size in the armor layer.

$$d = \frac{SH}{K_1 \left(n / D_{90}^{1/6} \right)^{3/2}} \quad (3.6-9)$$

Where d is the sediment size in the armor layer; S is the channel slope; H is the mean flow depth; K_1 is the constant number equal to 0.058 when H is in meters; n is the channel bottom roughness or Manning's roughness, and D_{90} is the bed material size where 90% of the material is finer.

To further examine the relationship between near bed velocity and maximum scour depth, Figure 3.6-3 was plotted. From Figure 3.6-3, at least three observations can be noticed.

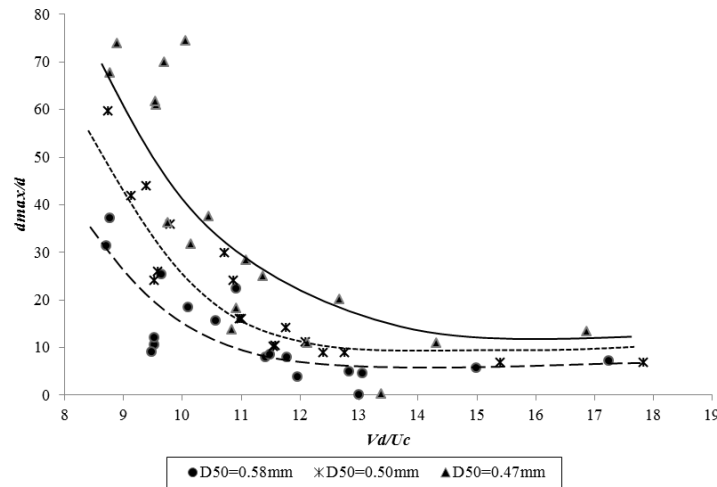


Figure 3.6- 3 Incipient motion of different sediments with the maximum scour depth

(1) For the same sediment, with the increase in V_d/U_c , the value of d_{max}/d decreases. From Figure 3.6-3, the slope of the curve represents the changing rate of scour depth. At the beginning, the scour depth increased quickly. Afterward, with the development of the scour hole and formation of the armor layer, the changing rate decreased correspondingly. The changing rate became 0 at the end, which means no variation in scour depth. In other words, the maximum scour depth was reached.

(2) Under the same flow condition with the same value of V_d/U_c , sediment with smaller D_{50} had a larger maximum scour depth. In this case, sediment with $D_{50}=0.47\text{mm}$ had the largest maximum scour depth.

(3) When the value of V_d/U_c reached about 14, the values of d_{\max}/d remained constant. During the scour hole development and formation of the armor layer, the velocity near the scour hole is higher than the critical velocity of D_{50} . When the maximum scour depth is constant, then the maximum scour depth is reached.

Dimensionless shear stress

In practice, the shear Reynolds number is usually used to study the incipient motion, which can be given by:

$$R_e^* = \frac{U_{*c} D}{\nu} \quad (3.6-10)$$

in which, U_{*c} is the shear velocity calculated by Equation 3.6-8, D is the grain size diameter, and ν is the kinetic viscosity of the fluid. Since the sediment used here is non-uniform sediment, the grain size diameter will be replaced by D_{50} , then Equation 3.6-9 can also be written as follows,

$$R_e^* = \frac{U_{*c} D_{50}}{\nu} \quad (3.6-11)$$

The dimensionless shear stress τ_* is calculated by using the following equation:

$$\tau_* = \frac{\rho U_{*c}^2}{g \Delta \rho D_{50}} \quad (3.6-12)$$

where $\Delta\rho$ is the difference in mass density between water and sediment.

The relation between shear Reynolds number and dimensionless shear stress is known as the Shields Diagram, which is widely used for predicting incipient motion in open channels. The calculated criteria for incipient motion of bed material is presented in Figure 3.6-4. For all three non-uniform sediments, with the increase in shear Reynolds number, the dimensionless shear stress increased correspondingly. However, with the same shear Reynolds number, finer sediment had a higher dimensionless shear stress. In this case, sediment with a $D_{50}=0.47\text{mm}$ had the largest dimensionless shear stress. With a high proportion of finer particles in the non-uniform sediment, the local scour can easily be triggered around bridge abutments. With the same bed material, the larger the shear Reynolds number, the larger the dimensionless shear stress. For the same dimensionless shear stress, the coarser the bed material, the larger the shear Reynolds number.

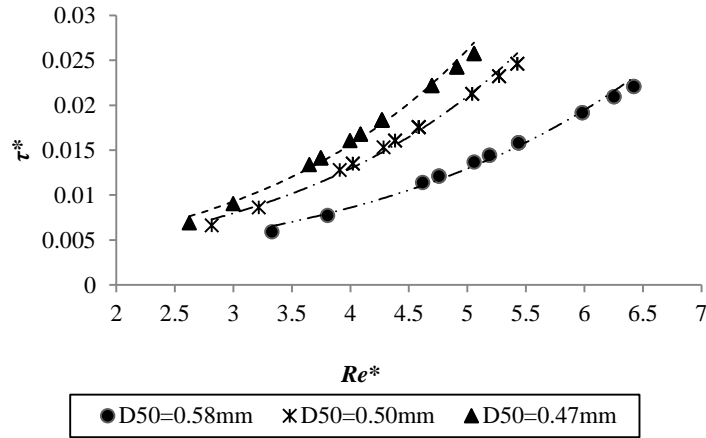


Figure 3.6- 4 The variation of shear Reynolds number with dimensionless shear stress

Since the maximum scour depth was our main interest in the scour estimation, the maximum scour depth versus dimensionless shear stress was presented in Figures 3.6-5, 3.6-6 and 3.6-7. The incipient motion for non-uniform sediment varied more in comparison to that of uniform sediment. To consider the impacts of armor layer in the maximum scour depth, the ratio of maximum scour depth to the particle size of armor layer was developed.

Figure 3.6-5 shows the variation of maximum scour depth with the dimensionless shear stress around a square abutment under both open channel and ice covered condition. The overall trend of the curve is increasing. With the increase in dimensionless shear stress, the maximum scour depth increases correspondingly. It is also indicated in the figure that the trend for open channel and covered conditions were the same for different non-uniform sediments. Due to the protection from the armor layer, after the dimensionless shear stress reaches the threshold value, the ratio of maximum scour depth to the particle size of armor layer would be close to constant. However, the experimental data in the present research was not enough to show the overall trend. More data are needed to prove this statement in the future, which means larger dimensionless shear stress will be needed for both open channel and ice covered flow.

Figure 3.6-6 compares the dimensionless shear stress under open channel condition with that of under rough ice covered condition around a square abutment. Figure 3.6-7 compared the dimensionless shear stress under smooth ice cover condition with that of under rough covered condition around a semi-circular abutment. For both types of abutments, the maximum scour depth increases with the increase in dimensionless shear stress. Under rough cover, less

dimensionless shear stress is needed to reach the same scour depth compared to that for open channel and smooth covered conditions. With the same dimensionless shear stress, rough cover results in a deeper scour depth around the abutment compared to that of open flow conditions. One can note that rough ice cover can cause a deeper scour depth compared to that under smooth ice covered condition.

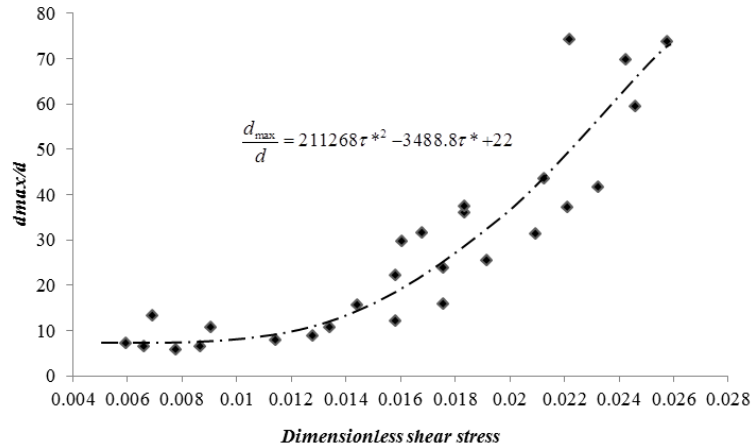


Figure 3.6- 5 The maximum scour depth variation with dimensionless shear stress around square abutment

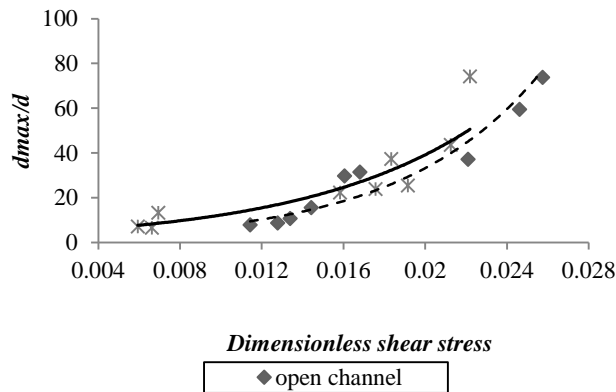


Figure 3.6- 6 The maximum scour depth variation with dimensionless shear stress under ice cover and open channel (square abutment)

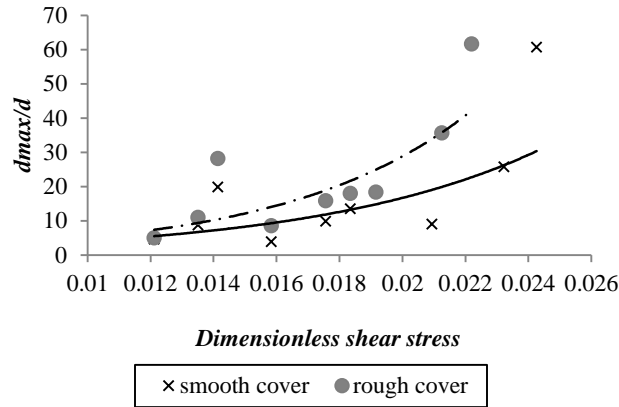


Figure 3.6- 7 The maximum scour depth variation with dimensionless shear stress under smooth ice cover and rough ice cover (semi-circular abutment)

3.6.3 Conclusions

The present study investigated the features of incipient motion under ice cover with non-uniform sediments. Experiments have been conducted by using two abutment models and three non-uniform sediments, under open flow condition and two ice-covered conditions. The following are the main conclusions that can be drawn from this study:

1. The average scour angle around a semi-circular abutment is around 10 degrees larger than that around the square abutment under clear water conditions. The streamline-like abutment with a solid foundation in the floodplain causes less local scour depth than that caused by the square abutment under ice-covered condition.
2. Based on the scour angle around bridge abutment, it was found that for same non-uniform sediment, due to the formation of an armor layer, the maximum scour depth remains constant.
3. With the increase in dimensionless shear stress, the maximum scour depth increases correspondingly. Additionally, the presence of ice cover can result in a deeper maximum scour depth compared to that under open flow condition. In reality, when the ice cover forms in early winter and breaks up in early spring, the roughness coefficient of ice cover (or ice jam) is surprisingly larger than the stable covered period during winter. Therefore the scour depth around bridge abutment at this time may increase due to the enlarged roughness coefficient.

The present research deals with the incipient motion and dimensionless shear stress for non-uniform sediments under ice covered condition. Further work needs to be carried out to investigate the velocity profile under ice cover in the scour hole around abutments with solid foundations.

Notation

C_D = drag coefficient at velocity V_d

C_L = lift coefficient at velocity V_d

d = sediment size in the armor layer

D_{50} = Mean diameter of sediment for which 50% of the sample is finer (mm)

F_D = Drag force for incipient motion

F_L = Lift force

F_R = Resistance force

g = gravity acceleration (ms^{-2})

H = mean flow depth

n = Manning's roughness value

Re^* = Reynolds number (-)

S = channel slope

U_{*c} = critical bed shear velocity

u = mean velocity at distance h from the bottom

W = Particle submerged weight

α = scour angle (-)

ρ = density of water

ρ_s = density of sediment

σ_g = geometric standard deviation (-)

τ^* = dimensionless shear stress (-)

References

1. Ackermann, N. L., Shen, H. T., Olsson, P. (2002) Local scour around circular piers under ice covers. Proc. Int. Conf. 16th IAHR International Symposium on Ice, IAHR, Dunedin, New Zealand.
2. Coleman, S. E., Lauchlan, C. S., Melville, B. W. (2003). Clear water scour development at bridge abutments, *J. Hydraulic Res.*, 41(5), 521–531.
3. Dey, S., Barbhuiya, A. K. (2005). Turbulent flow field in a scour hole at a semicircular abutment, *Can. J. Civ. Eng.*, 32, 213-232.
4. Duan, J. G., He, L., Fu, X., Wang, Q. (2009). Mean flow and turbulence around experimental spur dike, *Adv. Water Resour.*, 32, 1717-1725.
5. Ettema, R., Braileanu, F., Muste, M. (2000). Method for estimating sediment transport in ice covered channels. *J. Cold Reg. Eng.*, ASCE, 14(3), 130-144.
6. Ettema, R., Daly, S. (2004). Sediment transport under ice. ERDC/CRREL TR-04-20. Cold regions research and Engineering Laboratory, US Army Corps of Engineers.
7. Froehlich, D. C., (1995). Armor limited clear water construction scour at bridge. *J. Hydraulic Eng.*, 121, 490-493.
8. Graf, W. H., Acaroglu, E. R. (1966). Setting velocities of natural grains. *Bulletin of the International Association of Scientific Hydrology*, 11(4).
9. Hains, D. B. (2004). An experimental study of ice effects on scour at bridge piers. PhD Dissertation, Lehigh University, Bethlehem, PA.
10. Laursen, E. M., Toch, A. (1956). Scour around bridge piers and abutments. Iowa Highway Research Board Bulletin, No 4.
11. Melville, B. W. (1992). Local scour at bridge abutments. *J. Hydraulic Eng.*, 118, 615-631.
12. Melville, B. W. (1997). Pier and Abutment scour: integrated approach. *J. Hydraulic Eng.*, 123(2), 125-136.
13. Munteanu, A. (2004). Scouring around a cylindrical bridge pier under partially ice-covered flow condition. Master thesis, University of Ottawa, Ottawa, Ontario, Canada.

14. Munteanu, A., Frenette, R. (2010). Scouring around a cylindrical bridge pier under ice covered flow condition-experimental analysis. R V Anderson Associates Limited and Oxand report.
15. Sui, J., Faruque, M. A. A., Balachandar, R. (2009). Local scour caused by submerged square jets under model ice cover. *J. Hydraulic Eng.*, 135(4), 316-319.
16. Sui, J., Wang, J., He, Y., Krol, F. (2010). Velocity profile and incipient motion of frazil particles under ice cover. *International Journal of Sediment Research*, 25(1), 39-51.
17. Smith, B. T., Ettema, R. (1997). Flow resistance in ice covered alluvial channels. *J. Hydraulic Eng.*, 123(7), 592-599.
18. Wahl, T. L. (2000). Analyzing data using WinADV. 2000 Joint Conference on water resources engineering and water resources planning and management. Minneapolis, Minnesota, 1-10.
19. Wang, J., Sui, J., Karney, B. (2008). Incipient motion of non-cohesive sediment under ice cover – an experimental study. *Journal of Hydrodynamics*, 20(1), 177-124.
20. Yang, C. T. (2003). *Sediment transport, theory and practice*. Krieger publishing company, Krieger Drive, Malabar, Florida.

4 GENERAL CONCLUSION

Experiments have been conducted in a large scale flume to study the impact of ice cover roughness and non-uniform sediments on the local scour around two types of commonly used abutments. It is found that ice cover plays an important role in the development of local scour hole around bridge abutments, including bed morphology, maximum scour depth, maximum scour depth location, armor layer etc. The general conclusions are as follows.

The location of the maximum scour depth along the abutment is around 60° from the flume wall for semi-circular abutment. While the maximum scour depth around square abutment locates in the upstream corner. The results indicate that the impact of shape factor for semi-circular abutments on maximum scour depth is smaller in covered conditions than that in open channels. The range of shape factor is between 0.66 and 0.71. The downstream slope in the scour hole is also smaller compared to that in the upstream. Under ice cover, the average scour depth is always greater compared to that in open channels. The average scour depth under rough ice cover is 35% greater than that under smooth ice cover. In this research, densimetric Froude number is also used to investigate the impacts of non-uniform sediment composition on local scour. The scour volume and scour area are calculated and compared to open channel, smooth and rough cover conditions.

By using Buckingham Pi theorem for dimensional analysis, the impact of shape factor and ice cover roughness on maximum scour depth around abutments is investigated. Empirical equations of the maximum scour depth are developed, which indicates that with an increase in sediment grain size, the maximum scour depth decreased correspondingly.

Furthermore, the impact of armor layer development and ice cover roughness is discussed. The armor layer only forms in the scour hole while fine sediment deposition is located at the downstream of the abutment. The armor layer grain size has a strong impact on the dimensionless maximum scour depth. With the increase in the particle size of armor layer, the maximum scour depth decreases correspondingly. The relationships between maximum scour depth, water depth, densimetric Froude number, ice cover roughness, and armor layer grain size are derived by using dimensionless analysis.

By using a down-looking 3D ADV, the flow field at different locations and elevations around two abutments was measured. Compared to the flow in open channel, the velocity component in

Z direction contributes much to the development of scour hole under ice covers. Additionally, features of incipient motion under ice cover with non-uniform sediments are studied at the end of the research. It is interesting to find that the average scour angle around a semi-circular abutment is around 10 degrees larger than that around the square abutment under clear water conditions. The streamline-like abutment with a solid foundation in the floodplain causes less local scour depth than that caused by the square abutment under ice-covered condition. With the increase in dimensionless shear stress, the maximum scour depth increases correspondingly.

In reality, ice cover is a big issue in the northern hemisphere. When the ice cover forms in early winter and breaks up in early spring, the roughness of ice cover (or ice jam) is completely different, compared to that with stable covered period during the winter. Up to date, the impact of ice cover is beyond our knowledge. The present study indicates the necessity for further ice scour research as it relates to hydraulic engineering. Empirical equations developed from the present research can also be used for the estimation of scour depth under ice cover in hydraulic engineering.

5 APPENDIX

Table 5- 1 Experimental data collected at non-uniform sand ($D_{50} = 0.58$ mm)

date	abutment type	flume cover	maximum depth (cm)	average velocity (m/s)	approach depth	scour volume(cm^3)	scour area (cm^2)	average scour depth (cm)
0922	square	open	9.5	0.26	0.07	411.46	267.38	1.54
0923	square	open	4	0.21	0.07	288.18	355.35	0.81
0926	square	open	5.5	0.21	0.19	661.88	592.79	1.12
0927	round	open	0	0.21	0.07	0.00	0.00	0.00
0928	round	open	5.5	0.23	0.19	1433.09	1009.79	1.42
0929	round	open	2.7	0.26	0.07	570.46	782.08	0.73
0930	round	smooth	2.3	0.23	0.07	273.33	466.68	0.59
1001	round	smooth	3.2	0.2	0.19	696.74	907.55	0.77
1002	round	smooth	1	0.2	0.07	165.88	494.57	0.34
1003	square	smooth	3.1	0.2	0.07	167.72	264.03	0.64
1004	square	smooth	4	0.16	0.19	706.36	733.16	0.96
1005	square	smooth	8	0.23	0.07	1201.07	509.75	2.36
1006	square	rough	6.5	0.22	0.07	1400.24	904.46	1.55
1007	square	rough	5.7	0.21	0.07	993.01	766.47	1.30
1008	square	rough	5	0.14	0.19	785.24	518.72	1.51
1009	round	rough	2.2	0.21	0.07	238.63	540.96	0.44
1010	round	rough	3.5	0.2	0.19	459.50	376.34	1.22
1011	round	rough	4.7	0.22	0.07	1127.69	715.74	1.58

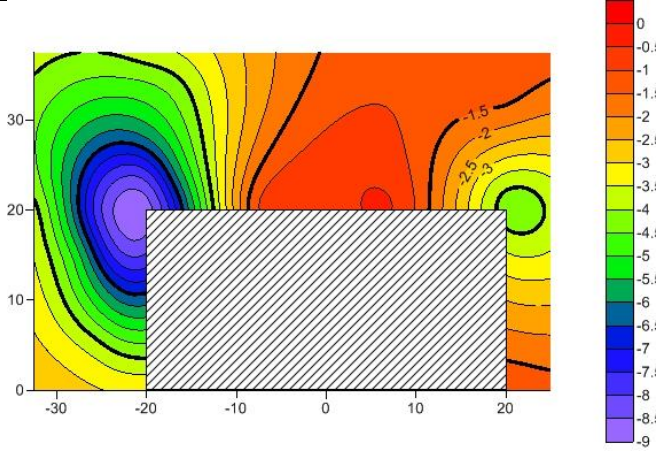
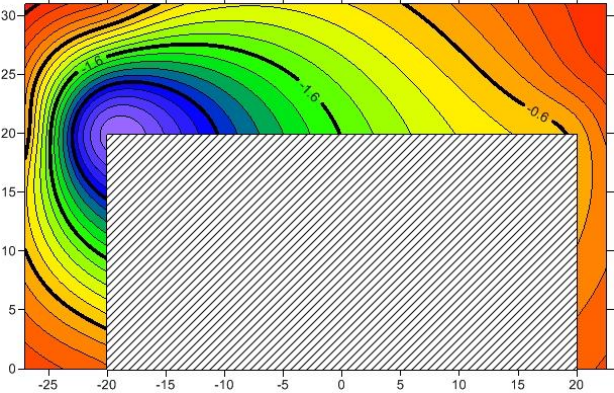
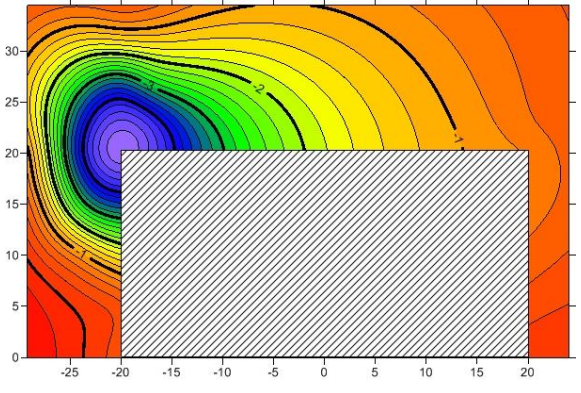
Table 5- 2 Experimental data collected at non-uniform sand ($D_{50} = 0.50$ mm)

date	abutment type	flume cover	maximum depth (cm)	average velocity (m/s)	approach depth (m)	scour volume (cm ³)	scour area (cm ²)	average scour depth (cm)
1018	square	open	16.4	0.26	0.07	24930.95	3977.91	6.27
1019	square	open	7	0.21	0.07	1131.11	1188.88	0.95
1020	square	open	6.5	0.21	0.19	1412.31	645.86	2.19
1021	round	open	0	0.21	0.07	0.00	0.00	0.00
1022	round	open	15	0.23	0.19	19095.94	3335.68	5.72
1023	round	open	15	0.26	0.07	16847.15	3401.70	4.95
1024	round	smooth	13.5	0.23	0.07	6520.80	1895.73	3.44
1025	round	smooth	12	0.2	0.19	5856.95	1758.72	3.33
1026	round	smooth	3	0.2	0.07	187.58	213.61	0.88
1027	square	smooth	8	0.2	0.07	1610.17	757.03	2.13
1028	square	smooth	6.5	0.16	0.19	1002.35	536.94	1.87
1029	square	smooth	15.5	0.23	0.07	12372.14	3101.20	3.99
1030	square	rough	16.5	0.22	0.07	14090.53	3885.92	3.63
1031	square	rough	8.3	0.21	0.07	3582.35	1421.59	2.52
1101	square	rough	8	0.14	0.19	2723.10	1151.93	2.36
1102	round	rough	4	0.21	0.07	565.81	469.97	1.20
1104	round	rough	17	0.2	0.19	13986.93	3020.83	4.63
1103	round	rough	13.7	0.22	0.07	3224.38	1150.13	2.80

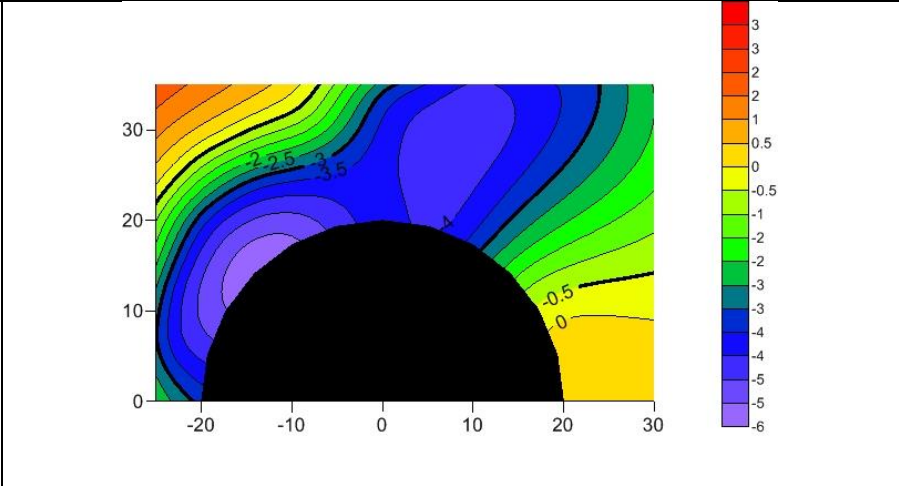
Table 5- 3 Experimental data collected at non-uniform sand ($D_{50} = 0.47$ mm)

date	abutment type	flume cover	maximum depth (cm)	average velocity (m/s)	approach depth (m)	scour volume (cm ³)	scour area (cm ²)	average scour depth (cm)
1107	square	open	15	0.26	0.07	8277.42	2002.30	4.13
1108	square	open	7.5	0.21	0.07	1007.74	532.61	1.89
1109	square	open	6	0.21	0.19	1010.42	652.13	1.55
1110	round	open	3.5	0.21	0.07	778.15	717.05	1.09
1111	round	open	7	0.23	0.19	3278.91	1528.65	2.14
1112	round	open	6	0.26	0.07	3712.67	2240.62	1.66
1113	round	smooth	6.5	0.23	0.07	1674.01	1187.83	1.41
1114	round	smooth	6	0.2	0.19	2350.44	1549.43	1.52
1117	round	smooth	2.5	0.2	0.07	361.83	511.09	0.71
1116	square	smooth	4	0.2	0.07	540.29	547.31	0.99
1115	square	smooth	4.5	0.16	0.19	608.74	643.44	0.95
1118	square	smooth	10.5	0.23	0.07	4752.10	1631.03	2.91
1119	square	rough	11	0.22	0.07	4343.89	1657.09	2.62
1120	square	rough	6	0.21	0.07	1537.33	832.45	1.85
1121	square	rough	4.5	0.14	0.19	999.56	808.63	1.24
1122	round	rough	4	0.21	0.07	481.45	507.46	0.95
1123	round	rough	7.5	0.2	0.19	2190.03	881.93	2.48
1124	round	rough	9	0.22	0.07	5892.06	2264.36	2.60

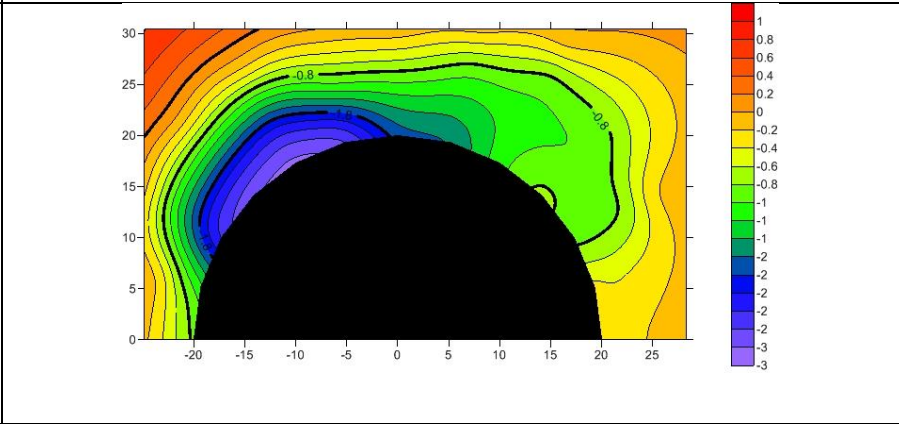
Table 5- 4 Scour contours at $D_{50} = 0.58$ mm

Date	Contour
0922	
0923	
0926	

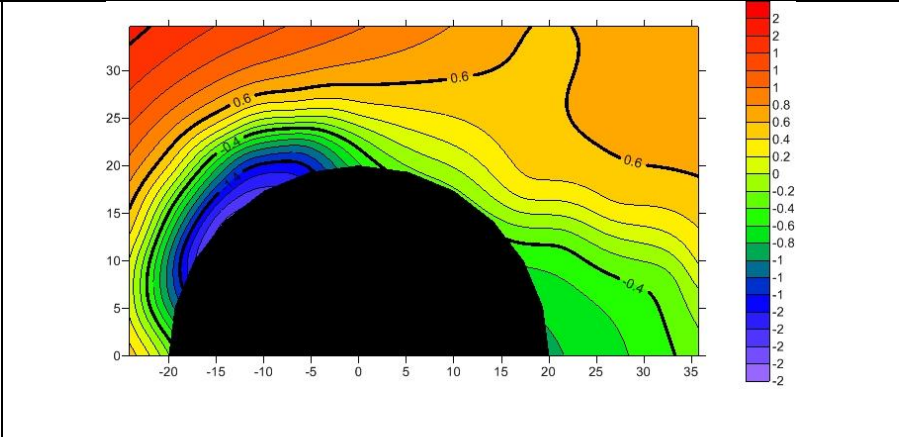
0928

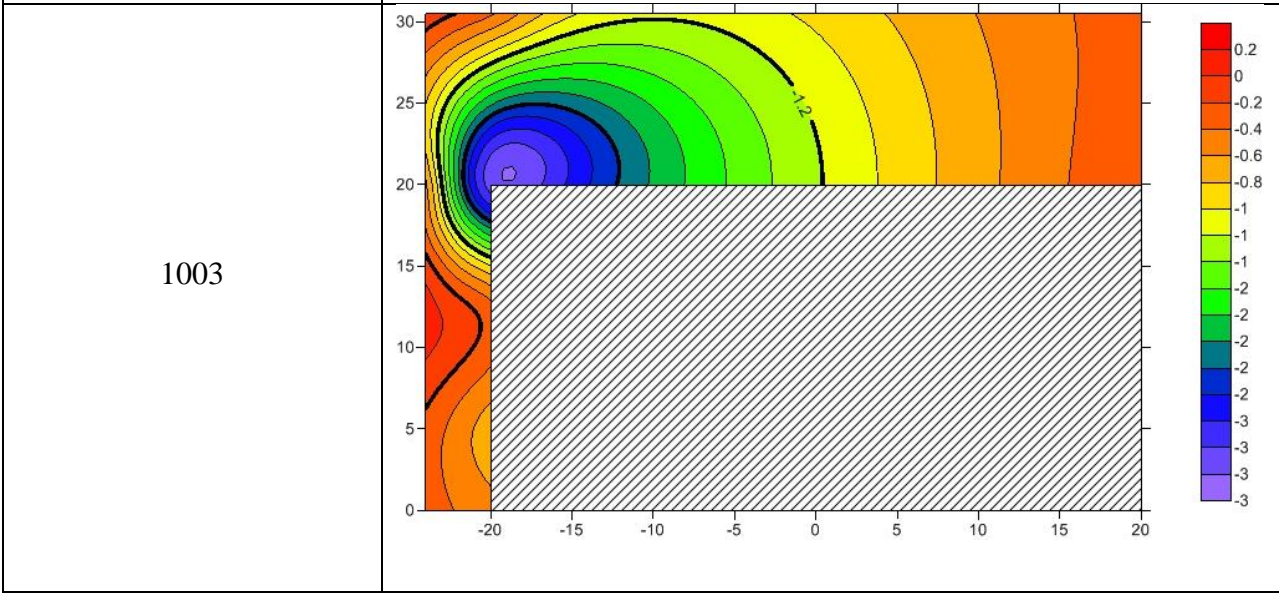
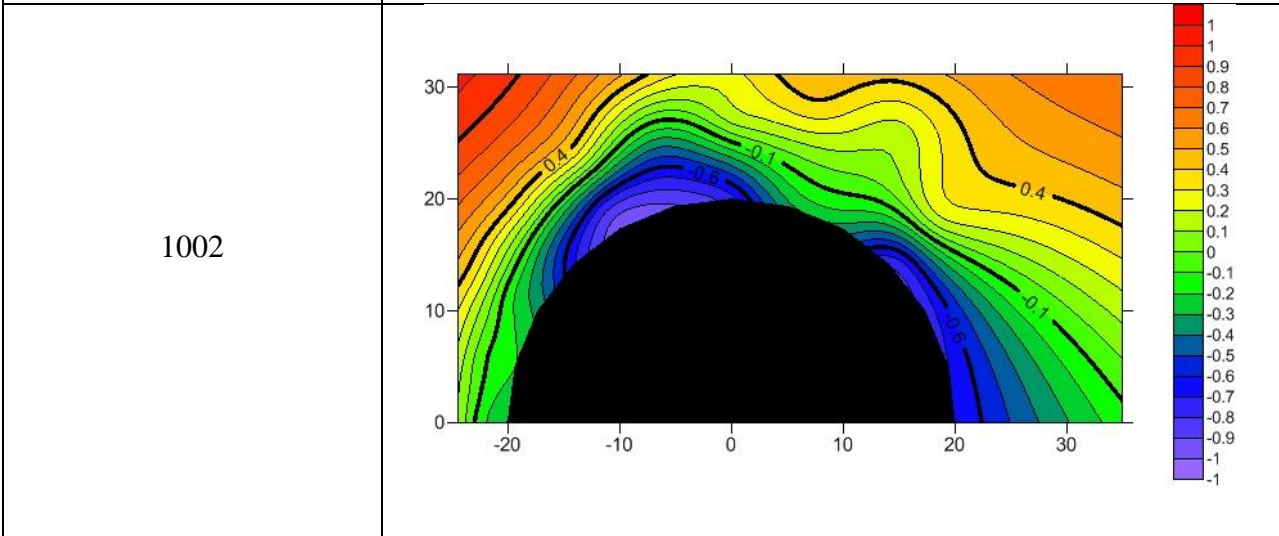
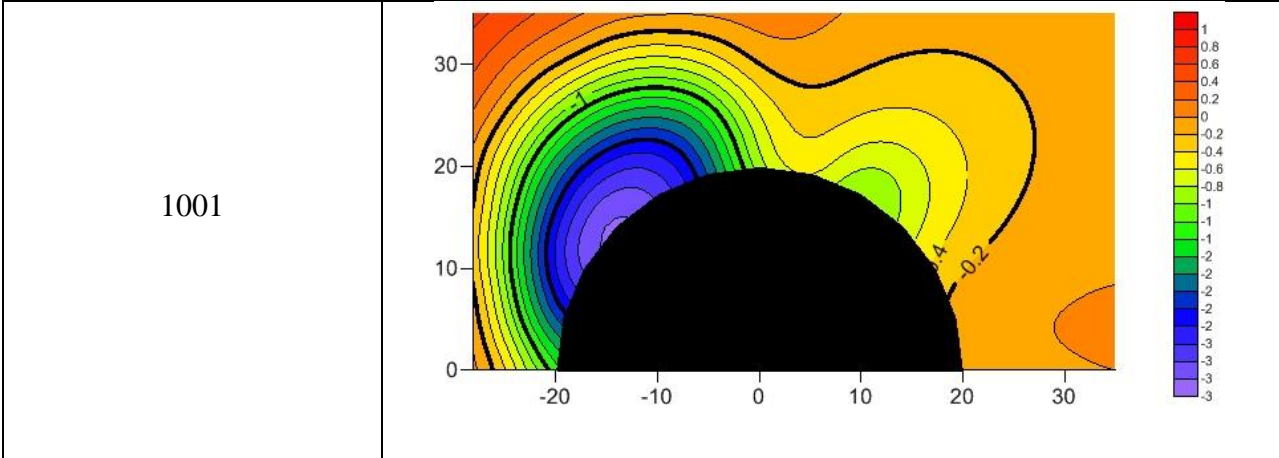


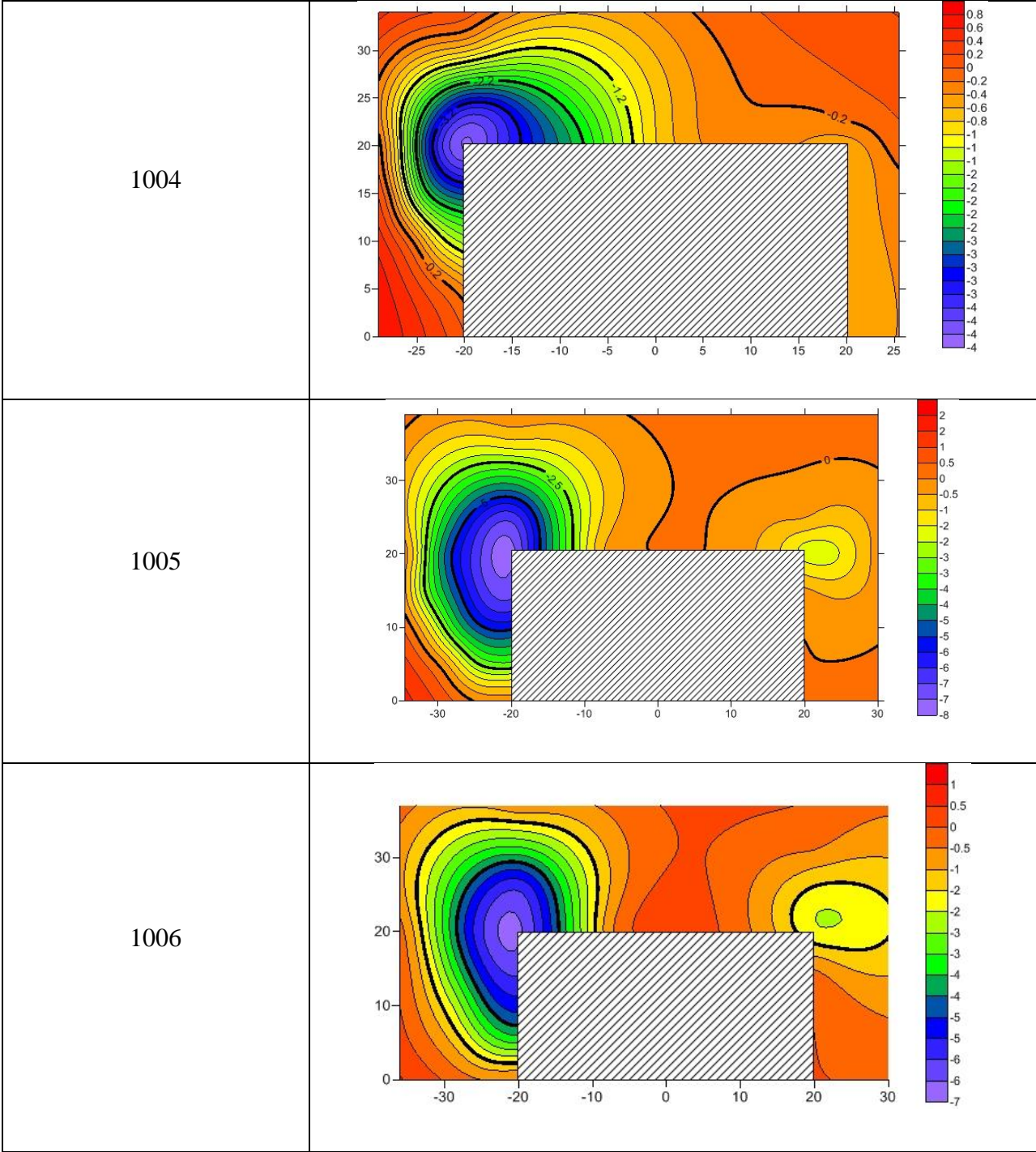
0929

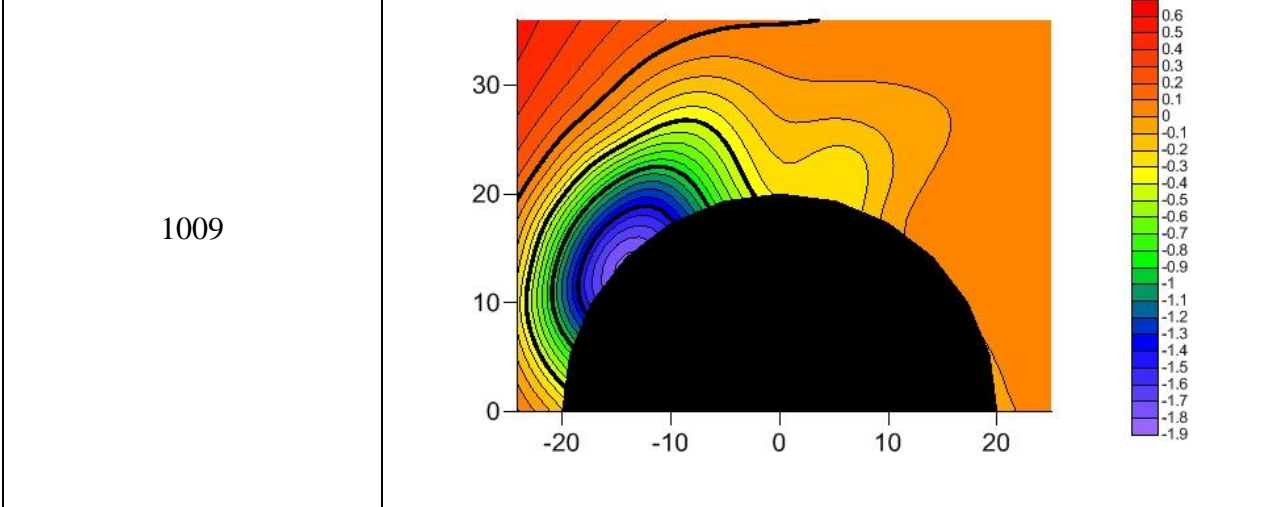
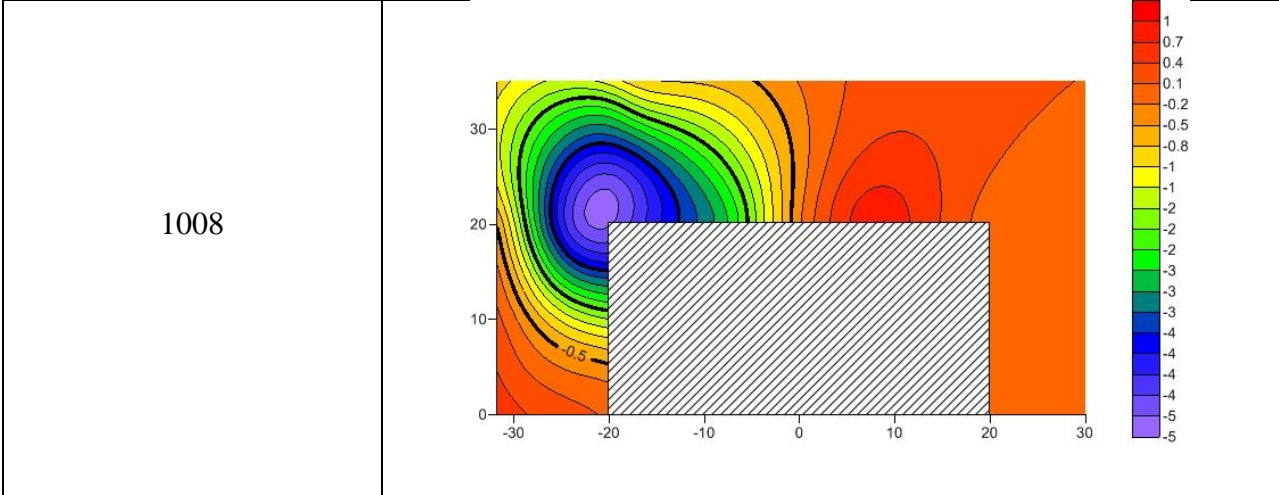
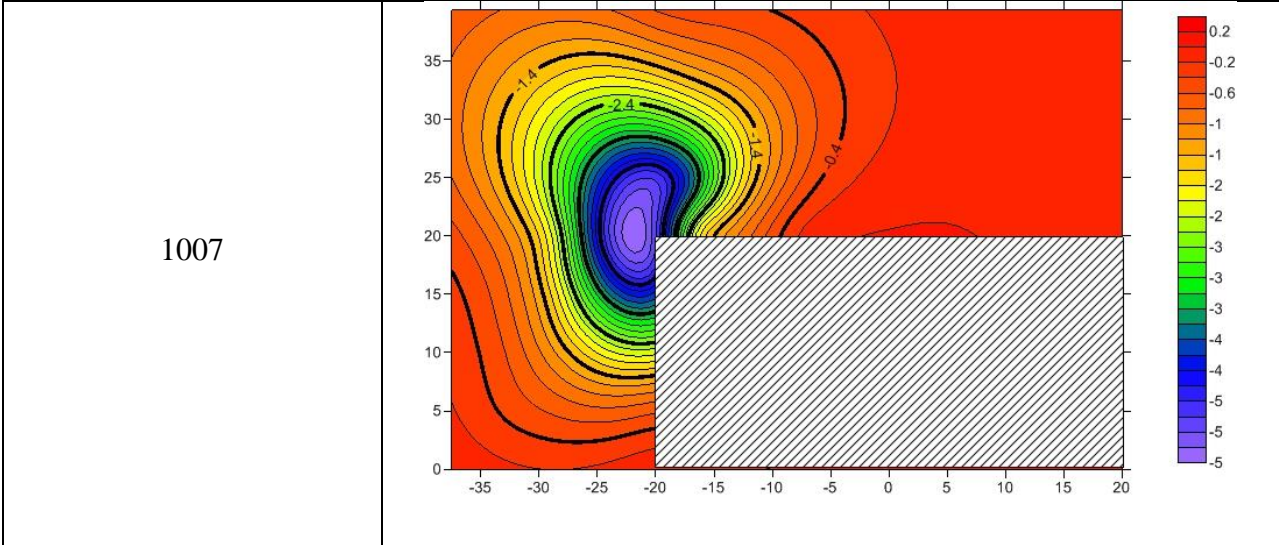


0930

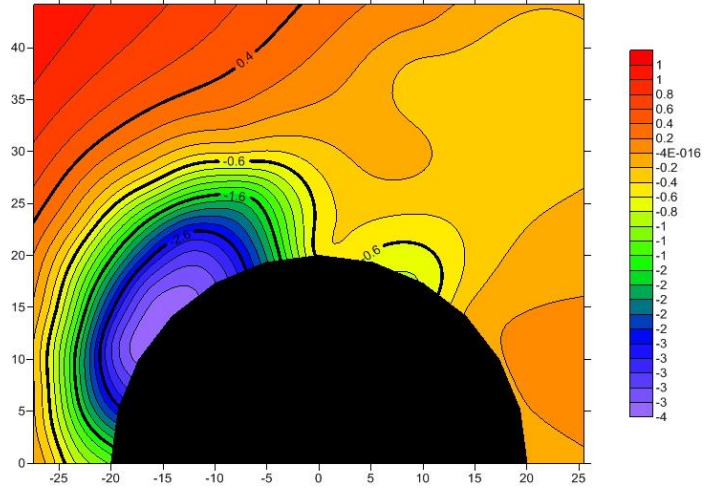








1010



1011

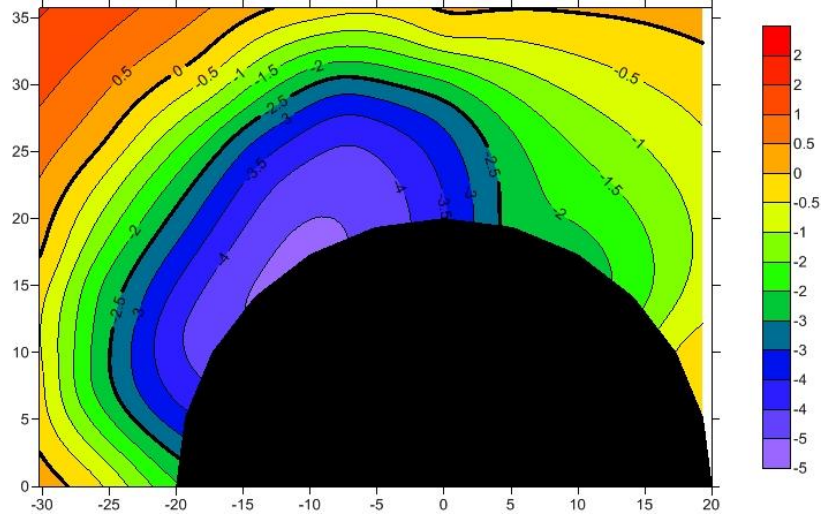
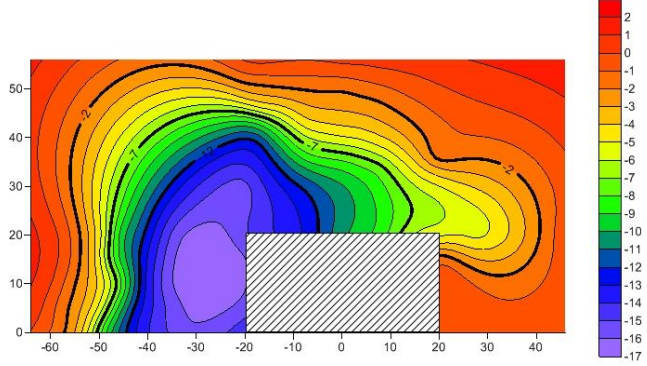
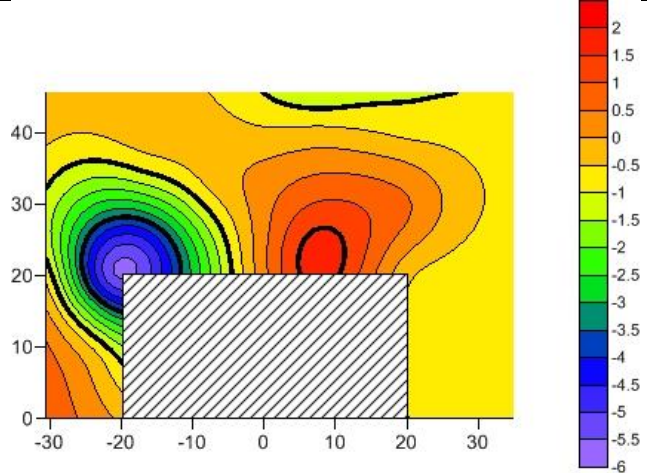
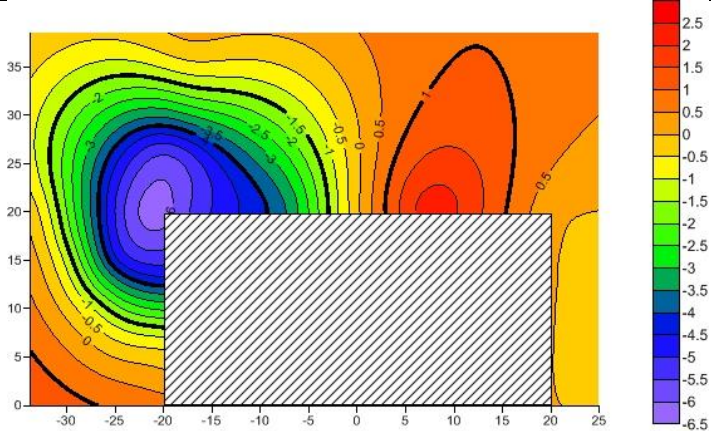
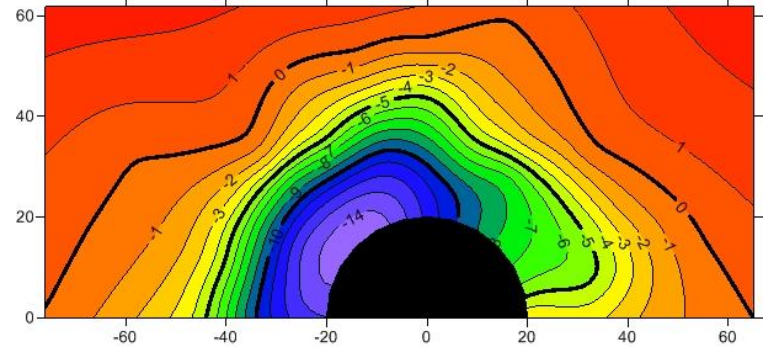


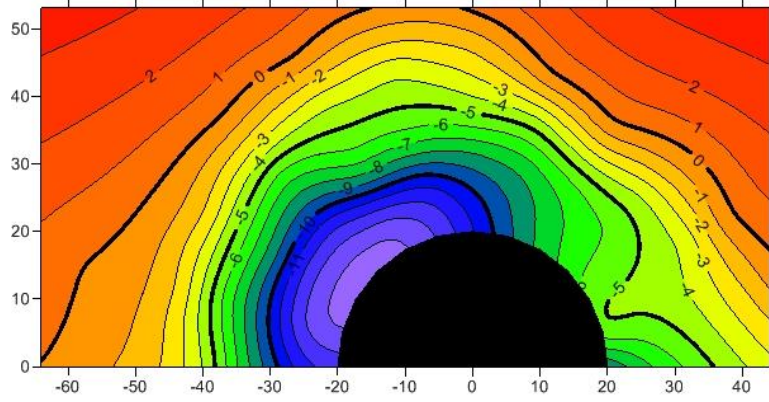
Table 5- 5 Scour contours at $D_{50} = 0.50$ mm

Date	Contour
1018	
1019	
1020	

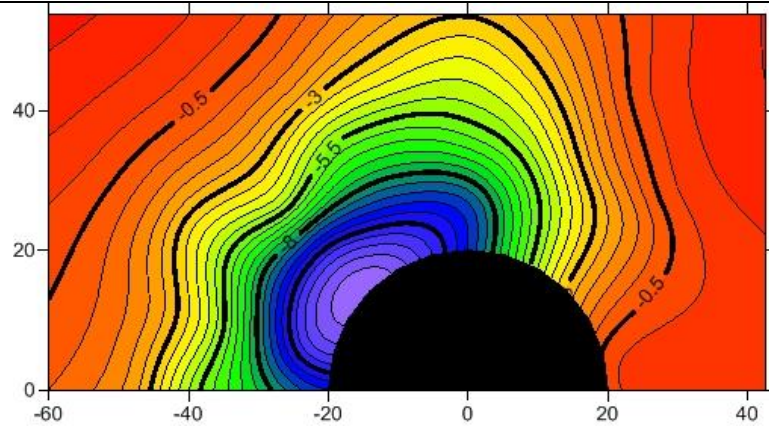
1022



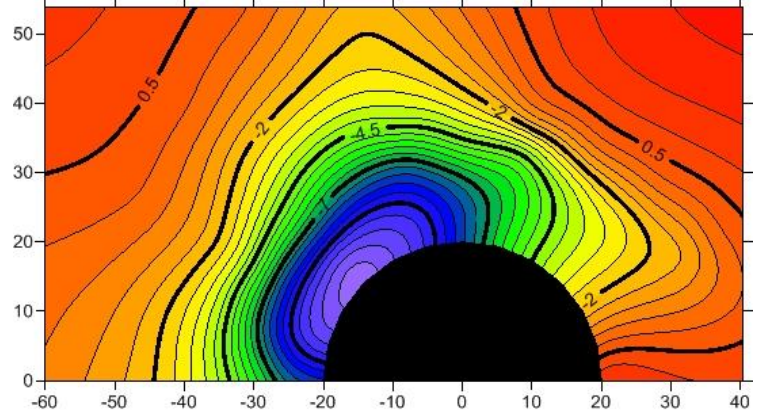
1023



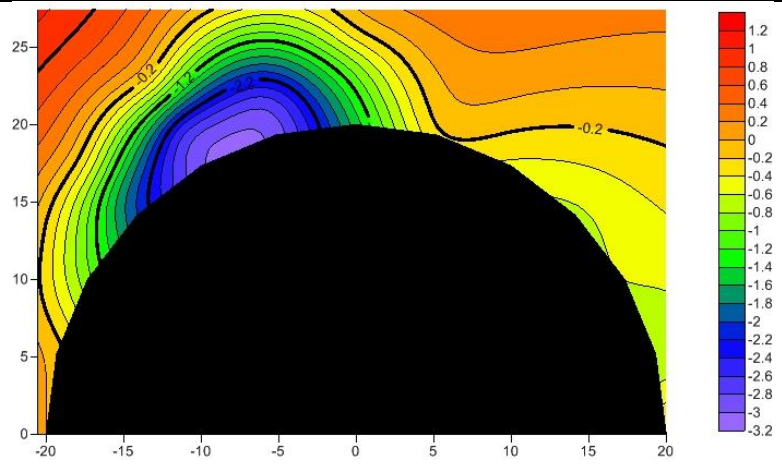
1024



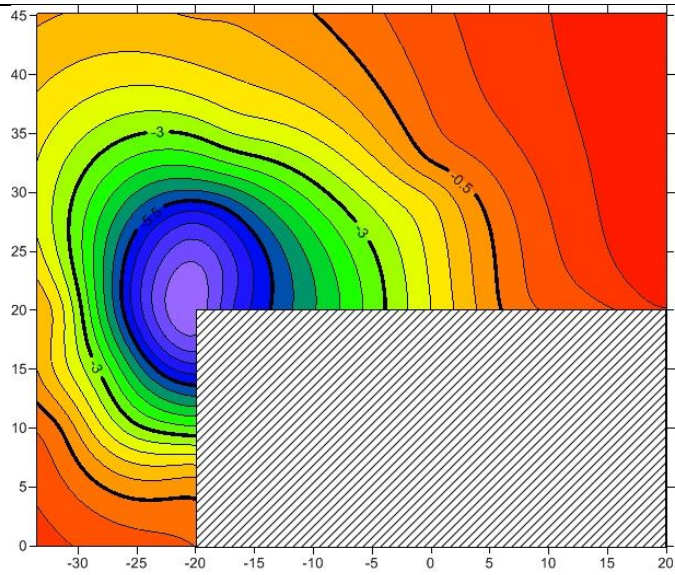
1025



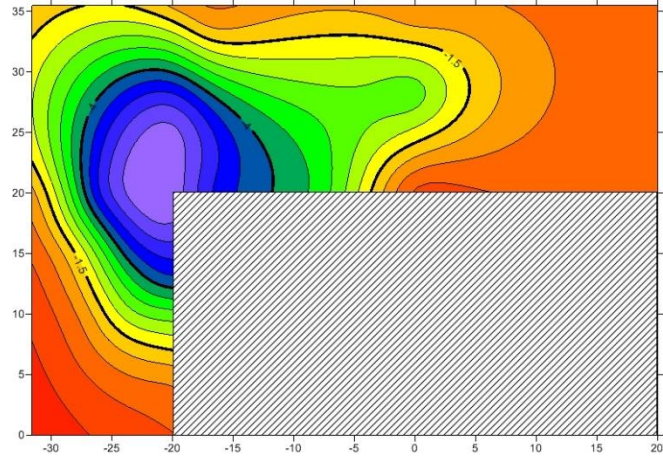
1026



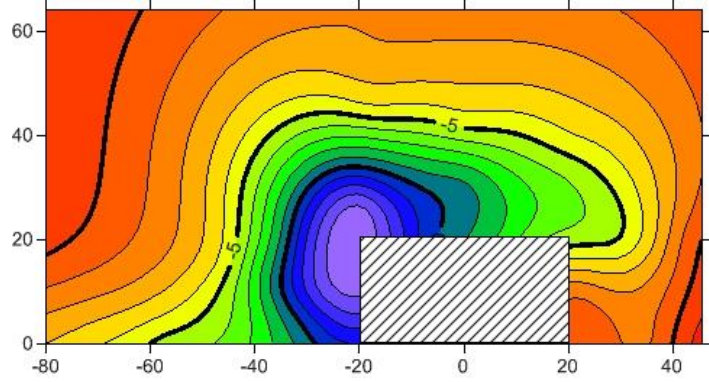
1027



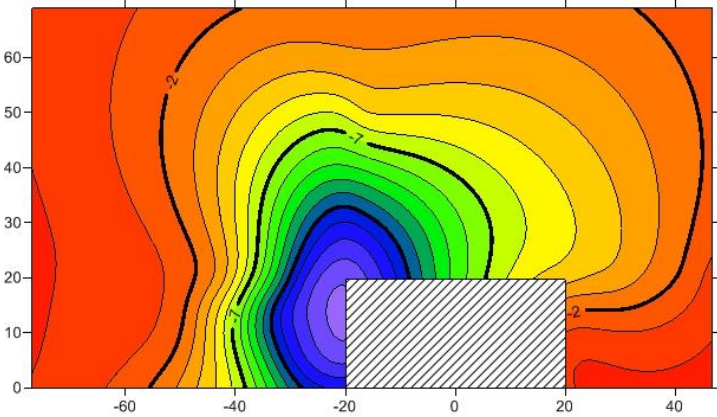
1028



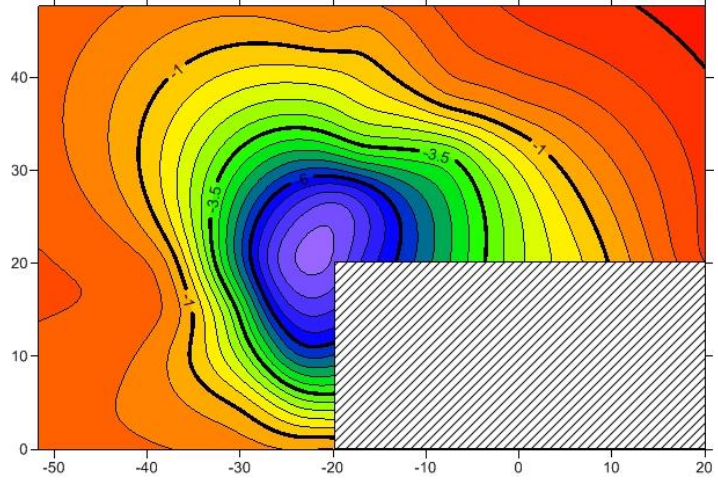
1029



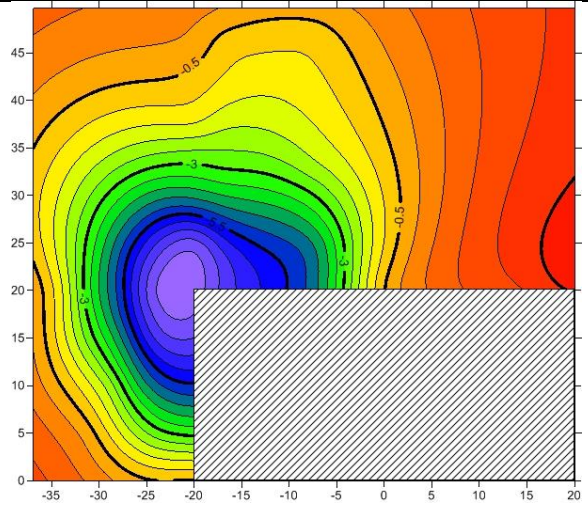
1030



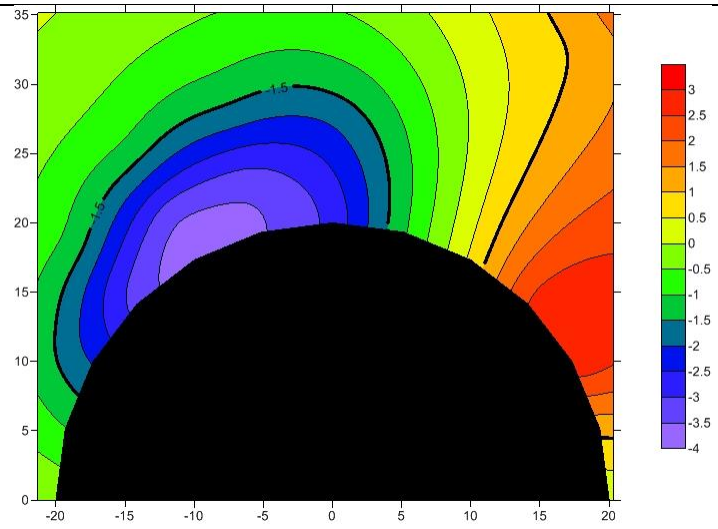
1031



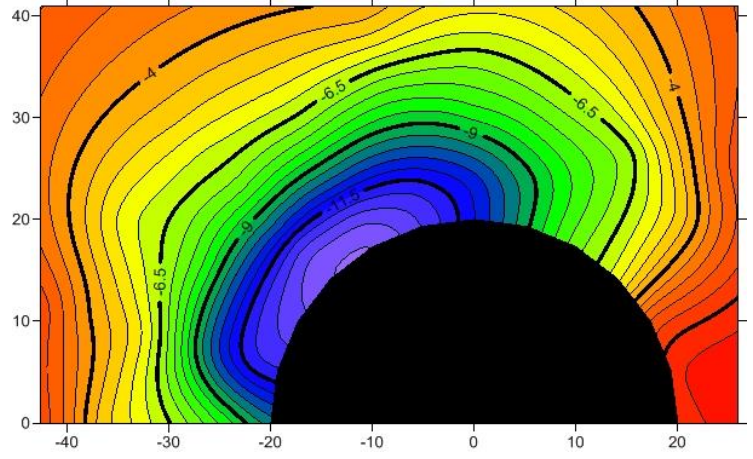
1101



1102



1103



1104

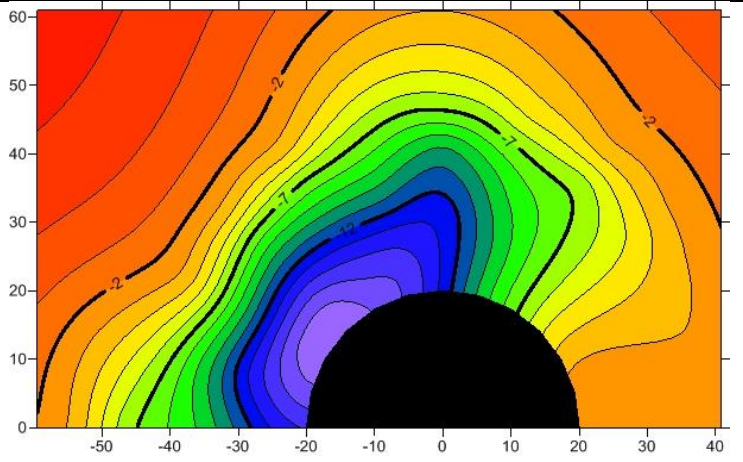
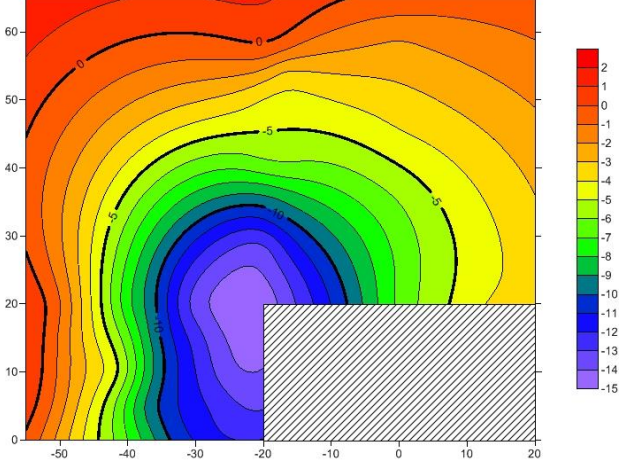
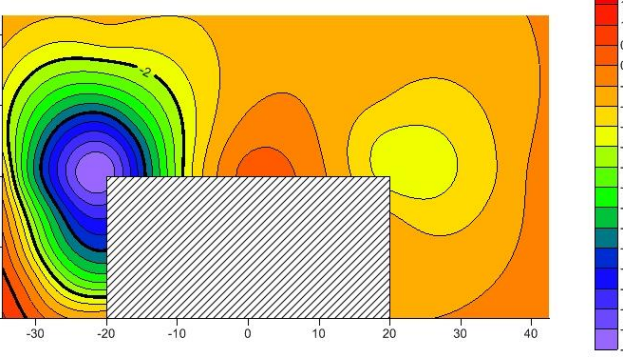
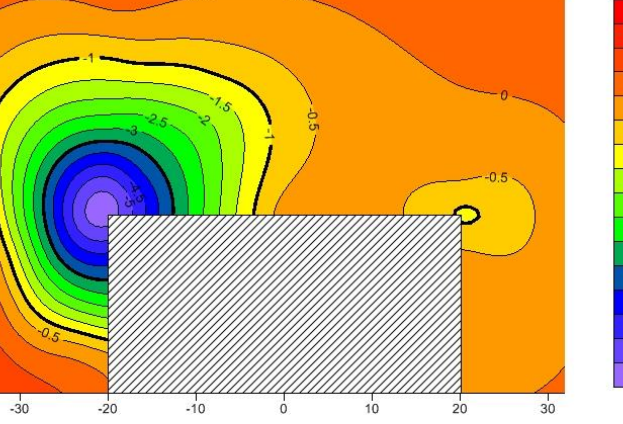
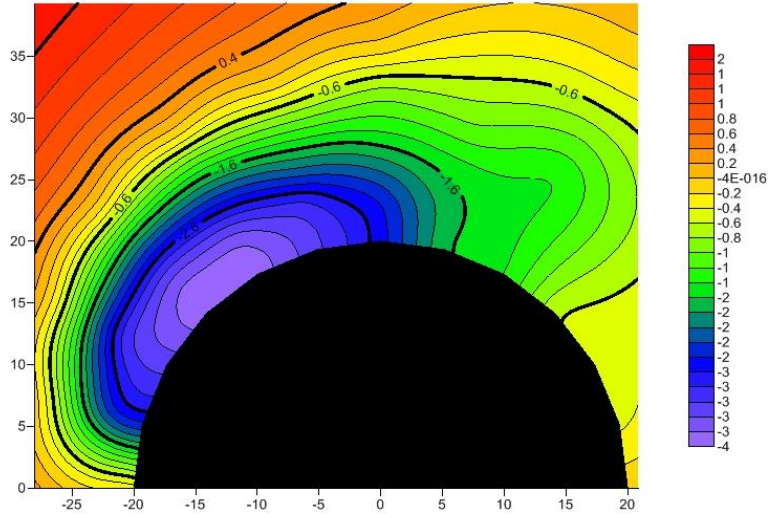


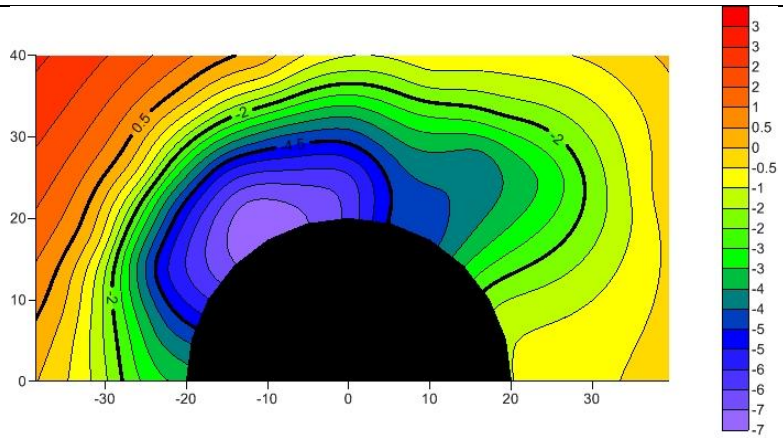
Table 5- 6 Scour contours at $D_{50} = 0.47$ mm

Date	Contour
1107	
1108	
1109	

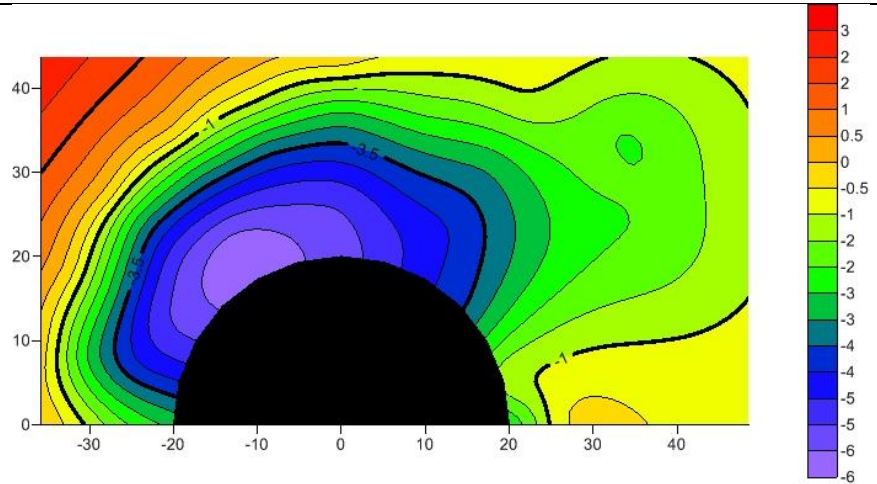
1110

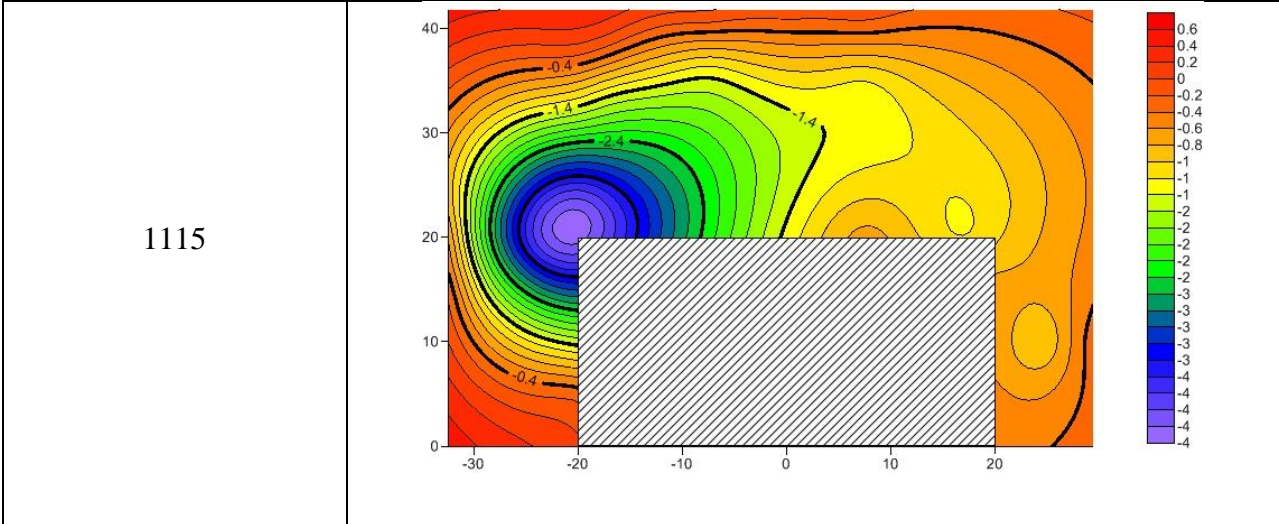
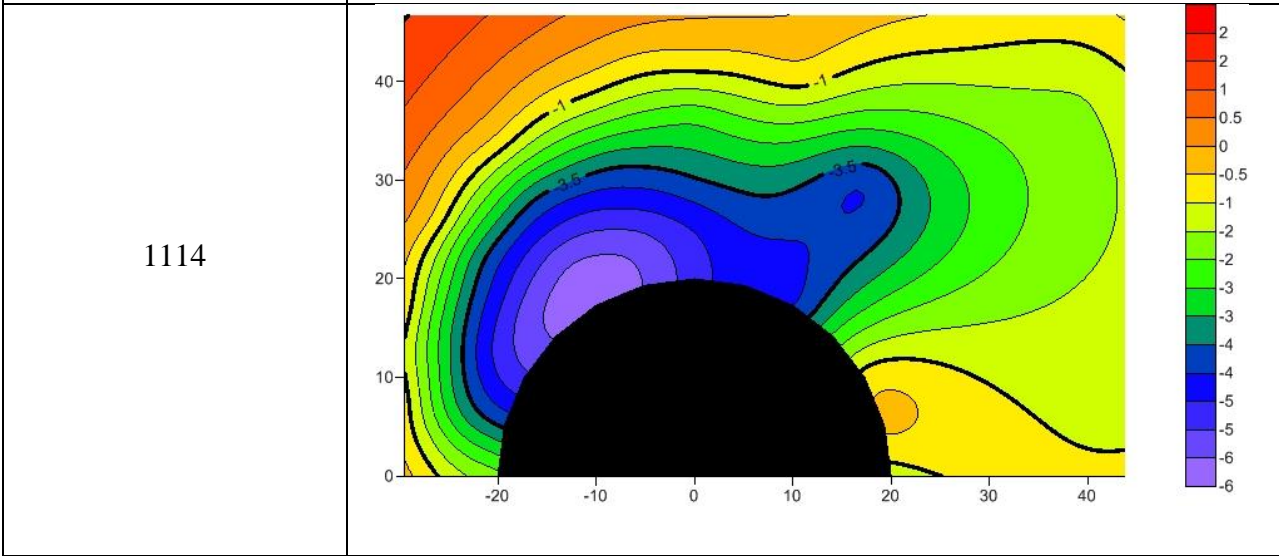
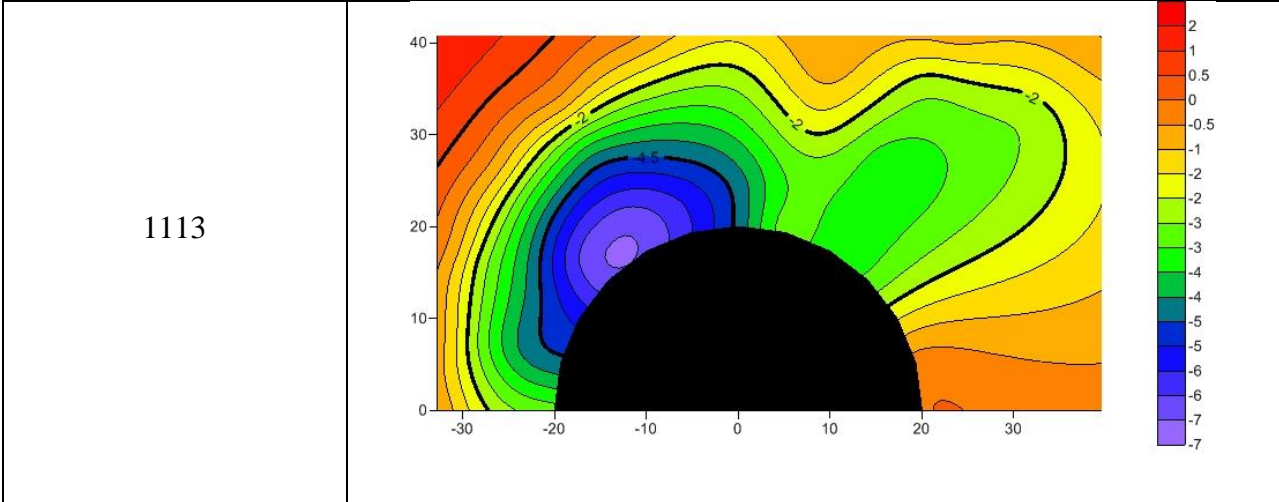


1111

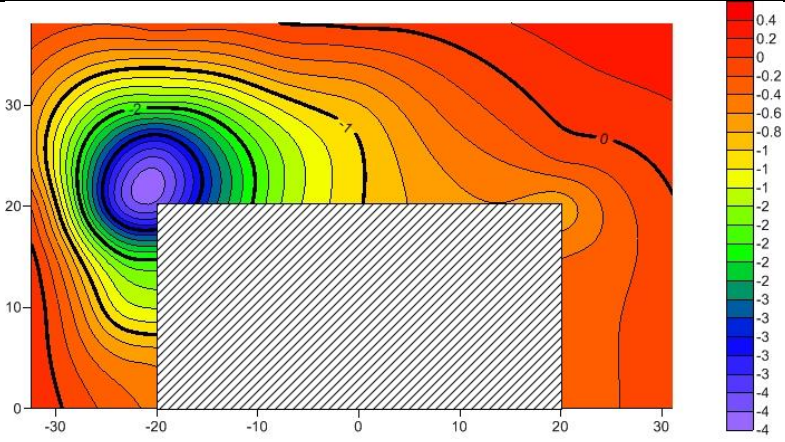


1112

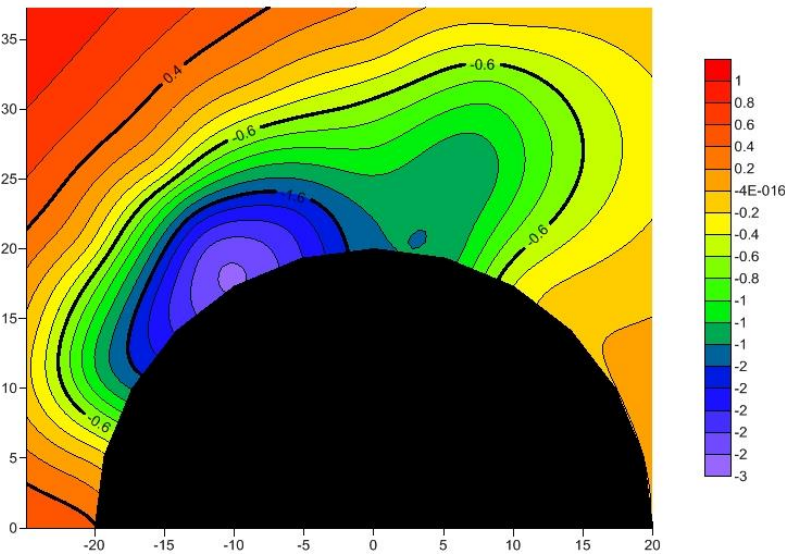




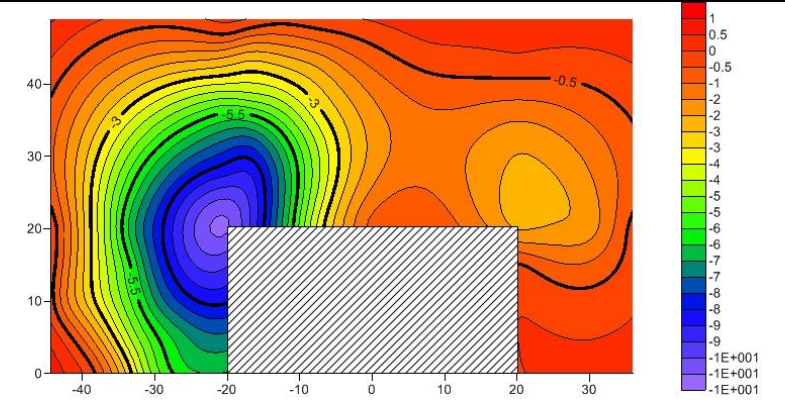
1116



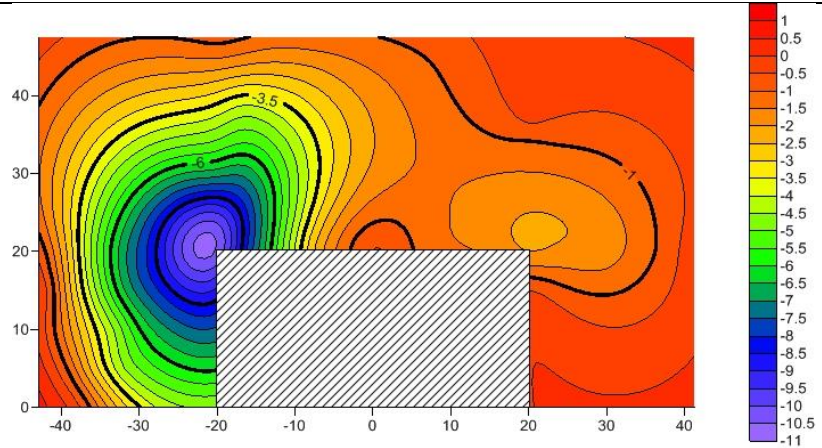
1117



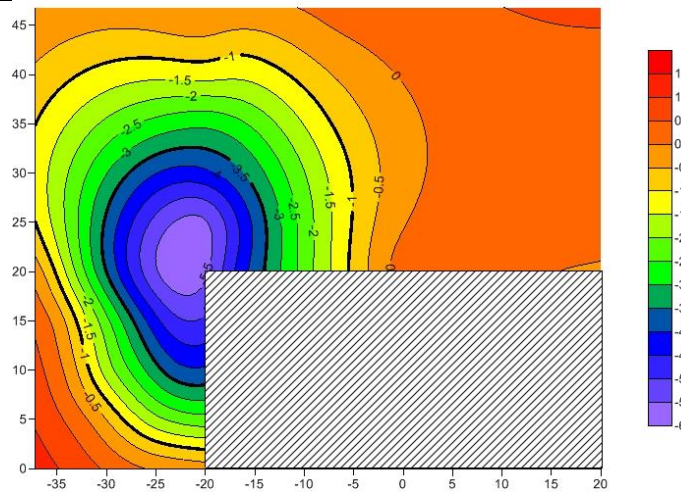
1118



1119



1120



1121

